NBS TECHNICAL NOTE 1002

U.S. DEPARTMENT OF COMMERCE / National Bureau of Standards

Measurements of Combined Axial Mass and Heat Transport in He II

0
753
1002
78
2

NATIONAL BUREAU OF STANDARDS

The National Bureau of Standards[1] was established by an act of Congress March 3, 1901. The Bureau's overall goal is to strengthen and advance the Nation's science and technology and facilitate their effective application for public benefit. To this end, the Bureau conducts research and provides: (1) a basis for the Nation's physical measurement system, (2) scientific and technological services for industry and government, (3) a technical basis for equity in trade, and (4) technical services to promote public safety. The Bureau consists of the Institute for Basic Standards, the Institute for Materials Research, the Institute for Applied Technology, the Institute for Computer Sciences and Technology, the Office for Information Programs, and the Office of Experimental Technology Incentives Program.

THE INSTITUTE FOR BASIC STANDARDS provides the central basis within the United States of a complete and consistent system of physical measurement; coordinates that system with measurement systems of other nations; and furnishes essential services leading to accurate and uniform physical measurements throughout the Nation's scientific community, industry, and commerce. The Institute consists of the Office of Measurement Services, and the following center and divisions:

Applied Mathematics — Electricity — Mechanics — Heat — Optical Physics — Center for Radiation Research — Laboratory Astrophysics[2] — Cryogenics[2] — Electromagnetics[2] — Time and Frequency[2].

THE INSTITUTE FOR MATERIALS RESEARCH conducts materials research leading to improved methods of measurement, standards, and data on the properties of well-characterized materials needed by industry, commerce, educational institutions, and Government; provides advisory and research services to other Government agencies; and develops, produces, and distributes standard reference materials. The Institute consists of the Office of Standard Reference Materials, the Office of Air and Water Measurement, and the following divisions:

Analytical Chemistry — Polymers — Metallurgy — Inorganic Materials — Reactor Radiation — Physical Chemistry.

THE INSTITUTE FOR APPLIED TECHNOLOGY provides technical services developing and promoting the use of available technology; cooperates with public and private organizations in developing technological standards, codes, and test methods; and provides technical advice services, and information to Government agencies and the public. The Institute consists of the following divisions and centers:

Standards Application and Analysis — Electronic Technology — Center for Consumer Product Technology: Product Systems Analysis; Product Engineering — Center for Building Technology: Structures, Materials, and Safety; Building Environment; Technical Evaluation and Application — Center for Fire Research: Fire Science; Fire Safety Engineering.

THE INSTITUTE FOR COMPUTER SCIENCES AND TECHNOLOGY conducts research and provides technical services designed to aid Government agencies in improving cost effectiveness in the conduct of their programs through the selection, acquisition, and effective utilization of automatic data processing equipment; and serves as the principal focus wthin the executive branch for the development of Federal standards for automatic data processing equipment, techniques, and computer languages. The Institute consist of the following divisions:

Computer Services — Systems and Software — Computer Systems Engineering — Information Technology.

THE OFFICE OF EXPERIMENTAL TECHNOLOGY INCENTIVES PROGRAM seeks to affect public policy and process to facilitate technological change in the private sector by examining and experimenting with Government policies and practices in order to identify and remove Government-related barriers and to correct inherent market imperfections that impede the innovation process.

THE OFFICE FOR INFORMATION PROGRAMS promotes optimum dissemination and accessibility of scientific information generated within NBS; promotes the development of the National Standard Reference Data System and a system of information analysis centers dealing with the broader aspects of the National Measurement System; provides appropriate services to ensure that the NBS staff has optimum accessibility to the scientific information of the world. The Office consists of the following organizational units:

Office of Standard Reference Data — Office of Information Activities — Office of Technical Publications — Library — Office of International Standards — Office of International Relations.

---

[1] Headquarters and Laboratories at Gaithersburg, Maryland, unless otherwise noted; mailing address Washington, D.C. 20234.

[2] Located at Boulder, Colorado 80302.

Measurements of Combined Axial Mass and Heat Transport in He II

N Bureau of Standards
3 1978
QC100
.5753
no. 1002
1978

Technical note no. 1002

Warren W. Johnson
Michael C. Jones

Cryogenics Division
Institute for Basic Standards
National Bureau of Standards
Boulder, Colorado 80303

U.S. DEPARTMENT OF COMMERCE, Juanita M. Kreps, Secretary

Sidney Harman, Under Secretary
Jordan J. Baruch, Assistant Secretary for Science and Technology

NATIONAL BUREAU OF STANDARDS, Ernest Ambler, Director

Issued February 1978

NATIONAL BUREAU OF STANDARDS TECHNICAL NOTE 1002

Nat. Bur. Stand. (U.S.), Tech. Note 1002, 84 pages (February 1978)

CODEN: NBTNAE

U.S. GOVERNMENT PRINTING OFFICE
WASHINGTON: 1978

For sale by the Superintendent of Documents, U.S. Government Printing Office, Washington, D.C. 20402

Stock No. 003-003-01889-9 Price $2.40 (Add 25 percent additional for other than U.S. mailing)

CONTENTS

		Page
1.	INTRODUCTION AND BACKGROUND	1
	1.1 The Two-Fluid Model	2
	1.2 Counterflow	3
	1.3 Limits to the Heat Current for Practical Applications	5
	1.4 Raising Those Limits Through Forced Convection	5
2.	THERMODYNAMICS OF HEAT TRANSPORT	6
	2.1 Conduction and Convection	6
	2.2 The Classical Analog	6
	2.3 The He II Energy Equation	10
	2.4 A Note on the Experiment	11
3.	EXPERIMENTAL METHODS	12
	3.1 Introduction	12
	3.2 The Temperature Measurement Systems	15
	3.3 Thermometer Calibration and Performance	16
	3.4 Pressure Difference Measurements	18
	3.5 Mass Flow Rate	24
	3.6 The Flow Tube	26
	3.7 The Energy Flow Measurement	29
	3.8 Extraneous Heat Flows	31
	3.9 Error Estimates	33
4.	RESULTS AND DISCUSSION	36
	4.1 The Net Fluid Velocity	36
	4.2 The Heat Current Density	44
5.	ENHANCEMENT OF HEAT TRANSPORT BY FORCED CONVECTION	54
6.	CONCLUSIONS	59
7.	ACKNOWLEDGMENTS	59
8.	REFERENCES	60
9.	NOMENCLATURE	62
Appendix 1		64
Appendix 2		76

MEASUREMENTS OF COMBINED AXIAL MASS AND HEAT TRANSPORT IN He II

Warren W. Johnson and Michael C. Jones

An experiment was performed that allowed measurements of both axial mass and heat transport of He-II in a long tube. The apparatus allowed the pressure difference and the temperature difference across the flow tube to each be independently adjusted, and the resulting steady-state values of net fluid velocity and axial heat transport to be measured. For the larger Reynolds numbers, it was found that the relation between pressure difference and net fluid velocity was nearly indistinguishable from that of an ordinary fluid in turbulent flow. The axial heat transported was found to be suppressed from the values that were calculated by assuming that "mutual friction" was unchanged by the net fluid flow, but it was always found to be larger than the "enthalpy rise" value. Taking this second value as a lower limit, it is shown that a mild extrapolation of these results suggests that (in appropriate circumstances) forced convection would allow much greater heat to be transported in long cooling channels than could be transported by "natural" convection alone.

Key words: Axial heat transport; forced convection; helium II; measurements; 1.4 - 2.1 K; pressure drop.

1. INTRODUCTION AND BACKGROUND

This is the first report of the results of an investigation of steady-state combined heat transport and fluid flow of the superfluid phase of helium 4 (known as He II) through a long tube.

The first experiments of this type, both at Leiden have been reported only in the last few years [1-4]. This is the first to be done in this country, and the first to investigate, with an unambiguous method, flow in which both fluid components are turbulent.

There are two motivations for this work, one scientific and one of an applied nature. A considerable amount is known about the extraordinary hydrodynamics of He II in certain idealized situations (i.e., where the velocities are small, and laminar or potential flow is taking place); rather little is known about the hydrodynamics of He II when the flow is turbulent, and so new types of experiments in this area, are of fundamental interest. From the standpoint of applications, He II is of interest mainly for its excellent heat transfer properties, which can be utilized in the construction of superconducting devices. This experiment is the first to attempt to determine the effect of forced convection, i.e., mass flow, on the heat transported by the fluid. The term heat transport in the context of this paper is used to mean heat transported in the axial direction by the fluid contained in a long tube which connects a cold fluid reservoir to a hot fluid reservoir. This is not to be confused with the more familiar problem of heat transfer from a solid wall into the liquid.

The measurements were made on a tube of length 60 cm and an inside diameter of 0.1149 cm. They covered a range in fluid flow (expressed as the "total" Reynolds number) of $3\text{-}90 \times 10^3$, and a range in heat current density of 0.01-1.4 W/cm^2.

The results at small net fluid velocities show that the usable heat transported by the fluid is predicted by an application of Vinen's expression for mutual friction. The measured usable heat transport falls considerably below this calculation at the larger velocities, but is always greater than the calculated enthalpy rise (the result for an ordinary fluid). It is argued that this latter value should be a lower bound for the heat transport, in which case an extrapolation suggests that forced convection might be expected to increase greatly the heat that can be removed from a heat source by liquid helium II.

1.1 The Two-Fluid Model

All of our understanding of the remarkable properties of He II is based on the two-fluid model. It supposes that He II can be treated as a mixture of two interpenetrating components: the superfluid component and the normal fluid component. (As is common, we will often use the term "superfluid" to signify both the superfluid component and the mixture of two components, trusting that the context will indicate which meaning is intended). The relative fractions of the two components is determined almost entirely by the temperature, the superfluid fraction changing from 0% to 99% in the temperature interval of 2.17 to 1.05 K. The extraordinary hydrodynamics comes from the fact that each component can have quite different and independent velocities. This is expressed by

$$\rho = \rho_s + \rho_n \tag{1}$$

$$\rho\vec{V} = \rho_s\vec{v}_s + \rho_n\vec{v}_n \ , \tag{2}$$

where ρ is the total mass density, ρ_s, ρ_n are the super- and normal-component densities, v_s, v_n are the super- and normal-component velocites and $\vec{V}$ represents the velocity at which mass is actually transferred. Mass conservation is expressed as

$$\frac{\partial\rho}{\partial t} + \vec{\nabla}\cdot(\rho\vec{V}) = 0 \ . \tag{3}$$

Other vital assumptions of the model are that: the superfluid component carries no entropy, the normal component has a viscosity η_n and satisfies the usual boundary conditions of an ordinary fluid, and that the superfluid component, at least under some conditions, can flow like an "ideal fluid", i.e., a fluid with no viscosity and a "slip" boundary condition at the walls. From these and a few other considerations can be derived the following equations - neglecting dissipation - that are supposed to govern the flow. [5]

$$\frac{\partial}{\partial t}(\rho s) + \vec{\nabla}\cdot(\rho s\vec{v}_n) = 0 \tag{4}$$

$$\rho_s\frac{\partial\vec{v}_s}{\partial t} + \rho_n\frac{\partial\vec{v}_n}{\partial t} + \rho_s\left(\vec{v}_s\cdot\vec{\nabla}\right)\vec{v}_s + \rho_n\left(\vec{v}_n\cdot\vec{\nabla}\right)\vec{v}_n = -\vec{\nabla}p + \eta_n\nabla^2\vec{v}_n \tag{5}$$

$$\frac{\partial \vec{v}_s}{\partial t} + \vec{v}_s \cdot \vec{\nabla} \vec{v}_s = - \vec{\nabla} \mu \qquad (6)$$

$$\vec{\nabla} \mu = - s \vec{\nabla} T + \frac{1}{\rho} \vec{\nabla} P \qquad (7)$$

The symbols P, T, s, μ stand for pressure, temperature, specific entropy, and specific Gibbs potential or chemical potential. (Throughout this report, specific thermodynamic quantities will refer to unit mass). Equation (4) represents entropy conservation, where all the entropy flow is associated with the normal velocity. Equation (5) is the analogue of the Navier-Stokes equation (momentum conservation). Equation (6) is the equation of motion of the superfluid component, and eq (7) is a well-known thermodynamic identity. The quantities $\vec{v}_s \cdot \vec{\nabla} \vec{v}_s$ and $\vec{v}_n \cdot \vec{\nabla} \vec{v}_n$ are usually neglected in the so-called linear hydrodynamics.

A great variety of experiments done with nonturbulent flows can be quantitatively analyzed with these equations, thus firmly establishing the two-fluid model. The reader unfamiliar with He II may consult Wilks [5], or several other texts [6-8], for a thorough review of the hydrodynamics in non-turbulent flows.

The difficulties arise with the nonlinear types of flow, particularly the turbulent ones. For a purely classical fluid, i.e., one that obeys the Navier-Stokes equation, turbulent flow problems still cannot be solved from first principles; most of what we know is empiricism based on a large body of experimental data. In He II, with extra variables, and where the possibility exists of still unknown terms in the equations of motion, we must rely even more on experimental results. As with classical fluids, it appears that the majority of practical applications of He II will probably involve turbulent flows.

1.2 Counterflow

There is one type of turbulent flow of He II that has received a lot of attention; it is termed "counterflow" or "internal convection". Its experimental realization is exactly like a thermal conductivity experiment, that is, it is a tube filled with He II that connects a heat source to a heat sink. The apparent thermal conductivity is always very high, usually much higher than any other known substance; it was the discovery of this property that first signaled the existence of a very unusual type of liquid. For small heat flows, typically much less than 0.1 W/cm^2, the temperature gradient is extremely small and all the facts are fully in accord with the equations of motion listed above. The origin of the enormous thermal conductivity is the ability of the two fluid components to flow "through" each other, essentially on an atomic scale, hence the term "counterflow". Entropy, hence heat, in the form of the normal component, is able to flow away from the heat source unimpeded except by its viscous resistance with the walls; the requirement that the net amount of fluid flow be zero is met by return flow of the super component. It is vital to note that the flow of heat, i.e., energy in the form of thermal agitation of the helium atoms, obeys a hydrodynamic equation of flow, rather than the usual diffusive one; this is in fact the main reason why a two-fluid model works. More detailed discussion of this point may be found in the texts [5-8].

At some critical heat current (or its equivalent in counterflow velocity) the character of the counterflow changes in that there arises a finite interaction between the normal and super components, termed "mutual friction", that impedes the counterflow. The temperature gradient is no longer proportional to the heat current $\dot{q}$; instead it rises much faster, approximately as

$$\frac{\partial T}{\partial x} \propto \dot{q}^3 \ . \tag{8}$$

The nature of mutual friction was revealed in a classic series of papers by Vinen [9]. He found that it is produced by a unique type of turbulence in the super component only, a type associated with a tangled mass of quantized vortex lines. These lines are the only locations where the super component has non-zero vorticity $\vec{\omega} \equiv \left(\vec{\nabla} \times \vec{v}_s\right)$. They are a structure in the super component; but they also have a drag force exerted on them by the normal component, thus they provide the means of interaction between the two components. Vinen argued that the force of mutual friction $\vec{F}_{sn}$ ought to be of the form

$$\vec{F}_{sn} = \beta L_o \left(\vec{v}_n - \vec{v}_s\right) \tag{9}$$

where β is a temperature-dependent constant, and L_o is the length of vortex line per unit volume. This mutual friction force changes the equation of motion for the superfluid (eq. 6) to

$$\frac{\partial}{\partial t} \vec{v}_s = - \vec{\nabla}\mu + \frac{1}{\rho_s} \vec{F}_{sn} \ . \tag{10}$$

Further, he deduced a dimension argument to conclude that

$$L_o \propto \left(\left| v_n - v_s \right| - v_o \right)^2 \tag{11}$$

where v_o is small. Since $\vec{v}_n - \vec{v}_s \propto \dot{q}$, combining eqs. (9,10 and 11) gives the experimental result, eq (8). The constant of proportionality is approximately $A\rho_n/s(\rho_s sT)^3$ where A, the Gorter-Mellink constant, is a weak function of temperature and is about 100 cm.s/g at 1.9 K.

One feature of this result is particularly remarkable, and it is the lack of any explicit geometrical dependence; the turbulence intensity, L_o, is only a function of the heat flux per unit area.

No serious challenge has been raised to the main features of Vinen's analysis. The most recent work [10,11] has shown that there are some additional features of the flow, at least for small diameters ($\lesssim 10^{-2}$ cm), and there are reports of different values for the constants (see the review of Arp [12]), but by and large the results of Vinen can still be recommended for large diameters ($\gtrsim 10^{-1}$ cm).

1.3 Limits to the Heat Current for Practical Applications

There must be some limit to heat that can be transferred by internal convection, and the weight of the evidence suggests that this is when the temperature and the pressure near the heat source assume values such that the vapor is the more stable phase, i.e., when the liquid is superheated [12-16]. In ordinary liquids, a small superheat of the liquid near a heated surface causes the formation of small vapor bubbles (nucleate boiling), but in He II this does not happen. Instead, at some modest value of superheat, which might depend on apparently extraneous variables, such as the level of mechanical vibration [15], it appears the He II goes directly into the film boiling stage, where the heated surface is coated by a layer of the (very low thermal conductivity) vapor.

For all the applications one can envisage, the onset of film boiling would be undesirable, perhaps disastrous. Therefore, we arrive at the following tentative prescription for the maximum allowed design heat current: from the geometry, the distribution of heat sources, and from eq (8) calculate the temperature distribution; if the liquid is superheated at any point (the pressure must be known and the phase diagram consulted) then the cooling channel must be expanded, or heat intensity reduced. It remains to determine an appropriate safety factor.

Examining eq (8) we see that for a uniform channel, with a heat source only at the end,

$$\dot{q}_{max} \propto (T_{max}/L)^{1/3}$$

At a typical value of $\Delta T = 0.05$ K and a length of 60 cm, the maximum heat current is about 1.0 W/cm^2. Because of the cube root dependence, and the limitations on ΔT ($T_{hi} < 2.17$ K) it is obvious that $\dot{q}_{max}$ cannot be much bigger than this.

1.4 Raising Those Limits Through Forced Convection

It is well known that total heat that can be transported through a long tube by a classical fluid can usually be greatly increased if the convection is forced by a pump. That this ought also to apply to He II was the motivation for this experiment.

The first task in such a program was to reformulate some of the equations of two fluid hydrodynamics in such a way that the transfer of energy away from a heat source by both internal convection and "real" or forced convection could be treated in a consistent manner. This is handled in section 2.

The design and performance of an experiment to measure the relevant quantities for a long tube is considered in the sections 3 and 4.

Because of the experiment's exploratory nature, and the resulting uncertainties, it turned out that the apparatus was not quite capable of reaching the region of flow where the forced convection would increase the total heat transported dramatically. However, the measured values of the relevant quantities are such that we can, with reasonable certainty extrapolate their behavior a modest amount, and conclude that, in certain circumstances, the heat transported per unit cross-sectional area of cooling channel can be increased to at least ten times the value allowed by counterflow. This conclusion is discussed in section 5.

2. THERMODYNAMICS OF HEAT TRANSPORT

2.1 Conduction and Convection

The case we wish to treat is when both conduction and convection are important for the axial heat transport. This is not a common case for any ordinary cryogenic fluid. For ordinary fluids, the thermal conductivity is so small that it is of significance only for the "heat transfer coefficient," i.e., the transport of heat through the boundary layer near the wall. Axial energy transport is ordinarily dominated by the physical movement of hot fluid, whether by natural (gravity-driven) convection or forced convection.

In He II, the counterflow process seems to share some attributes of both conduction and ordinary convection, and we also wish to consider the effect of forced convection; therefore a consistent treatment of the whole process is vital.

2.2 The Classical Analog

It is illuminating to consider a somewhat idealized version of this same problem for a classical fluid. The situation is shown in Fig. 1. Heat is generated at a point source in the middle of a channel connecting two heat sinks. We wish to know the relationship between the heat $\dot{Q}''$, the impressed average fluid velocity V, and the temperature rise ΔT.

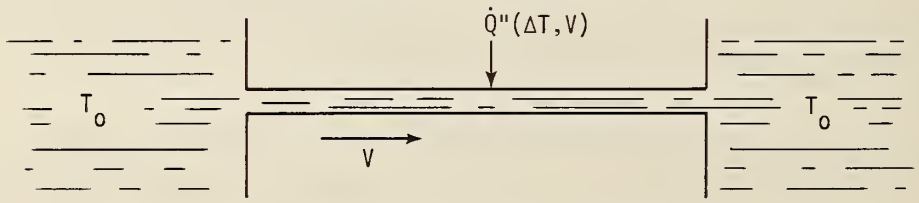

Figure 1. A schematic diagram of a long cooling channel with a localized heat source, $\dot{Q}''$.

We can derive a differential equation that governs the axial energy transport from the energy conservation equation of the fluid. In the form we will find particularly useful, it is

$$\frac{\partial}{\partial t}\left[\rho(u+V^2/2)\right] + \vec{\nabla} \cdot \left\{\rho\vec{V}[h+V^2/2] + \vec{\dot{q}}\right\} \simeq 0 \qquad (12)$$

Here u is the specific internal energy, $h = u + P/\rho$ is the specific enthalpy, $\vec{v}$ is the velocity vector, and $\dot{q}$ is the heat current density vector. This equation is derived in many texts on fluid mechanics, e.g., Ref. [17], p 184. One term, the viscous energy flux, has been dropped because it can be shown to be negligible for the flows of interest to us.

In this equation, the first term in square brackets is the total energy density (internal plus kinetic); this implies that the term in curly brackets is the <u>total energy flux</u> vector, $\vec{J}_u$, for a fluid. This form of the energy equation is particularly useful because it requires no explicit calculations of the rate at which flow work is degraded to thermal energy, nor has any assumption been made about the functional dependence of heat conduction.

In steady fully-developed turbulent flow through a tube, if we express V, h, and $\dot{q}$ as sums of steady and fluctuating components, the equation may be time-averaged, as shown for example in Ref. [18]. If we now integrate the equations over the cross-sectional area A_x of the tube, we get

$$\frac{d}{dx}\left\langle \rho V_x h \right\rangle + \frac{d}{dx}\left\langle \dot{q}_x \right\rangle = \frac{1}{A_x}\frac{d\dot{Q}(x)}{dx} \qquad (13)$$

where angular brackets indicate cross-sectional averages, $d\dot{Q}(x)/dx$ is the local rate of heat addition per unit length, x is the axial coordinate, and we have taken the cross-sectional area to be a constant. The quantities V_x, h, and $\dot{q}_x$, in eq (13) must now be interpreted as time-averaged quantities: $\dot{q}_x$ is now no longer just the molecular energy flux, but also contains a turbulent energy flux (the time correlation of the enthalpy fluctuations and the axial velocity fluctuations).

We can use well-known thermodynamic relations to rewrite h in terms of the specific heat at constant pressure C_p, and other quantities

$$\frac{\partial h}{\partial x} = \left(\frac{\partial h}{\partial T}\right)_P \frac{\partial T}{\partial x} + \left(\frac{\partial h}{\partial P}\right)_T \frac{\partial P}{\partial x} \simeq C_P \frac{\partial T}{\partial x} + \frac{1}{\rho}\frac{\partial P}{\partial x} \qquad (14)$$

where the second equality is an excellent approximation because we can neglect the compressibility of the liquid. In a long tube, with no wall heating, the axial temperature and pressure gradients are not a function of transverse position, so that the first term of eq (13) becomes

$$\rho V C_p \frac{\partial T}{\partial x} + V \frac{\partial P}{\partial x} ,$$

where

$$V \equiv \left\langle V_x \right\rangle .$$

Let us assume that the liquid has the usual form for the molecular thermal conductivity k, and that it is much larger than any turbulent mixing contribution. Then for the configuration of Fig. 1,

$$\rho V C_p \frac{\partial T}{\partial x} + V \frac{\partial P}{\partial x} + \frac{\partial}{\partial x}\left(- k \frac{\partial T}{\partial x}\right) = \frac{\dot{Q}''}{A_x} \delta(x - x_o) \qquad (15)$$

where δ is the Dirac delta function which represents the point heat source located at x_o.

The appropriate boundary conditions are the values of the temperature at the ends of the tube and at the point heat source. The value of $\dot{Q}''/A_x$, where A_x is the cross-sectional area of the tube, is found by solving for T(x), and then calculating the discontinuity of the energy flux, i.e., the discontinuity of $-k(\partial T/\partial x)$.

When the pressure gradient is small enough, we can obtain an explicit solution for T in terms of an exponential. The character of the solutions is shown in Fig. 2.

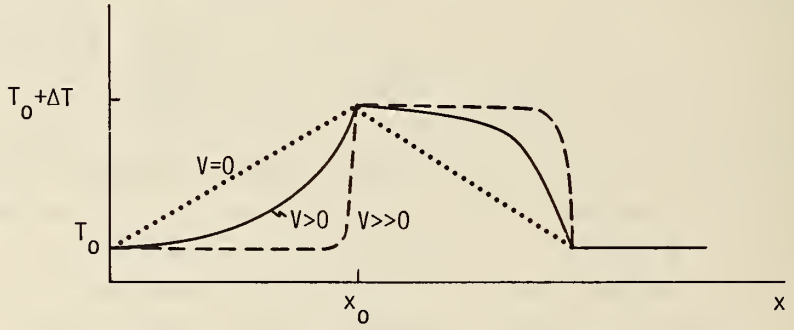

Figure 2. The temperature of the fluid in the channel of Figure 1, for various values of the impressed fluid velocity V.

It is apparent that the heat transported away from the source can be divided into an upstream part and a downstream part. In the configuration of Fig. 3, which is essentially the geometry of our experiments, we find we can measure the contribution of each part separately, thus obtaining a more complete picture of the whole process.

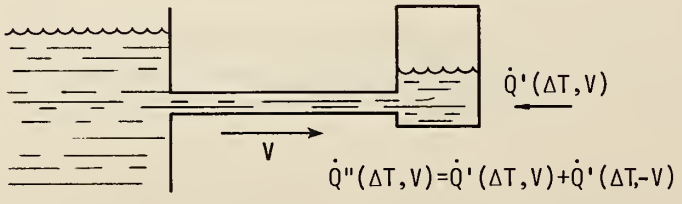

Figure 3. Schematic diagram of a configuration that allows us to measure separately the heat removed by each half of the cooling channel shown in Fig. 1, and the equation that relates the results for the two configurations.

The calculated result for the heat absorbed in this second configuration is shown in Fig. 4.

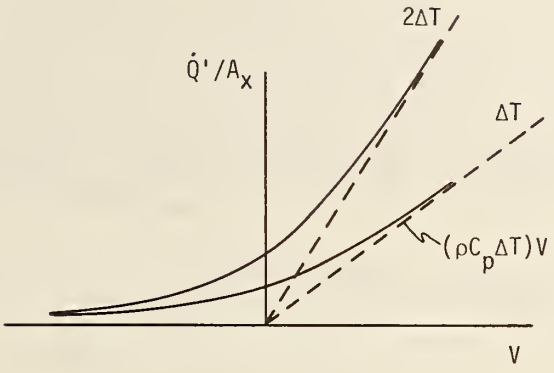

Figure 4. The expected results for Fig. 3 for two different temperature rises at the heat source, if the fluid has a high thermal conductivity. Asymptotically, the heat removed is given by the enthalpy rise of the fluid.

The solutions display the appropriate values in the two limiting cases. For $V = 0$, we recover the pure conduction equation, with the result $\dot{Q}'' = 2\dot{Q}' = 2k(\Delta T/x_0)A_x$. For the case $V \gg 0$, we find that the upstream part approaches asymptotically the value $\rho V(\Delta h)A_x \tilde{=} \rho V C_p(\Delta T)A_x$, and the downstream part approaches zero, i.e., we obtain the familiar result that, if axial conduction is small except near the heat source, then the heat transported away from the source is given by the enthalpy rise of the fluid.

There is another representation for the energy flux vector which we will find useful. It is found by using the definition of the chemical potential

$$\mu = u + \frac{1}{\rho} P - sT = h - sT \tag{16}$$

to obtain

$$\vec{J}_u = \rho\vec{V}(\mu + V^2/2) + [\rho s\vec{V}T + \vec{\dot{q}}] \tag{17}$$

the term in square brackets can be identified as T times the total entropy flux. If there is no mass flow, then the heat and energy fluxes are the same, and the entropy flux differs only by a factor of T, so that the distinctions between the three quantities tend to become lost. With mass flow present, it is obviously important to maintain the distinctions between them [19].

2.3 The He II Energy Equation

As discussed in Section 1, eqs (1-6) are often presented as the basic two-fluid model equations. Also discussed were the counter-flow experiments that necessitate the replacement of eq (6) by eqs (9 & 10). At least one other modification of the two fluid equations is required.

For the cases we wish to consider it is obvious that entropy is being increased by the heat transport, so that the equation for entropy conservation, eq (4), is not correct. While explicit modification of this equation has been proposed [20], we have preferred to use the approach of finding the total energy flux, as was done above for the classical fluid case, and thus we replace equation (4) with an energy equation.

An explicit energy equation has been derived for He II from several different viewpoints (Ref. [8], p 28; Ref. [5], p 168). To a good approximation it is

$$\frac{\partial}{\partial t}\,[\rho u] + \vec{\nabla}\cdot\{\rho\vec{V}\mu + \rho s T\vec{v}_n\} \cong 0 \tag{18a}$$

or

$$\frac{\partial}{\partial t}\,[\rho u] + \vec{\nabla}\cdot\{\rho\vec{V}h + \rho s T(\vec{v}_n - V)\} \cong 0 \tag{18b}$$

All dissipative flux terms have been dropped: by comparison with the ordinary fluid equation we expect the normal fluid viscous stress part to be small, the irreversible heat flux term is always 3-5 orders of magnitude smaller than the heat flux defined below, and numerical estimation of the remaining terms suggests they are even smaller.

By comparison with eqs (12) and (17), we see that the same relations hold, as in the classical case with the new identifications of the total entropy flux as

$$\rho s T\vec{v}_n$$

and the heat flux as

$$\vec{\dot{q}} = \rho s T(\vec{v}_n - \vec{V}) = \rho_s s T(\vec{v}_n - \vec{v}_s) \tag{19}$$

where the second equality follows from eqs (1) and (2).

In many treatments of He II, the heat flux has incorrectly been identified with the entropy flux, probably because there have been almost no previous experiments on heat flow where $V \neq 0$. The correct identification for the heat flux has been stated recently [21]; evidently the argument just given is the explicit justification for it.

We can use the same steps as before to derive a one-dimensional, steady state, energy conservation equation. It is

$$\frac{\partial}{\partial x}\left[\rho V h + \dot{q}\right] = \frac{1}{A_x}\frac{\partial \dot{Q}(x)}{\partial x} \tag{20}$$

where it is understood that V and $\dot{q}$ are the cross-sectional averages. Again the right hand side represents the external heat sources.

As in the classical case, this form of the energy equation does not require any detailed knowledge of the hydrodynamic mechanisms that give rise to the pressure and temperature gradients; it only requires their measured values. But $\dot{q}$ represents the total heat flux from whatever microscopic mechanism, be it molecular or eddy conduction, or "internal convection."

The experimental problem then is straightforward: what is the functional dependence of V and $\dot{q}$ on the pressure and temperature gradients and on the geometry? Note that because of the hydrodynamic character of $\dot{q}$ for He II, we must not expect it to be solely a function of the temperature gradient. Ideally we would like to compute these from the two fluid equations, but that is not practical for the reasons discussed in section 1.

2.4 A Note on the Experiment

The experiment was done using essentially the configuration of Fig. 3. Not only does this allow the separate examination of the upstream and downstream components of the heat transported, it also allows the net flow velocity V to be measured by a straightforward volumetric technique. This is important because there is no conventional flowmeter that we can be confident will work in its usual manner [22]. Vortex-shedding and turbine meters depend on the shed or bound vorticity having particular values. We know that vorticity, at least in the superfluid component, is not generated in the conventional manner, e.g., from the high shear in the boundary layer, but rather its main source is apparently the relative velocity between the normal and super components, and so we have no good reason to expect the conventional values. Orifice meters, pitot tubes and venturi meters all depend on a surface of flow separation being in a certain position, but flow separation is really the same as a bound vortex sheet, and so the same objection applies to these meters.* The only type of flow meter that we can be reasonably certain would work in He II is an acoustic one; unfortunately it seems nearly impossible to build one for small diameter tubes.

* Work done in this laboratory [23] has suggested that a venturi meter might still work in some reasonable manner in He II, but no direct test could be made in that experiment.

3. EXPERIMENTAL METHODS

3.1 Introduction

In the previous section it was shown that the axial transport problem is essentially the determination of the functional relations between the two fluxes and the two gradients. Then the energy and mass conservation equations can be used to determine the effect of distributed heat sources, of changes in flow tube cross-section, etc. We found it convenient to choose the two fluxes to be the net average velocity V and the average heat current density $\dot{q}$, rather than the normal- and super-fluid velocities v_s and v_n. The gradients that drive the fluxes were taken to be the pressure and temperature gradients. In general, any two of the four quantities can be chosen to be the independent variables, whose values, and the hydrodynamics, then determine the two remaining (dependent) variables.

The general plan for the experiment was to use several feedback systems to maintain a fixed temperature difference and pressure difference between the ends of a tube filled with liquid helium -- the independent variables for this experiment. The tube was surrounded by an insulating vacuum, so that no heat was transferred through its walls. The resulting steady state values of overall mass flow and energy flow through the tube -- the dependent variables -- were then measured.

A schematic diagram of the experimental apparatus is shown in Fig. 5. In Fig. 6 we show a photograph of the apparatus with vacuum can removed. The flow tube (FT) was the only connection between the outside helium bath (O) and the inside helium vessel (I). The inside vessel (I) was surrounded by a vacuum maintained by the stainless steel vacuum can (VC). This inside vessel was constructed in two parts, an upper section with a large horizontal cross-sectional area, and a lower section with a small horizontal cross-sectional area. The temperatures of O and I were sensed by identically mounted carbon resistors (TCO, TCI), which controlled the voltages applied to the two resistance heaters (IH, OH) so as to maintain a fixed temperature in each space. The actual temperatures in O and I were determined from the germanium resistance thermometers T1, T2 and TB.

The entire assembly of vacuum can (VC), inside helium vessel (I), and associated instruments, was surrounded by a copper heat shield (HS) and was suspended by a single support tube (ST). This support tube also acted as the pumpout tube for the vacuum space, and as a conduit for the electrical leads. An exterior motor-driven mechanism and a sliding seal for ST allowed adjustment of the vertical position of VC in the helium bath O, and hence adjustment of the hydrostatic pressure difference applied across the flow tube (FT). The difference between the inside and the outside levels was sensed continuously by the coaxial capacitors C1 and C2. This signal was used to control that motor so as to maintain a fixed level difference. Of course, steady state flow could be maintained only for the length of time it took for the inside vessel (I) to be filled or emptied.

The first dependent variable, the mass flow through the tube, was determined by noting the average value of the vertical speed of the vacuum can (VC) that the motor-controller system had set in order to maintain the fixed level difference. The second dependent

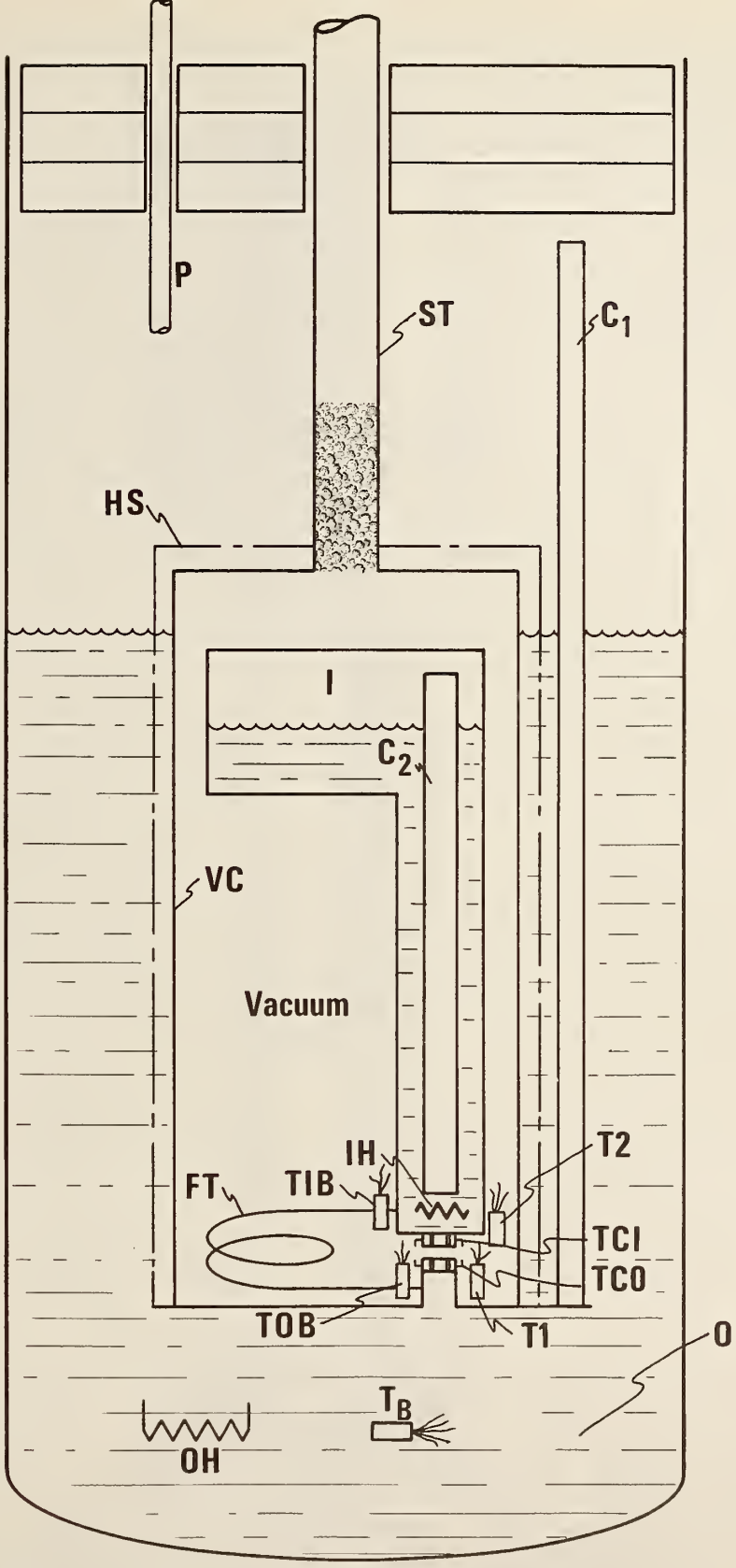

Figure 5. A schematic diagram of the apparatus.

Figure 6. A photograph of the apparatus with the vacuum can removed.

variable, the rate at which energy flowed through the tube, could be determined by noting the value of the heat being supplied to the inside heater (IH) by the inside temperature control system.

The inside heater consisted of 60 cm of 0.04 cm diameter manganin wire wound around the bottom end cap of the inside capacitor, where it would always be immersed in the liquid. The heater current was brought through the vacuum space by superconducting wires, which led from a heat sink on the base plate to the inside space. Their low thermal conductivity allowed the current to be transmitted without adding a significant thermal link through the insulating vacuum. The (cold) resistance of the heater was measured to be 664 ohms, of which less than 1 ohm was the room temperature to helium temperature lead resistance.

Data were taken at four temperatures (1.39, 1.65, 1.92 and 2.10 K), which span a range in the normal fluid component fraction from 7 percent to 74 percent. Time permitted data to be taken for only a single tube (diameter = 0.115 cm, length = 60 cm), and at only a few, but widely-spaced ΔT's. Fifteen or twenty points were taken at each ΔT, covering a range of approximately two orders of magnitude in pressure difference.

All of the data presented in this report were taken during a single thirty-five day period. They are presented in tabular form in Appendix I, and in graphical form in the results and discussion sections. During this long run, the liquid helium in the outer helium bath was replenished every two or three days, and the apparatus was never allowed to warm up. Two of the main variables, temperature and temperature difference, were varied from day to day in an irregular manner, and also there was enough duplication, so that we can conclude that there was no significant progressive change in the data throughout this long run. Some data taken during several preliminary runs were also reproduced (to within about 2% in the dependent variables) during this long run.

3.2 The Temperature Measurement Systems

The two independent temperature control systems had identical carbon resistor temperature sensors. Each resistor mounted in the vacuum space was filed flat on opposite sides down to a thickness of about 2 mm, wrapped in a layer of cigarette paper saturated in varnish and then wrapped in copper foil, whose loose end was varnished onto a copper piece in contact with one of the helium spaces. The resistor was connected as one arm in a dc Wheatstone bridge, whose null detector fed a signal to a temperature controller. Power dissipation in each resistor was 10^{-5} -10^{-6} W. The outside controller was of local design. The inside controller was a commercial temperature controller used in the proportional mode. The error signal from the inside null detector was attenuated greatly (100:1) so that the control fluctuations were quite weak. This meant that the fixed offset had to be adjusted manually for each change in conditions, but this was necessary to ensure that the voltage on the inside heater could be read with sufficient precision.

Judging from the null detectors and the germanium resistor thermometers, short term fluctuations (minutes to seconds) in the two temperatures were less than 0.0002 K. The very high effective thermal conductivity of He II makes this possible even in a large

system with fluctuating heat loads. However, there were significant long term drifts in the carbon resistors, occasionally as large as 0.0001 K/hour. These were not seriously damaging to the measurements, because readings from a set of germanium resistance thermometers were used to determine the actual temperatures for almost every data point.

There were a total of five germanium resistance thermometers mounted on the apparatus. Two were mounted in the vacuum space near the carbon resistors, and were intended to measure the temperatures of the inside helium vessel (T2) and the outside helium bath (T1). Two others were mounted on the flow tube itself in an attempt to measure the fluid temperature at points near the ends; TIB was mounted 1.5 cm from the inside end and TOB 1.5 cm from the outside end. A fifth thermometer (TB) was laid on the bottom of the helium dewar and also was intended to measure the outside helium temperature. T1 and T2 were inserted into vacuum grease-coated thermometer wells. Their leads were thermally tempered to copper surfaces by 5 cm of 28 gauge copper wire (for thermal contact) and then by 5 cm of 36 gauge manganin wire (for isolation from any residual heat being conducted from room temperature). All leads (36 gauge manganin) then ran 10-20 cm to a second tempering station on the base plate, which accepted the main heat leak, and then up the inside of the support tube to room temperature. TIB and TOB were mounted in similar fashion on a small copper fitting, which was soldered onto the outside of the stainless steel flow tube. The contact area between the fitting and the tube was approximately 0.15 cm x 0.5 C, where C = circumference = 1.6 cm. A typical installation is shown in Fig. 7.

All the (four terminal) germanium resistors were placed in series, with two oil filled standard resistors and a reversing constant current source. A 5 1/2 digit high impedance digital voltmeter was used to measure the dc voltage drop for current in each direction and their average was used to determine the resistance. 1 μA of current was used throughout the experiment, thus power dissipation in each resistor was always less than 10^{-8} W.

One possible source of systematic error in the temperature measurements was discovered to be the placement of the inside heater. It had originally been a resistance wire varnished onto the outside of the copper walls of the inside helium vessel. Later calculations indicated that, at contemplated heating levels, the thermal boundary resistance (Kapitza resistance) might cause a significant temperature difference between the walls and the liquid, thus biasing the inside temperature measurement. This problem was solved by moving the resistance wire to the inside of the vessel, where it was wrapped loosely around the bottom of the inside level gauge.

3.3 Thermometer Calibration and Performance

At least once each day, usually more often, a series of "equilibrium" points were taken. The procedure was as follows: first, the inside heater was shut off entirely, and the motor-controller system (see pressure control section below) altered to maintain the vacuum can position constant relative to the outside level, and then, when the inside had come to equilibrium with the outside, the offset between the level gauges was measured, the thermometer resistances recorded and the vapor pressure of the bath recorded. This was usually repeated for several nearby temperatures. Selected equilibrium data for the entire

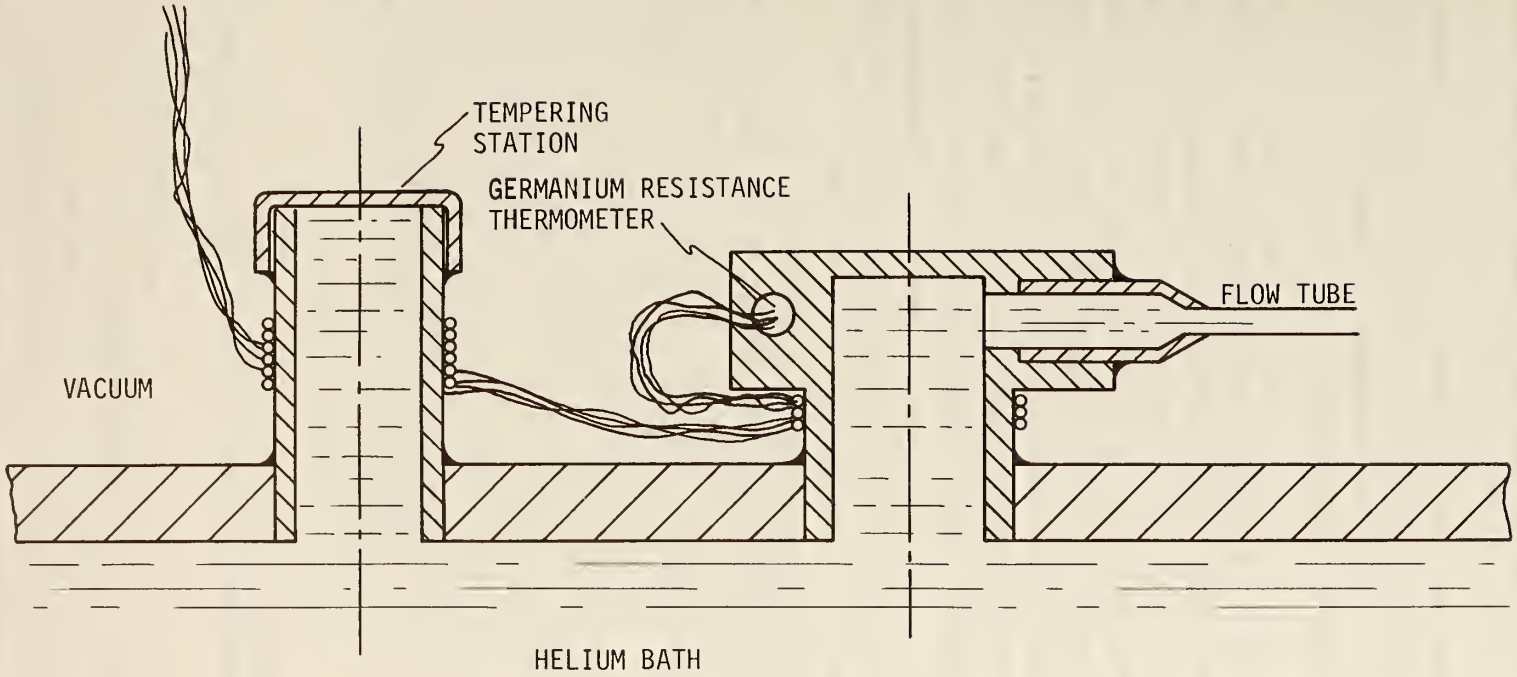

Figure 7. A typical germanium thermometer installation.

long run were combined to determine a single resistance vs. He vapor pressure for each resistor. The T_{58} temperature scale [24] was then used to convert the vapor pressures to temperatures.

The vapor pressure measurement was made by a commercial capacitance manometer with a 0-1000 mm Hg pressure head. Precautions were taken to avoid several known sources of systematic error: refluxing vapor, pumping pressure drops, thermo-acoustic oscillations, and zero shifts in the pressure gauge. The mobile He II film is known to cause refluxing vapor which biases pressure measurements made with capillary tubes connected to vapor bulbs [25] therefore the "bath pressure" was measured. The pressure probe was a 3/16 inch diameter tube (P of Figure 5.) whose open end in the vapor space penetrated 5-10 cm below the bottom of the dewar radiation shield, (R of Figure 5.), thus the mobile film was probably evaporating from the dewar walls below the shield, and at any rate the estimated vapor flux would be too small in this situation to cause a measurable pressure drop. No change was observed due to vertical motion of the probe, as long as its end was below the bottom of the radiation shield. This location for the probe also prevented any bias due to the pressure difference across the radiation shield caused by the steady flow of evaporating vapor. The probe was stuffed with coarse "brass wool" to damp out any thermo-acoustic oscillations that might bias the manometer. It was found that the zero of the manometer drifted 0.2-0.4 mm Hg/day, and was also a function of the absolute pressure (not solely the pressure differential). Therefore the pressure-to-resistance calibration was based on only those equilibrium points which followed a zero-adjustment of the manometer done with both ports of the pressure head pumped to a good vacuum. Most equilibrium points were not taken under this condition, so the pressure recorded on the data sheets is usually subject to some unknown zero-shift error: of course, all these equilibrium points are still useful for consistency checks between the resistors and for checking at a single point by occasional measurements of local atmospheric pressure, which were compared to a mercury barometer; the two always agreed to within one part in 1000. The measurements were all converted to units of mm Hg at 0° C and standard gravity (1 mm Hg = 133.32 Pa). The manufacturer's calibration indicated that the scale remained linear throughout its range to better than 1 part per 1000; it was not attempted to verify this in the pressure range of the vapor pressure measurements.

3.4 Pressure Difference Measurements

The pressure difference between the two ends of the flow tube was determined from the following equation,

$$\Delta P = P_{sv}(T_2) - P_{sv}(T_1) + \rho g(z_2 - z_1) \qquad (21)$$

where, the subscripts 1 and 2 represent the outside and the inside helium vessels respectively P_{sv} is the saturated vapor pressure at the indicated temperature, ρ is the helium density, g is the local acceleration of gravity (= 979.60 cm/s^2), and z is the

liquid level height. The presence of the first term is dictated by the fact that the pressure of the vapor above the liquid is different for the two sides. This effect is quite large at the higher temperatures, where the vapor pressure curve has a large slope, but could be quite accurately measured because of the way that the temperature calibrations were taken (see above). Because the resistances of the thermometers were calibrated against the manometer measuring the vapor pressure, those calibrations give the vapor pressures directly. The resulting difference in vapor pressure should be far more accurate than absolute pressure.

The second term in the pressure difference equation is due to the hydrostatic pressure difference. The liquid level difference was determined from the difference in capacitance of the two matched capacitance level gauges, C_1 and C_2 of Fig. 5.

The capacitors, illustrated in Fig. 8, consisted of two vertical concentric stainless steel tubes and an end cap assembly. Designed as a three terminal capacitor, the inside tube (o.d. = d_1 = 0.6407 ± 0.0003 cm) acted as the "hi" electrode, the outside tube (i.d. = d_2 = 1.733 ± 0.001 cm) acted as the "lo" electrode, and the grounded end caps acted as the guard electrodes for the outer tube. With such a configuration, the capacitance in the end regions is not sensed.

The capacitance per unit length for infinitely long coaxial tubes in a vacuum is given by

$$\frac{C_v}{\ell} = \frac{2\pi\varepsilon_o}{\ln(d_2/d_1)} = \frac{0.5563\ \frac{pF}{cm}}{\ln(d_2/d_1)} \qquad (22)$$

The active length ℓ of the outside tubes was 30.480 and 60.960 cm for the inside and outside capacitors respectively. The dimensions imply a calculated capacitance (at room temperature and in a vacuum) of 17.04 and 34.08 pF, which can be compared to the measured values for these conditions of 17.071 and 34.116 pF, which are higher by 2 and 1 parts per thousand respectively. This is within the estimated error of the measurement of the dimensions, and demonstrates the good match. The values actually used in the subsequent calculations are values derived from the measured low temperature values of C (measured in low pressure He vapor, and corrected to vacuum values), and the values of ℓ given above multiplied by 0.9970 to correct for the thermal contraction.

When a capacitor is partially filled with liquid, its measured capacitance should be

$$C(z) = \frac{C_v}{\ell}\left[\varepsilon z + \varepsilon'(\ell - z)\right] \qquad (23)$$

where z is the liquid level height referred to the bottom of the active section, and ε and ε' are the dielectric constants of the liquid and saturated vapor respectively. If both capacitors have the same value of C_v/ℓ, then their difference will be

$$\Delta C\left(z_2 - z_{1\ell}\right) = \frac{C_v}{\ell}(\varepsilon - \varepsilon')\left(z_2 - z_1\right) + \Delta C(0) \qquad (24)$$

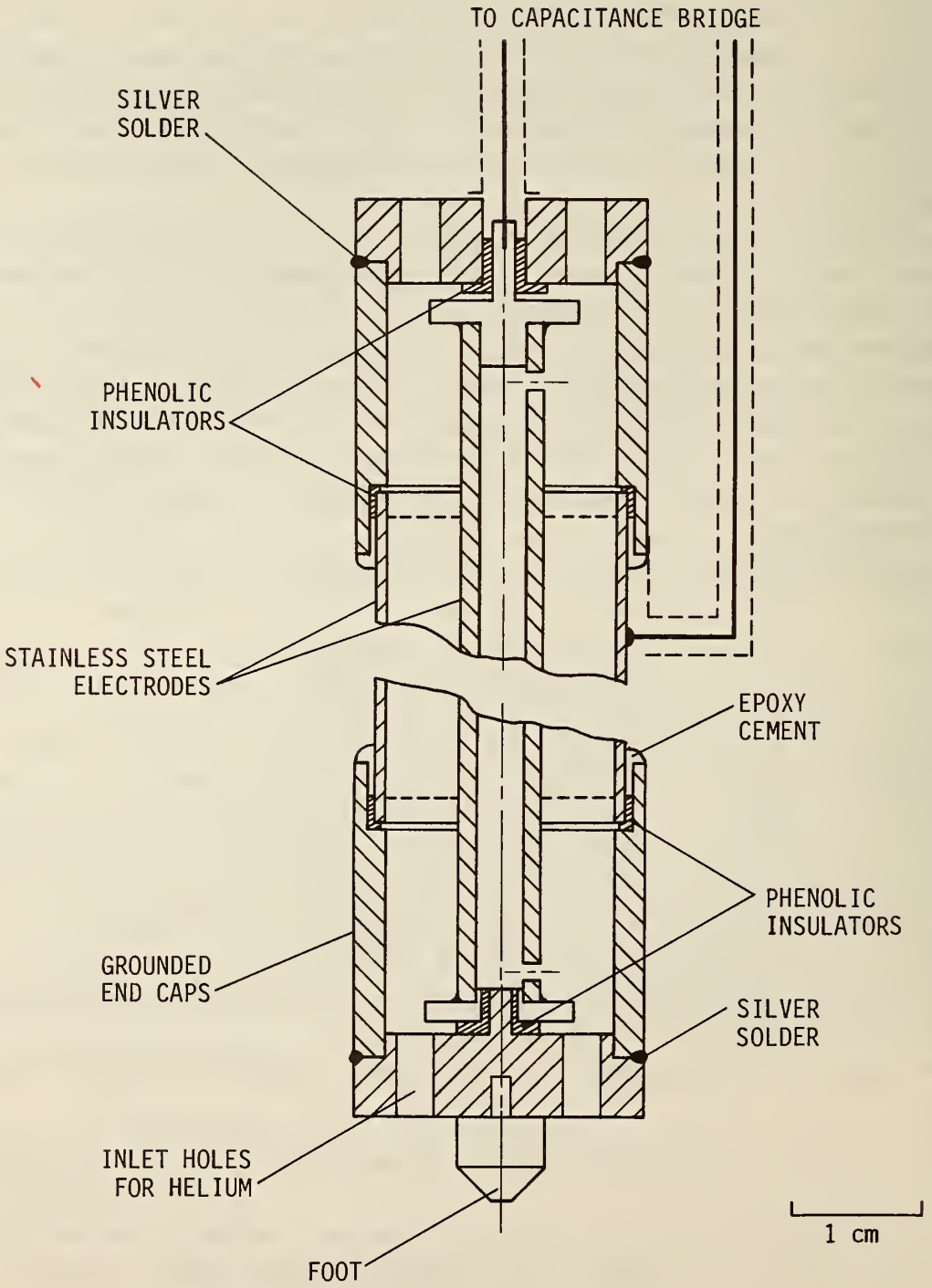

Figure 8. A drawing of the level sensing capacitor.

where z_2 and z_1 are the liquid levels on the inside and outside respectively, referred to some arbitrary point. The difference in the vacuum capacitance, and the (small) vertical offset, are contained in the factor $\Delta C(0)$, which is the capacitance difference measured while the outside and inside are in equilibrium.

The vapor inside the capacitor was assumed to be at the temperature of the liquid. This was obviously true for the inside capacitor, and was assured for the outside capacitor by placing it inside a copper tube whose lower end was immersed in the liquid. Any residual radiation leak to the capacitor could be absorbed by the high conductivity of the superfluid helium film.

The capacitance difference was measured directly by the use of the system shown in Fig. 9, which incorporates the use of a commercial capacitance bridge of the ratio-transformer type. The outside capacitor was connected to the "unknown" ports of the bridge, and the inside capacitor was connected to the "external standard" ports of the bridge. With the appropriate settings, the indicated capacitance at balance is equal to the difference of these two capacitors.

In order to maintain a fixed level difference between the inside and the outside, the desired capacitance difference was set on the bridge, then the corresponding level difference was approximated by manual adjustment of the vertical level of the vacuum can, and then the level control feedback system indicated in Fig. 9 was activated. The signal conditioner produced a signal derived from the error signal and its time integral. This was combined with a large manually controlled offset signal to form the velocity command for the motor-controller system. A digital volt-meter at this point served to monitor the vertical speed of the vacuum can. A gain-of-one amplifier (not shown) was used to float the velocity command voltage so as to meet the input requirement of the motor-controller. When running smoothly, the system was capable of maintaining a set capacitance difference within 30-50 ppm. The main trouble encountered was rough movement in the pulley used to counterbalance the weight of the moving system. It was quite obvious when the system became stuck, and so the data could be retaken.

The configuration of Fig. 9 was altered slightly for the equilibrium data points. First, as mentioned earlier, the inside heater was turned off, then the controls on the bridge changed so that the off-balance signal was determined by the difference of C_0 from a set value, and then the control system was activated. This had the effect of maintaining the outside level fixed relative to the vacuum can. When transients had died away, this allowed measurement of several parameters with the inside and outside at complete equilibrium, i.e., no mass or heat flow, no temperature or pressure difference. As mentioned earlier, the temperatures were recorded as a check on their stability. Also measured was the small downward velocity necessary to maintain a fixed outside level, because this allowed determination of the evaporation rate of the outside He bath. Then the velocity was fixed at this value, and the bridge controls changed back so that $\Delta C(0)$ could be measured.

The dielectric constants were at first computed from the Clausius-Mossotti equation and polarizability found in NBS Technical Note 631 [26], the liquid densities taken from

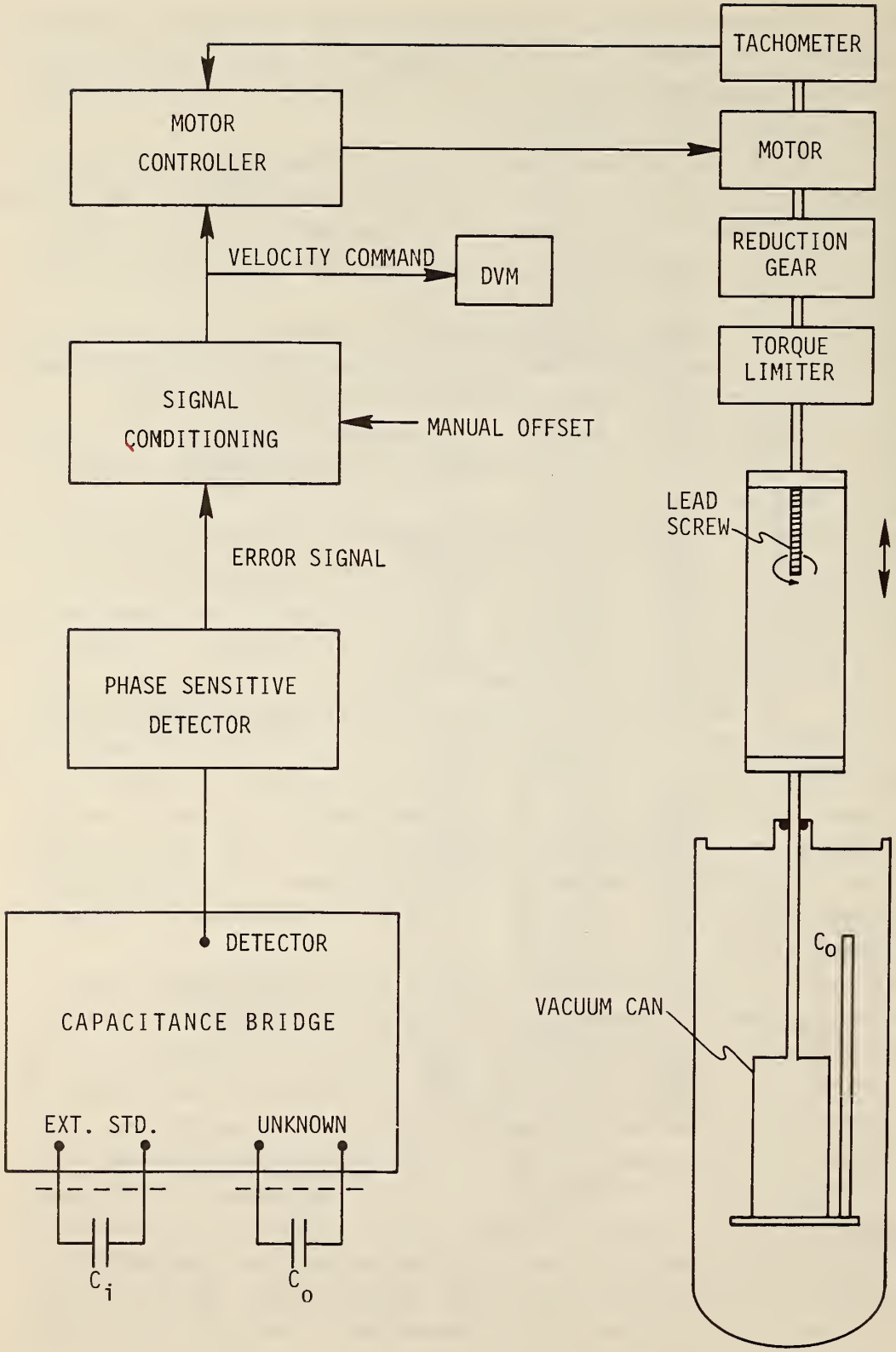

Figure 9. A schematic drawing of the system used to maintain a constant difference between the inside and outside levels.

the text of Donnelly [7], and the vapor densities from the ideal gas equation of state. They could also be derived from full vs. empty measurements, which were found not to agree with the calculations. The reason was found to be inconsistent units in the Clausius-Mossotti equation as found in the above reference, which had the effect of making the polarizability too small by a factor of $4\pi/3M \tilde{=} 1.047$ (M = molecular weight). With this correction, the agreement was excellent between the calculated value of ε at 1.92 K of 1.05736 and the measured value of 1.05740. It was found that while the values of ε and ε' varied significantly with temperature, their difference was constant to within a part per thousand over our temperature range. Therefore, the calculated value of $\varepsilon - \varepsilon' = 0.05714$, appropriate for the highest temperature, where other results depend most sensitively on its value, was used for all temperatures. C_v/ℓ was taken to be 0.5599 pF/cm, the average of the values measured for the two capacitors. Combining all these factors leads to the expression for z_2-z_1 actually used in equation (21),

$$z_2 - z_1 = -31.27 \frac{\text{cm}}{\text{pF}} \left(\Delta C(z_2-z_1) - \Delta C(0)\right) \qquad (25)$$

where $\Delta C(0)$ was slightly different for the different temperatures.

This single simple calibration served for the entire long run, because the capacitors proved to have excellent stability and linearity, as determined by the regular measurement of $\Delta C(0)$. By varying the point at which the outside level was fixed during an equilibrium point, the two capacitors could be compared with each other over a significant fraction of their lengths. It was desirable to keep equilibration times short, so that equilibrium points were taken only where the inside level was still in the narrow section, thus limiting the comparison to the lower 2/3 of the inside capacitor and the lower 1/3 of the outside capacitor. Within this range, $\Delta C(0)$ was found to be essentially independent of height and time. Expressed as a height difference, via equation (25), the standard deviation of $\Delta C(0)$ for all the equilibrium points was 0.01 cm. It is thought that the good stability and linearity of the capacitors is due in part to several design features arrived at by trial and error. They are: (1) a mounting for the inside tube that allows some small axial movement, which prevents compression and bowing of this long slender column, and (2) the rather wide gap, whose proportions appear to be about the optimum compromise between sensitivity to level change and insensitivity to dimensional errors, particularly lack of coaxiality.

A remark should be made about the limitations that the experimental method placed on the pressure difference measurements. They are due to the vapor pressure difference caused by the temperature difference between the inside helium vessel and outside bath [the first term in eq (21)]. If this term was large, then the liquid level difference had to be large and of opposite sign for those flow regimes in which the total pressure difference was small (essentially flows for which V was small). For an extreme example, at T = 1.92 K with $\Delta T = 0.047$ K and V = 0, the inside level z_2 was 25 cm below the outside level, z_1.

3.5 Mass Flow Rate

The volumetric flow rate through the flow tube was determined from the geometry of the apparatus and from the vertical speed of the vacuum can that was necessary to maintain a fixed level difference between the inside and the outside helium spaces.

The functional relation between these quantities was determined by application of the mass conservation relation to the geometry sketched in Fig. 10. The upward velocities of the outside liquid surface, the inside liquid surface, and the vacuum can (all with respect to some fixed point in the laboratory), are designated by V_o, V_i and V_b respectively. The areas of the inside liquid surface, the outside liquid surface, and the dewar are designated as A_i, A_o and A_d.

The small amounts of mass entering or leaving the vapor phase can be ignored, so that mass conservation can be expressed in terms of the liquid volumes as

$$\text{volume added outside} + \text{volume added inside} + \text{volume evaporated} = 0$$

During the small time interval dt, the volume added inside is $(V_i - V_b)A_i dt$. If we designate $V_e (< 0)$ as the velocity of the vacuum can during an equilibrium data point, and assume that the evaporation rate is not time dependent, then the volume evaporated in time dt is $-V_e A_d dt$. (The correct area is A_d and not A_o because the volume displaced by the vacuum can remains constant during the equilibrium point.) The volume added outside has two contributions: the added volume on the surface area of $V_o A_o dt$, and the volume that has been vacated by the movement of the can = $V_b(A_d - A_o)dt$. The result is

$$V_o A_o + V_b(A_d - A_o) + (V_i - V_b)A_i - V_e A_d = 0 \qquad (26)$$

But under the conditions of the experiment, the level difference between the inside and the outside remains constant, therefore

$$V_i = V_o \qquad (27)$$

The average velocity of net fluid flow through the flow tube (V) is expressed as

$$V = (V_i - V_b)A_i/A_x \qquad (28)$$

where A_x is the cross-sectional area of the tube. Combining the above equations gives

$$V = -\frac{A_i}{A_x}\frac{A_d}{A_o + A_i}(V_b - V_e) \qquad (29)$$

As defined, V is positive for flow toward the inside.

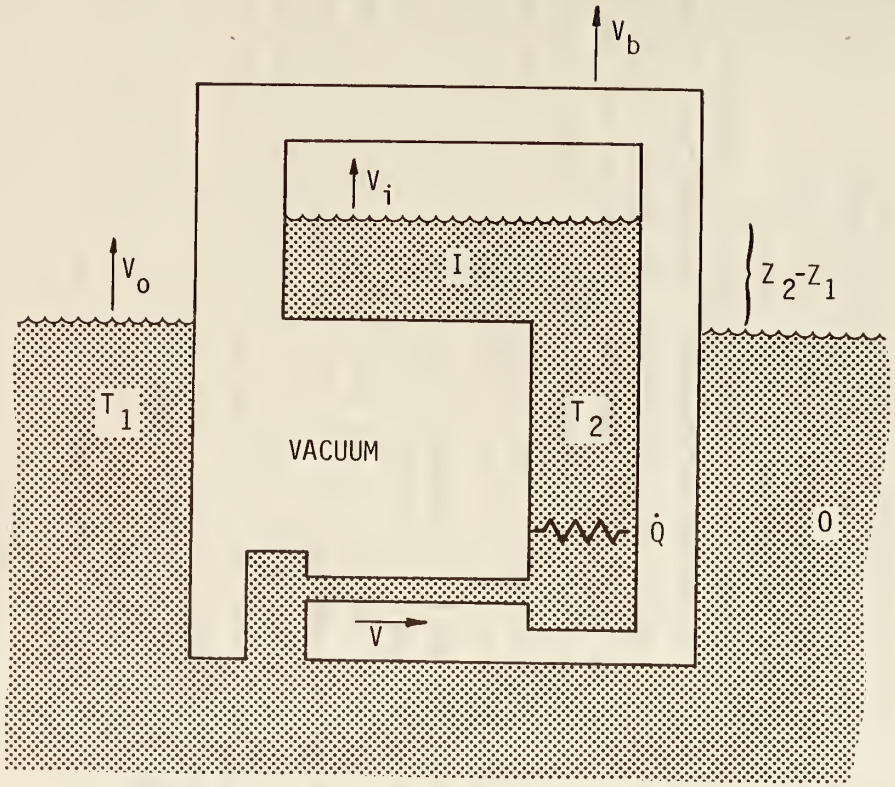

Figure 10. A schematic diagram of the main variables of the experiment.

In order to cover a wider range in flow rates, the inside helium space was constructed with a wide cross-section for the top one-third of the inside capacitor, and a narrow cross-section for the bottom two-thirds. In order to allow large level differences for inflow it was often necessary to have the outside level well above the top of the wide section of the inside space, hence well above the top of the vacuum can. In all then, there were four different combinations of inside and outside surface areas for which data could be taken; the parameters, and the "mode" identification numbers used on the data sheets, are listed in Table 1.

3.6 The Flow Tube

The flow tube used in this experiment was a commercial quality stainless steel tube with an o.d. = 0.160 cm, and an i.d. determined to be 0.1149 ± 0.0006 cm. It had a length (L) of 60 cm and was wound in two turns of 10 cm diameter. The inside end was mounted about 3.5 cm above the outside end. The ends were cut off square.

The inside diameter was determined by room temperature gas flow measurements performed after the experiment, but while the tube was undisturbed in its mounting on the apparatus. The results seemed inconsistent until it was realized that, in laminar flow, even the rather small curvature of the tube could have large effects on the gas flow. Helium gas and nitrogen gas were used to cover a range in Reynolds' number (Re) from 55 to 1930. The volumetric flow rate of gas was measured by a wet test meter whose calibration against a bell prover had a standard deviation of 0.6%. The pressure drop (ΔP) across the flow tube was measured by the commercial capacitance manometer used in the experiment. The volumetric flow rate was multiplied by the factor $(1 - P_s/P_o)$ to correct for the water vapor added by the wet test meter (where P_o is the ambient pressure, and P_s is the vapor pressure of water at the ambient temperature). The ideal gas equation of state was used, the temperature taken to be ambient, and the density of the gas taken to be the mean of the values calculated for the ends of the tube. The fractional pressure drop never exceeded 0.18. Thus we obtain the equivalent volumetric flow rate Ω of dry gas.

The data were analyzed by using the laminar flow equation for a straight tube applied to the lowest Re data to deduce a diameter D. This was then used to calculate the (Fanning) friction factor f as a function of Re. The equations used were

$$f = \frac{\pi^2}{32}\frac{D^5}{\Omega^2}\frac{\Delta P}{L}\left(1 + \frac{\Delta P}{2P_o}\right) \tag{30}$$

$$Re = \frac{4P_o\Omega}{\pi D\eta}$$

where P_o is the mass density of dry gas at ambient temperature and pressure. The viscosity η was taken from [26] and [27]. We have plotted in Fig. 11 the experimental friction factor divided by the expected values for a straight tube in laminar flow; the solid line

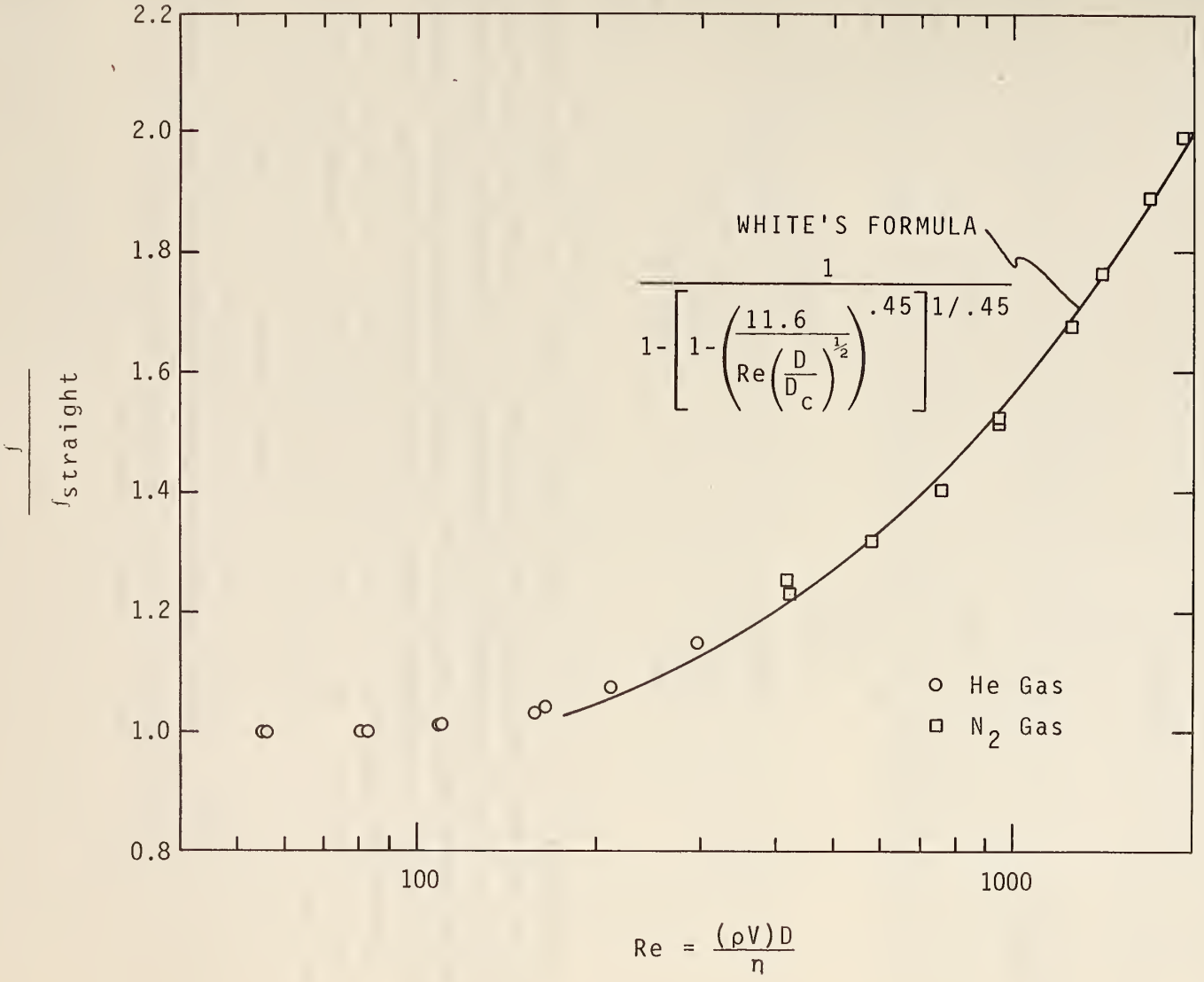

Figure 11. The results of the room temperature gas flow measurements on the flow tube.

Table 1.

	Mode Number	Inside Interface Location: Narrow	Wide
Outside Interface Location	Vacuum Can	1	3
	Support Tube	2	4

A_i (narrow)	=	4.96 cm^2
A_i (wide)	=	78.4 cm^2
A_o (VC)	=	A_{dewar} - 105.2 cm^2
A_o (ST)	=	A_{dewar} - 2.8 cm^2
A_{dewar}	=	219.4 cm^2

is the formula of White [28] for curved tubes calculated for our diameter of curvature D_c. The good agreement makes us confident that the correct value of the diameter has been found. The principle uncertainty in its measurement is the uncertainty in the volumetric flow measurement and its corrections. The deviations from the calculated values over the entire range of the measurement indicate a standard deviation for D of about 0.5%.

Precautions were taken to prevent or reduce any effects on the flow due to the presence of frozen air. The first was the protected location of the outside end of the flow tube; it was in a chamber which was recessed about one inch into the bottom of the base plate (see Fig. 7.). Such a location appears inaccessible to condensing air or falling air particles. Of course, only helium gas was allowed to be present in the dewar during the cooldown. Another precaution was the addition of a filter (which used ordinary chemical filter paper) onto the transfer line used to fill the helium dewar, in an effort to reduce buildup of frozen air during the long run.

The only problem which could not be definitely eliminated was a cumulative buildup of those particles small enough to remain in suspension in the liquid helium; they might be expected to accumulate from air introduced during the insertion of the transfer tube, etc. There was no way to measure their concentration, nor are we aware of any data on the sizes of particles that might be expected to remain in suspension. However, the lack of any significant cumulative shifts in data points that were repeated during the 35-day run, we take to be good evidence that suspended solic particles were not a significant problem. See, for example, the good reproducibility (~ 1%) of the $T = 1.39$, $\Delta T = 0.019$ data taken at the very beginning and end of the long run (e.g., data points 9 422 and 10 515).

That evidence is reinforced by a mishap that took place early on October 1. A technician working nearby accidentally knocked off a large rubber vacuum hose used to pump on the helium dewar. At the time, the liquic helium was probably warm enough to be at a vapor pressure above atmospheric pressure, but still, in the 30-60 seconds it took him to replace the hose, we would guess that more air should have been introduced than during all the previous activities. Again, no significant changes in the repeated data can be seen following that date.

3.7 The Energy Flow Measurement

The inside helium vessel and the flow tube were surrounded by an insulating vacuum. Thus the energy flow through the tube could be determined from an energy balance calculation. The essential elements of the situation are shown in Fig. 10. The unusual feature of this calculation turns out to be the large influence of the vapor that is present.

The energy balance is done in two parts; first we calculate the change in total energy of the helium in the inside vessel (the control volume) from thermodynamics applied to a small change in its mass. The conditions of the change are that the temperature, and hence the vapor pressure, remain fixed and that the total volume is fixed, even though the total mass is changing. Designating the specific volumes of the liquid and vapor as v and v' (not to be confused with the velocities v_n, v_s, V), and the specific internal energies as u and u', we find that the increases of total mass M, of total volume, and of total energy U are given by

$$dM = dm + dm'$$

$$d(\mathrm{Vol})\Big|_{T,P} = v\, dm + v'\, dm' = 0$$

$$dU\Big|_{T,P,\mathrm{Vol}} = u\, dm + u'\, dm' \qquad (31)$$

where dm and dm' are the increases in the liquid and vapor masses. Combining these equations gives

$$dU\Big|_{T,P,\mathrm{Vol}} = \frac{v'u - vu'}{v' - v}\, dM \qquad (32)$$

We can use the definition of the chemical potential, eq (16), and the well known fact that the chemical potentials of the liquid and vapor are equal in equilibrium, to find that

$$u' = u - P(v' - v) + T(s' - s) \tag{33}$$

Substituting into the previous equation and using the Clausius-Clapeyron equation for the slope of the vapor pressure curve $\left(\frac{\partial P}{\partial T}\right)_{svp}$ and the definition of dM in terms of the tube cross-section and the average velocity

$$dM = \rho V A_x dt \tag{34}$$

we find

$$dU\Big|_{T,P,Vol} = [\rho Vh - VT\left(\frac{\partial P}{\partial T}\right)_{svp}]A_x dt \tag{35}$$

In the second part of the energy balance calculation we express dU in terms of the external sources of energy, i.e., in terms of the energy that flows through the boundaries of the control volume. They are the heating rate $\dot{Q}$ of the internal heater and the energy flux $j_u A_x dt$ that enters through the flow tube. As discussed in section 2, this energy flux can be expressed in terms of the enthalpy flux and the heat current $\dot{q}$, using equations (18b) and (19). Equating this to the previous equation gives

$$\dot{Q} + (\rho Vh + \dot{q})_{ent} A_x = [\rho Vh_2 - VT_2\left(\frac{\partial P}{\partial T}\right)_{svp,T2}]A_x \tag{36}$$

The energy flux on the left hand side is to be evaluated at the entrance of the flow tube to the inside helium vessel. The energy change on the right hand side is to be evaluated at the temperature and pressure that prevail within the inside vessel, whose values are indicated by the subscript 2. Let us define the heat flux density $\dot{q}_2$ by

$$\dot{q}_2 = -\frac{\dot{Q}}{A_x} - VT_2\left(\frac{\partial P}{\partial T}\right)_{svp,T_2} \tag{37}$$

If the temperature and pressure are essentially continuous at the entrance, which we expect to be true in most cases, we have $h_{ent} = h_2$, and so $\dot{q}_{ent} = \dot{q}_2$. In any case, by application of eq. (20), we can find $\dot{q}(x)$ at some location x, if we know $\dot{q}_2$ and the temperature and pressure at x. For our case the relation is

$$\dot{q}(x) = \dot{q}_2 + \rho V\left(h_2 - h(x)\right) \tag{38}$$

We shall quote all our results for the energy transport as values of $\dot{q}_2$. As defined, the

sign convention of $\dot{q}_2$ is consistent with the one for V [eq. (29)], so that heat flow away from the (higher temperature) inside vessel has a negative sign.

The second term of eq (37) is readily interpreted as the heat of condensation (or evaporation) that must be absorbed by the liquid in order to change the volume of vapor. Its presence is due to the particular configuration used to perform the experiment. At the higher temperatures of this experiment, it becomes nearly as large as $\dot{Q}/A_x$ for the larger values of V, and thus its presence causes a significant deterioration in the measurement accuracy of $\dot{q}_2$. It is the quantity $\dot{q}_2$ that is most significant (not $\dot{Q}/A_x$) because it is the quantity to be compared to the $\dot{Q}/A_x$ of section 2.

This heat of condensation also introduced an extra limitation in the range of velocities for which data could be taken. For fixed ΔT, it was often found that for inflow ($V > 0$), when this term acts like an extra heat source, that its magnitude increased more rapidly with V than the heat conducted out ($\dot{q}_2$). Therefore, it was not possible for eq (37) to be satisfied with positive values of $\dot{Q}$ if V was greater than some particular value. When encountered, this limiting value of V is indicated on the graphs of $\dot{q}_2$ vs. V (figs. 22-25) by a vertical bar.

We have neglected the kinetic energy terms in the total energy balance because they can be shown to be quite small for all the conditions encountered in this experiment. We have also left out gravitational potential energy terms, because a careful accounting of them found that they just cancelled the work done on the fluid by the movement of the container. In Appendix 2, we rederive eq (36) with a full accounting of potential energy terms and the work done on the fluid in raising or lowering the vessel.

3.8 Extraneous Heat Flows

The energy balance equations that have been given for determining the heat flow are correct only if we have accounted for all the energy exchanges, i.e., only if there are no extraneous heat flows between the inside and the outside helium vessels. Below are explained the precautions taken and the tests made to ensure that these extraneous heat flows were small.

The poor thermal conductivity of the stainless steel walls of the vacuum can dictated that it be surrounded by a heat shield, HS of Fig. 5. This took the form of a thin (0.04 cm) copper sheet fitted to surround the sides and top of the vacuum can. Its lower end was always immersed in the liquid, and its upper end was soldered to the support tube $\sim$ 10 cm above the top of the vacuum can, thus intercepting the heat conducted down the support tube. On the inside of the support tube, the lower 10 cm was stuffed with coarse brass wool to act as a radiation shield.

The inside helium space was supported by three long, thin-wall stainless steel legs that attached to the bottom (or base plate) of the vacuum can. The rather close fit suggested the precaution of mounting three sharpened nylon screws on the legs just below the wide section of the inside space; they could be extended so as to maintain a fixed spacing between the inside space and the vacuum can. All electrical leads that went to the inside

space were first thermally "tempered" to the base-plate and were of low thermal conductivity wire.

It was not practical to maintain a good vacuum at all times in the vacuum space, because this prevented the inside helium space from ever cooling down enough to fill with liquid. Therefore the inside space was filled before cool-down with hydrogen gas at a pressure of a few Torr.* This acted as a thermal exchange gas, as long as the vacuum can remained above ∿ 10 K. Once the vacuum can was cooled below ∿ 3 K, the hydrogen gas was frozen to the walls or adsorbed onto about 3 cm^3 of "molecular sieve" that was present. After the first transfer was completed and the vacuum gauge outgassed, the seals were checked by monitoring the vacuum space for several hours with a He leak detector; it was checked again several days later. The vacuum was monitored throughout the long run by a Phillips-type vacuum gauge mounted on the top of the support tube. It registered 2-5 x 10^{-5} Torr during data taking, except for jumps of an order of magnitude (which lasted 1-2 minutes) that were caused by the sudden withdrawals of a good fraction of the vacuum can from the liquid; this was almost certainly due to slight desorption of hydrogen from the suddenly warmer walls.

The thermal isolation was checked directly at the beginning of the run by measuring the total thermal conductance between the inside and the outside at temperatures above the lambda point. This was done by maintaining a fixed outside temperature T_2 = 2.31 K, providing a small heat input with the inside heater, and waiting 1-2 hours for the temperature to equilibrate at a value 0.5-1.5 K higher than the outside temperature. The vacuum can was completely immersed for these measurements, but the higher temperature of the inside prevented liquid from entering. (It was found that this type of test can be very misleading if there exist any pockets on the inside that can trap liquid; the relatively large latent heat of the liquid that is being evaporated on the inside and condensed on the outside can cause a large and long-lived false conductivity).

Assuming that the thermal conductance linking the inside and the outside is temperature independent, the three data points that were taken yielded a value for the thermal conductance of 1.5 x 10^{-3} W/K. This value is about 1 1/2 orders of magnitude larger than was calculated for conduction through the legs, electrical leads, etc. It was found that conduction through the low pressure hydrogen gas could account for the conductance, if the indicated pressures at the Phillips gauge were taken at face value. Still, this value for the conductance was low enough so that we could choose to ignore the unexpected persistence of unchanged indicated pressures (2 - 5 x 10^{-5} Torr) at the lower temperatures, where the calculated vapor pressure of hydrogen should be considerably smaller.

These same measurements indicated that a heat input of 2 x 10^{-4} W remained at $\Delta T = 0$. This could represent a real heat leak (e.g., incomplete radiation shielding), or it could reflect a small temperature dependence in the thermal conductivity. This heat leak, if real, would require that all values of $\dot{q}_2$ be corrected by the addition of -0.019 W/cm^2. Since data could not be taken at low enough ΔT's to distinguish between the two alternatives, we have not made this correction to the data, and instead view this as an upper limit to the possible systematic error in $\dot{q}_2$.

*1.0 Torr - 133.3 Pa.

3.9 Error Estimates

The errors of this data are not always as small, nor as accurately known, as might be wished, primarily because of the exploratory nature of the experiment. The method was new, the results could be only crudely anticipated, and it seemed more desirable to emphasize a broad range for the measurements rather than concentrate on their accuracy. Given these conditions, they seem satisfactory. The errors for quantities given in Appendix 1 vary, depending on the conditions, and are summarized in Table 2.

A part of the random error in the temperature and pressure difference measurements could be evaluated quite reliably from the variation of the equilibrium point data. This variation should include the effect of electronic noise, intrinsic sensor resolution, drift in the sensor characteristics, and inaccuracies in the data reduction. Including all the equilibrium point data, we find that the temperature difference had a standard deviation of (4, 3, 2, and 4) x 10^{-5} K at the four temperatures of 2.10, 1.92, 1.65 and 1.39 K respectively. The standard deviations for the height difference were 0.016, 0.012, 0.009 and 0.011 cm respectively. Through eq (21), these figures imply a standard deviation for the pressure difference of 0.4, 0.2, 0.1 and 0.1 Pa respectively.

For the regular data points there may exist an extra source of random error that is not included in the figures given above; it is the fluctuations that might be introduced by the control systems that are used to maintain a "constant" temperature and pressure difference. The short term fluctuations in the altitude and temperature differences (time constants of a few seconds) were judged by the error signals of the feedback systems to be rarely more than 0.02 cm and 0.0001 K. However, because it is the time-average values that count, it is the longer term fluctuations (the drift during the 3-5 minutes it took to record the data) that determine the real error. For the altitude difference, we estimate that this source of error was negligible. Unfortunately, the temperature sensors of the control system (but not the temperature measuring system) were found to drift. On bad days, these drifts caused progressive shifts in the measured ΔT of 2-3% over the course of the day. In the worst cases, the rate of drift suggests that ΔT should change by an amount somewhat less than the errors given above. Somewhat arbitrarily then, we increase the error estimates of ΔT by 50%. Our final estimate of the random error (one standard deviation) in ΔT is (6, 4, 3 and 6) x 10^{-5} K, and in ΔP is 0.6, 0.3, 0.2 and 0.1 Pa, respectively, for the four mean temperatures.

The systematic error in temperature difference is determined by the systematic error in the pressure measurement during calibration as discussed below. This leads to a systematic error in temperature difference of between 0.5% and 0.7%.

The pressure difference is subject to systematic error, due to uncertainties in the capacitance-to-altitude conversion. Estimated at 2 parts per thousand, it implies a possible systematic error of $\sim 2.8 \times 10^{-2} \times (z_2 - z_1)$Pa, where z is expressed in centimeters. This error becomes significant only for the large ΔT, small V, data at the higher temperatures.

The errors in the mean temperature are determined by the errors in the vapor pressure measurements used to calibrate the thermometers. We could evaluate the random errors in

Table 2. Estimated Errors

Measured Quantity (Units)	Temperature			
	2.100	1.919	1.650	1.395
Random Error (1σ)				
T (K)	0.2 mK	0.2 mK	0.3 mK	0.4 mK
Systematic Error	1.1 mK	1.1 mK	1.1 mK	0.8 mK
ΔT (K)	0.06 mK	0.04 mK	0.03 mK	0.06 mK
	0.005 ΔT	0.006 ΔT	0.006 ΔT	0.007 ΔT
Δz (cm)	0.01 cm	0.01 cm	0.01 cm	0.01 cm
	0.002 Δz (cm)	0.002 Δz	0.002 Δz	0.002 Δz
ΔP (Pa)	0.6 Pa	0.3 Pa	0.2 Pa	0.1 Pa
	0.03 Δz (cm)	0.03 Δz	0.03 Δz	0.03 Δz
V (cm/s)	0.02 V	0.02 V	0.02 V	0.02 V
	0.02 V	0.02 V	0.02 V	0.02 V
$\dot{q}_2$ (W/cm^2)	$0.01(\dot{q}_2+0.047$ V)	$0.01(\dot{q}_2+0.030$ V)	$0.01(\dot{q}_2+0.013$ V)	$0.01(\dot{q}_2+0.004$ V)
	$0.01(\dot{q}_2+0.047$ V)	$0.01(\dot{q}_2+0.030$ V)	$0.01(\dot{q}_2+0.013$ V)	$0.01(\dot{q}_2+0.004$ V)

the calibrations at 1.92 and 1.39 K, from the standard deviations for data taken on several different occasions; they were 0.2 and 0.4 mK respectively. A few simple tests indicated that systematic errors due to placement of the pressure probe could not be too much larger than this. The absolute calibration of the pressure gauge could not be confirmed in the region of interest; if we take the manufacturer's estimate and increase it by a factor of three, we arrive at a systematic error in pressure of about 0.3%. This implies a systematic error of about 1 mK in mean temperature on the T_{58} scale.

The random error in V is determined from the standard deviation in the voltage-to-speed conversion (1.5%), the estimated accuracy to which the voltage fluctuations could be averaged by eye, (1%), and the non-uniformity in the geometry (1%). Combined in quadrature, this gives a random error of 2%. An estimate of the error in geometry suggests that each mode might have a systematic error as large as 2% of V.

The relative error in $\dot{q}_2$ (both random and systematic) depended rather strongly on the conditions of the measurement, because of the sometimes large value for the vapor's latent heat correction (second term of eq (37)). Assuming an error in V of 2%, we find that the error in $\dot{q}_2$ is given by αV (V in cm/s), where α has the values of (4.8, 3.0, 1.3 and 0.4) $\times 10^{-4}$ W/cm^2 for the temperatures of 2.10, 1.92, 1.65 and 1.39 K respectively. At the most extreme value of V (70 cm/s), this corresponds to errors of 0.033, 0.020, 0.009 and 0.003 W/cm^2. When V is small, and $\dot{q}_2$ is large, this error is not too significant, and we must include the estimated random and systematic errors of the first term in eq (37) of 1% and 1% respectively.

4. RESULTS AND DISCUSSION

Data were collected at four values of the mean of the outside and the inside temperature. Using the formulas given in section 3, each data point was reduced to give values for the actual pressure and temperature differences between the ends of the flow tube and the resulting steady state values for the net fluid velocity V and the heat flux density $\dot{q}_2$. These results are presented in tabular form in Appendix 1, along with some other data and derived quantities of interest.

4.1 The Net Fluid Velocity

Nearly all the results for the net fluid velocity V (the actual mass flow rate divided by the total density and the flow tube cross-sectional area) are shown in Figs. 12-15. The absolute values of V have been graphed there as a function of the absolute value of the pressure difference, so that data for both directions of flow are superimposed. The value of the nominal temperature difference is indicated by the symbols; the measured temperature differences may differ from the nominal by as much as 3%, due to the drifts discussed earlier.

More than half of the results might be summarized in a very simple statement: they are largely indistinguishable from those of an ordinary fluid in fully developed turbulent flow. This statement applies for those flows at the larger velocities or Reynolds numbers, which are the ones most likely to be of interest for applications.

These graphs of $|\Delta P|$ vs $|V|$ reveal quite distinctly one of the important results of this experiment: V depends primarily on ΔP -- its dependence on ΔT is significant only at the lower velocities. This result is only to be expected for an ordinary (single-phase) fluid, because the temperature gradient does not appear in the equation of motion of the fluid (we are excluding indirect effects due to buoyancy forces). In contrast, the temperature gradient appears explicitly in the (simple) superfluid equation of motion, eq (6), as part of the chemical potential gradient. Even though that simple equation for v_s is not expected to remain valid for our conditions, it suggests the possibility that v_s might be a function mainly of $\Delta\mu$; this would make V also a function of $\Delta\mu$, at least if ρ_s/ρ is not too small. This possibility is completely excluded (for our conditions) by the weak dependence of V on ΔT. To make a numerical comparison, we can use the expression

$$\rho\Delta\mu = \Delta P - \rho s\Delta T$$

which we have included in the data listing in Appendix 1. We find that under most conditions, the temperature difference dominates the chemical potential difference, and that neither one has much influence on the net mass flow. As a typical example, we can examine the data for T = 1.92, ΔT = 0.019; not until ΔP is about 50 times smaller than $\rho s\Delta T$ ($\sim$ 2150 Pa) do we see much effect of the latter on V.

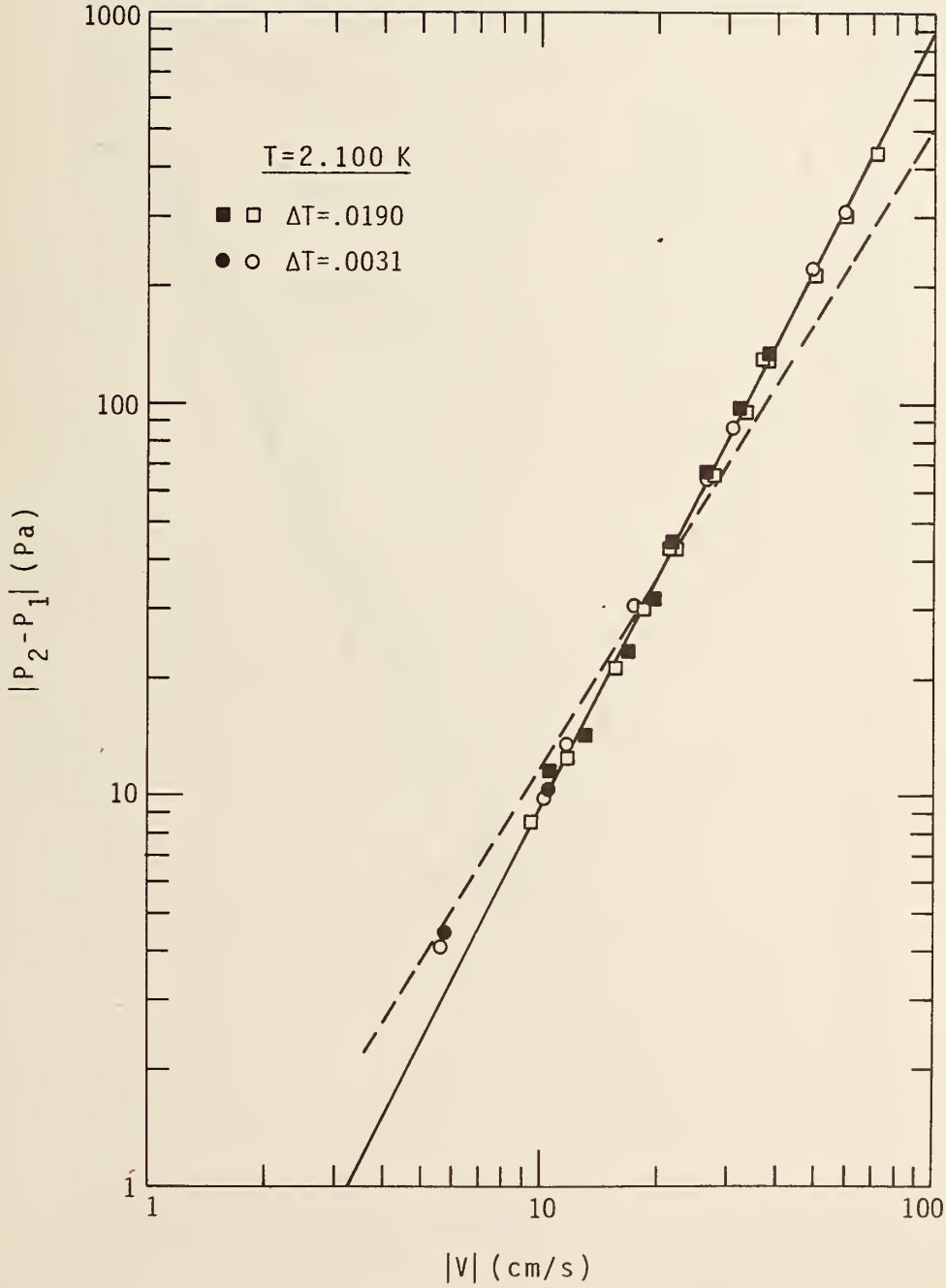

Figure 12. The pressure difference vs the net fluid velocity at 2.100 K. The dashed [solid] line is eq (41) [(42)].

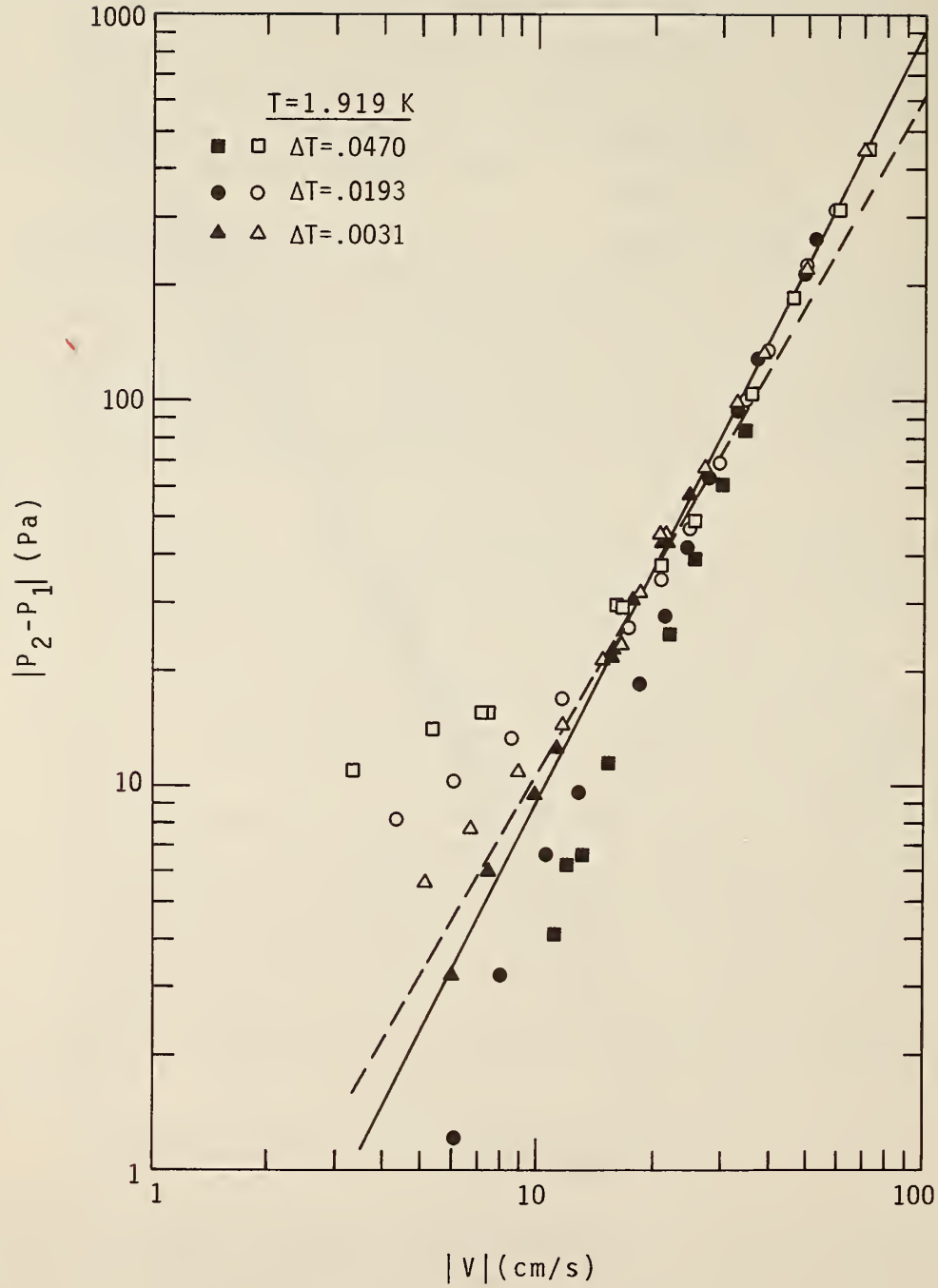

Figure 13. The pressure difference vs the net fluid velocity at 1.919 K. The dashed [solid] line is eq (41) [(42)].

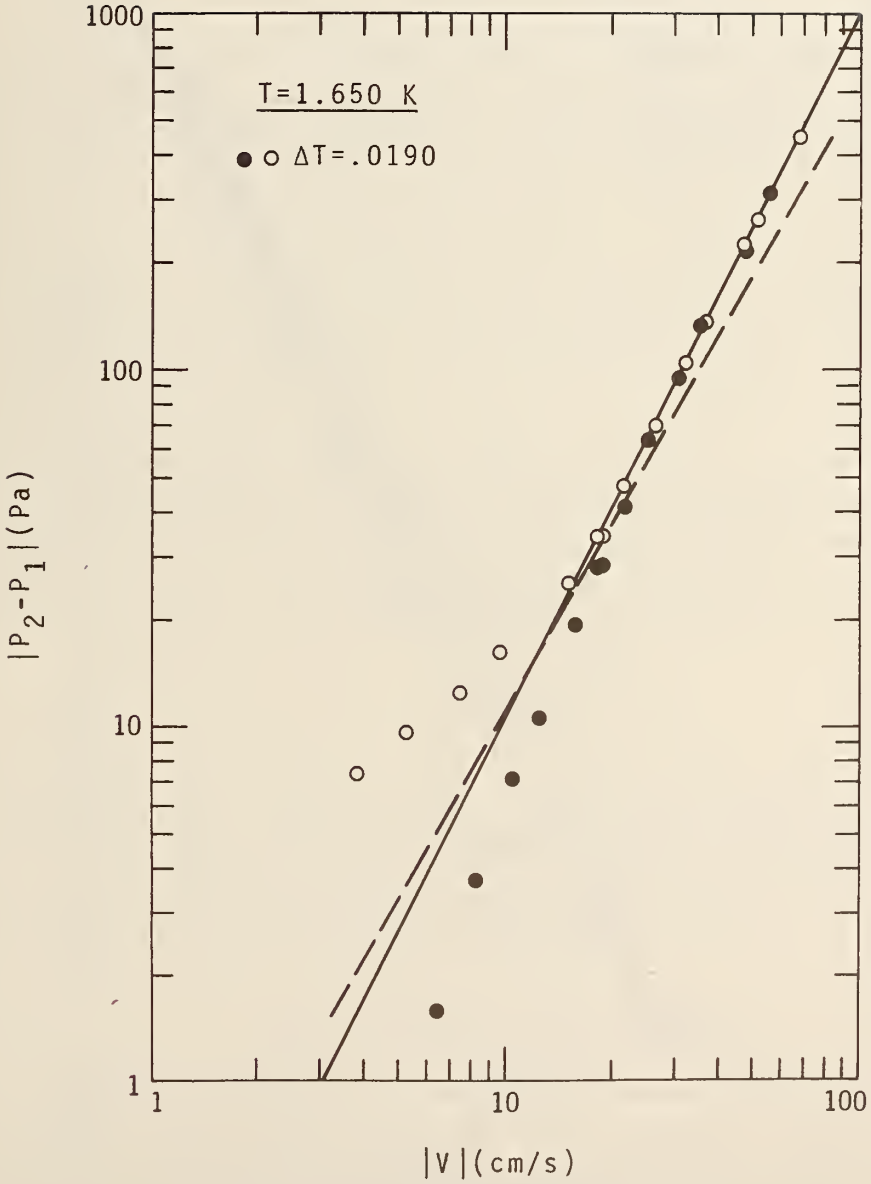

Figure 14. The pressure difference vs the net fluid velocity at 1.650 K. The dashed [solid] line is eq (41) [(42)].

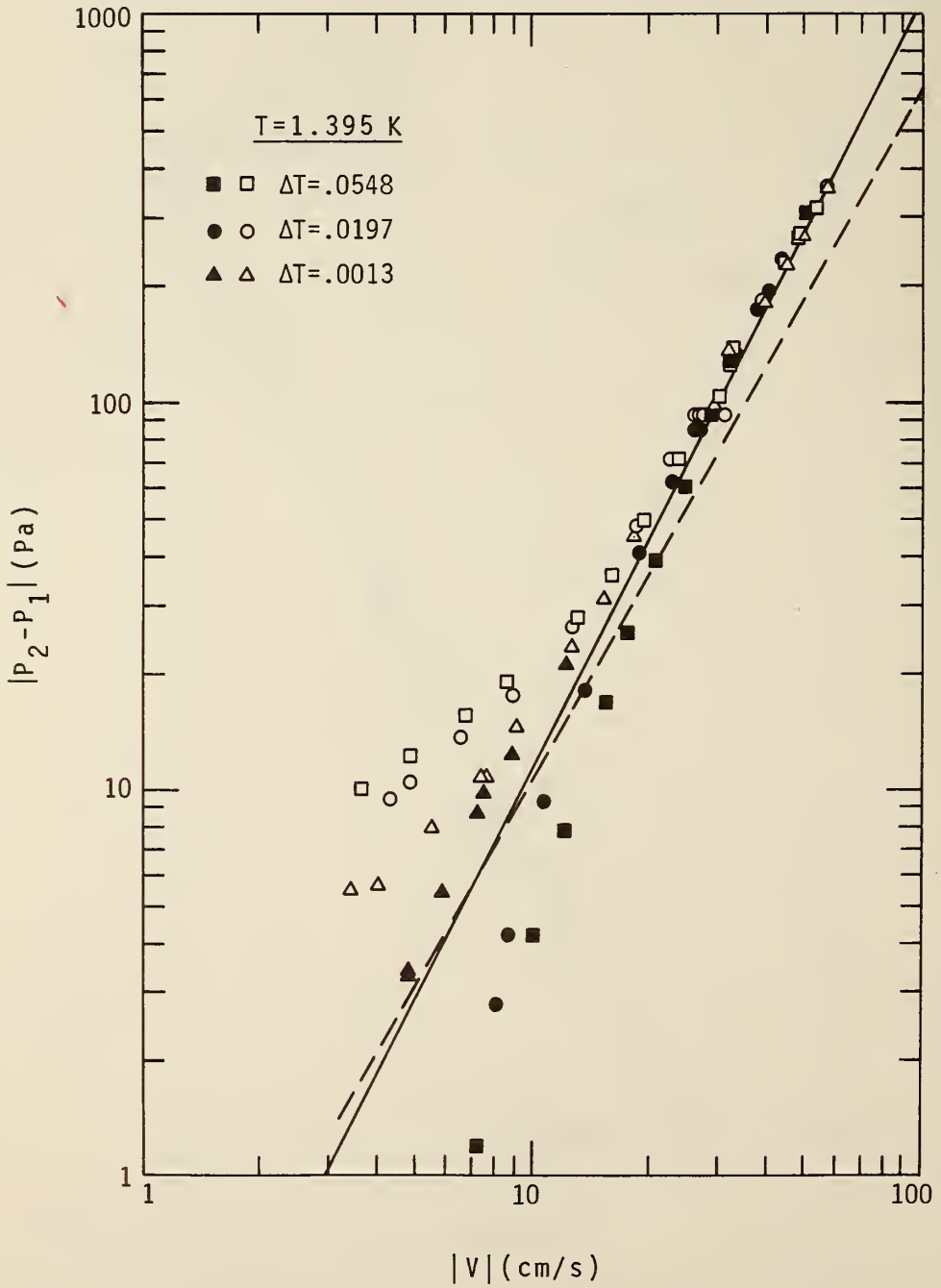

Figure 15. The pressure difference vs the net fluid velocity at 1.395 K. The dashed [solid] line is eq (41) [(42)].

A related, but not equivalent, observation is that neither v_s nor v_n becomes solely a function of ΔP in this same limit. This comparison is not quite as clear-cut as for V vs ΔP, because v_s and v_n (unlike V) can vary significantly along the flow tube, as can be seen from the expressions obtained from eqs (1, 2, and 19).

$$v_n = V + \frac{\dot{q}}{\rho s T} \qquad v_s = V - \frac{\rho_n}{\rho_s}\frac{\dot{q}}{\rho s T} \tag{39}$$

The variation of both $\dot{q}$ and T can cause substantial changes in v_n and v_s. Nevertheless, the average of the velocities at the ends of the flow tube, plotted against the overall pressure difference, ought to give a good indication of whether or not the local value of velocity is solely a function of ΔP. Such plots of the two worst cases of correlation between v_n or v_s and P are shown in Fig. 16 and 17. The data for a particular ΔT fall on two lines, whose difference is correlated with the sign of ΔT (relative to ΔP). These worst cases are also the cases where v_n and v_s differ the most from V. In those cases where there is a good correlation of v_n or v_s with ΔP (e.g., v_n at T = 2.10, v_s at T = 1.39, or all the small ΔT data) then it is also true that these velocities do not differ significantly from V.

The final major observation to make is that the numerical results for V vs P are largely indistinguishable from what we would expect for an ordinary fluid at these velocities. For an ordinary fluid, the flow is known to be turbulent for Reynolds numbers greater than $2 - 4 \times 10^3$. The most reasonable choice (but not the only one!) of a counterpart for He II might be the "total" Reynolds number, defined by

$$Re = \frac{\rho V D}{\eta_n} \tag{40}$$

For all our conditions, this is equal (to within 15%) to 1.15×10^3 V, for V expressed in cm/s. Then the range in velocities that we could cover corresponded to a range in Re of $5 - 85 \times 10^3$, all apparently above the threshold for classical turbulent flow. If the inside surface of the flow tube were smooth enough, we know that the pressure drop for an ordinary fluid should be given by the "Blasius Formula"

$$\Delta P_B = 0.079\ Re^{-(1/4)}\ \frac{4L}{D}\ [(1/2)\rho V^2] \tag{41}$$

This formula is shown on each of the graphs (Figures 12-15) as a dashed line. We see that the main trend of the data is reproduced. In the high velocity region, the formula underestimates the pressure drop, but for an ordinary fluid, a rather modest surface roughness would be capable of making up the difference. We have no data on the surface roughness of our flow tube, so that we are not able to determine if this accounts quantitatively for the difference.

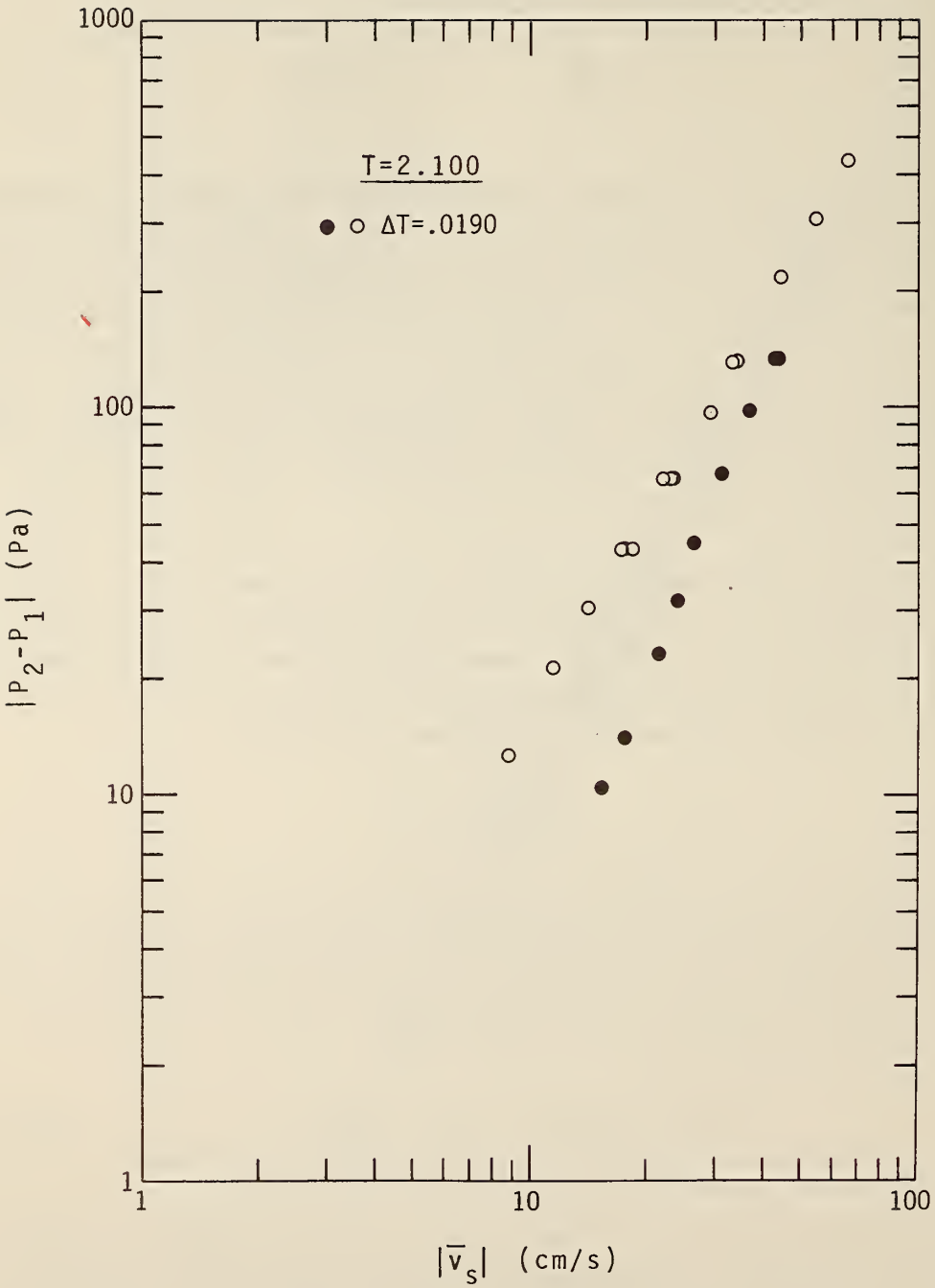

Figure 16. The pressure difference vs the average superfluid velocity at 2.100 K. Cf. Fig. 12.

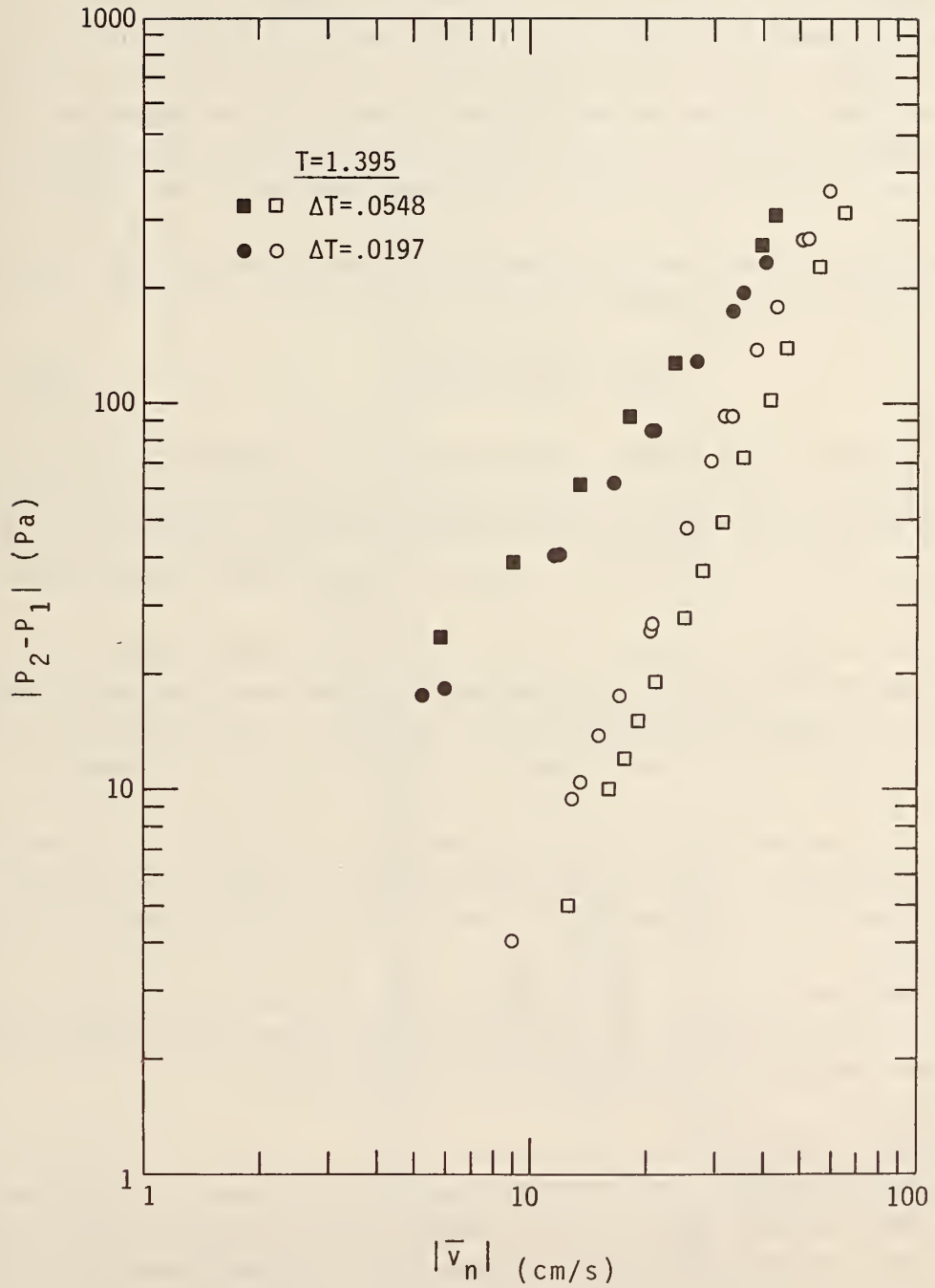

Figure 17. The pressure difference vs the average normal fluid velocity at 1.395 K. Cf. Fig. 15.

This result is very appealing, because it suggests that the two-fluid dynamics reduces to ordinary fluid dynamics in some limiting cases. It suggests, even if only further experiment can prove, that the pressure drop should change with L and D in the same way as the ordinary fluid results eq (41.). It might be suggested that the superfluid fraction has been reduced to zero by the large flow velocities but that can be ruled out on a number of grounds, including the results reported in the next section, which would display no heat transport above the "enthalpy rise" value if the heat current were only the thermal conduction of He I. Actually, it presents a difficult problem, because there is no obvious way to derive such results from the current versions of two-fluid hydrodynamics.

For the purpose of a more sensitive comparison of the data, we have made a rough fit to a constant friction factor formula, defined by

$$\Delta P_c = f \frac{4L}{D} [(1/2)\rho V^2] \qquad (42)$$

where f has the values 0.0062, 0.0062, 0.0067 and 0.0075 for the temperatures 2.10, 1.92, 1.65 and 1.39 K respectively. This formula is plotted as the solid line in figures 12-15. The fractional deviations of the data from this formula have been plotted in Figs. 18-21. This plot gives a more exact impression of the data coverage, scatter and departure from a simple behavior.

We have not yet found any simple correlation for the lower velocity data, nor have we been able to specify what condition it is that determines just where that region starts. However, in all the conditions encountered in this experiment, this ignorance is in regions where the pressure drop is small enough so that it may be mainly of academic interest.

No correction was made for end effects, because we have no experience that indicates that they should be made. If such an extra pressure drop were present, of about the same size as for ordinary fluid flow (say $1/2\ \rho V^2$), then it would represent about a 6% correction to the data.

If the change due to the curvature of the flow tube were about the same for He II as for an ordinary fluid in turbulent flow, then there would be about 1% extra pressure drop at 10 cm/s, and about 12% extra pressure drop at V = 70 cm/s [29].

4.2 The Heat Current Density

We have shown in sections 2 and 3 that the quantity $\dot{q}_2$ represents the useful heat (per channel cross-sectional area) that can be removed from a heat source by the fluid in a cooling channel. We showed that for a heat source which is a small heated section in the middle of a cooling channel of length 2L, assuming the other conditions are matched, our experimental result for $\dot{q}_2(V)$, $V > 0$, would represent the heat absorbed by the incoming fluid, and that the result for $\dot{q}_2(V)$, $V < 0$ would represent an additional heat conducted away by the departing fluid.

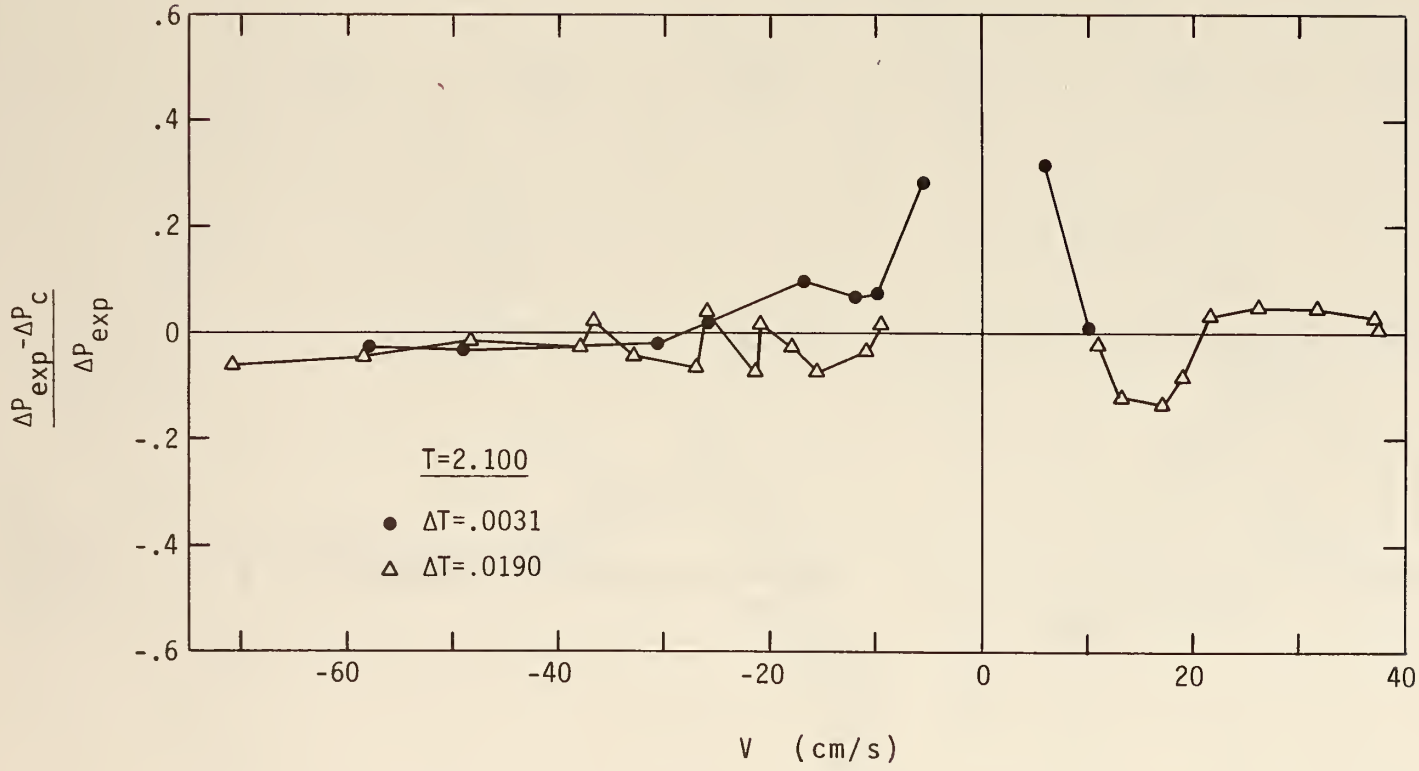

Figure 18. The data of Fig. 12, plotted as deviations from eq (42).

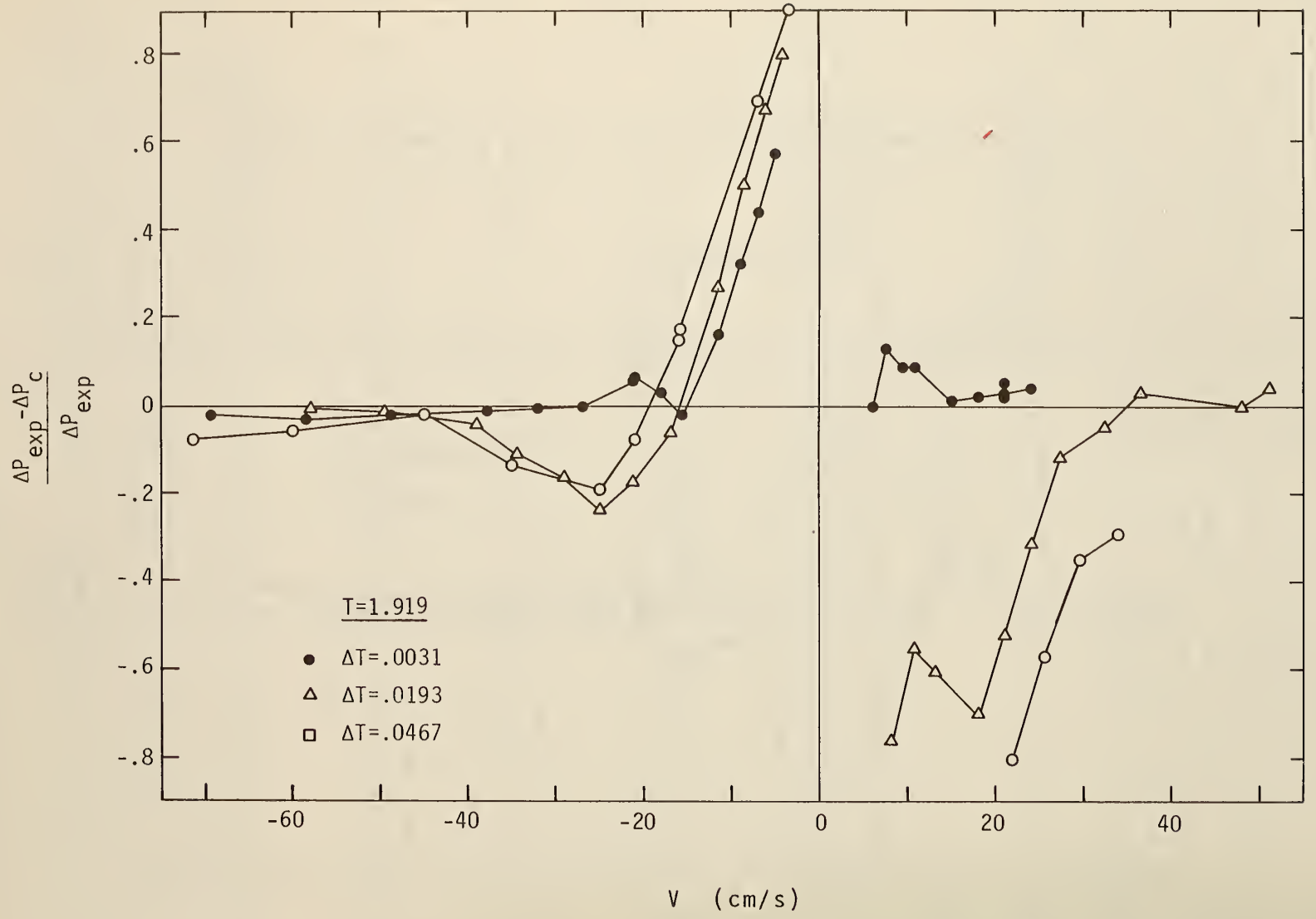

Figure 19. The data of Fig. 13, plotted as deviations from eq (42).

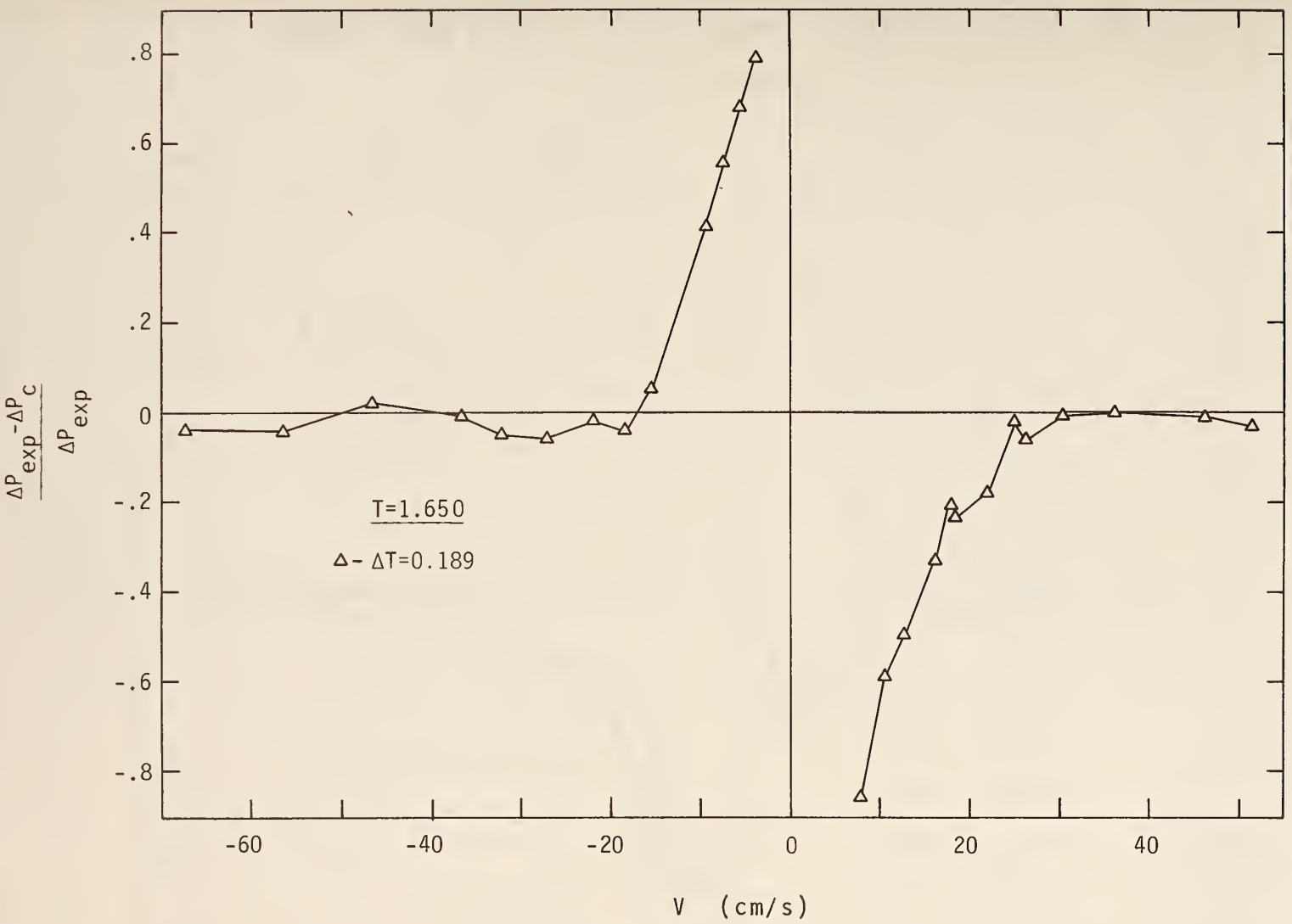

Figure 20. The data of Fig. 14, plotted as deviations from eq (42).

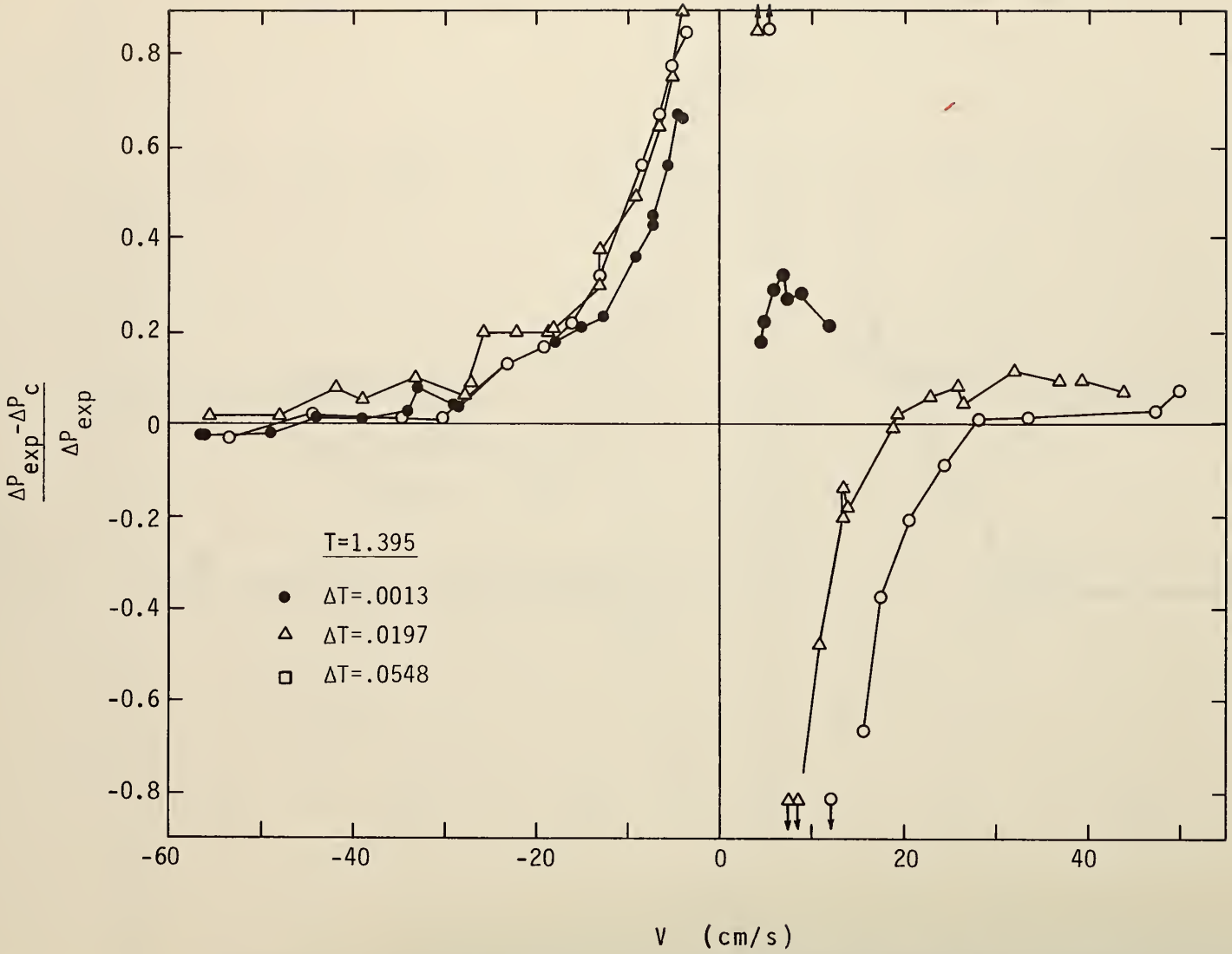

Figure 21. The data of Fig. 15, plotted as deviations from eq (42).

The results for $\dot{q}_2$ are shown in Figs. 22-25, where they are plotted as a function of V. The symbols indicate the nominal values for ΔT, but the explicit dependence on ΔP is not indicated; it can be inferred from the value of V.

Constructing a correlation for this data is not so straightforward as for the net fluid velocity. In that case, mass conservation required that V be a constant, so that once it was found that ΔP is mainly a function of V, we can infer that the local and average pressure gradients are nearly the same. In this case, the temperature gradient and the heat current density can turn out to be strong functions of position along the tube.

We proceed in a manner similar to that found in section 2.2 The one-dimensional energy equation [eq (20)] gives us an expression that relates $\dot{q}(x)$ to $T(x)$, and to the velocity and the local pressure; the latter two quantities can be taken directly from experiment. The model building comes in trying to devise a successful second equation that will allow solution for the unknowns $\dot{q}$ and T.

The most natural choice we have come up with so far is to set the chemical potential gradient equal to one of the mutual friction expressions using eq (10) with $\partial v_s/\partial t = 0$. This amounts to setting $\dot{q}$ equal to some simple function of $\nabla\mu$.

We used Vinen's expression [9],

$$\rho_s \frac{d\mu}{dx} = A\rho_s\rho_n \left(|v_n - v_s| - v_o \right)^2 (v_n - v_s) \qquad (43)$$

and took the values for A from his graph. The value of v_o (not very influential in the calculation) was arbitrarily fixed at 0.5 cm/s, a value near his.

The equations were integrated numerically, the T at x_2 fixed at T_2, and $\dot{q}$ given various starting values, until the temperature at the other end matched. The resulting values of $\dot{q}_2$ are displayed as the solid lines on the graphs of $\dot{q}$ vs V, Fig. 22-25.

The calculations do reproduce some features of the data. First, they do a reasonable job of doing what they were originally designed to do, i.e., predict the V = 0 data, the poor spots being T = 1.395 and T = 2.100, where the calculated values are all about 10% high. Second, for the higher T's they do a reasonable job of predicting the slope of $\dot{q}_2$, near V = 0. Finally, one curve (Fig. 25) does go through zero (albeit much more steeply) about where the data reverses sign, at the lowest T and ΔT. This last feature, and the other sharp drop at negative V, are found only for the conditions in which ΔP becomes large enough to cause $\Delta\mu$ to reverse sign; we have the interesting possibility of a heat current flowing toward higher temperatures. Unfortunately, the experimental evidence for this current reversal is not quite compelling. The data had a small scatter, and were reproducible, but the possibility of a systematic error (an extraneous heat input) of about the size needed to cancel the effect, cannot be excluded.

Overall, though, this simple theory does not work very well, the most striking result being that for both $V < 0$ and $V > 0$ the observed $\dot{q}_2$ is less than expected. As originally formulated, Vinen's arguments that lead to eq (43) clearly suggest that the equation should remain valid when $V \neq 0$. These results lead us to conclude otherwise.

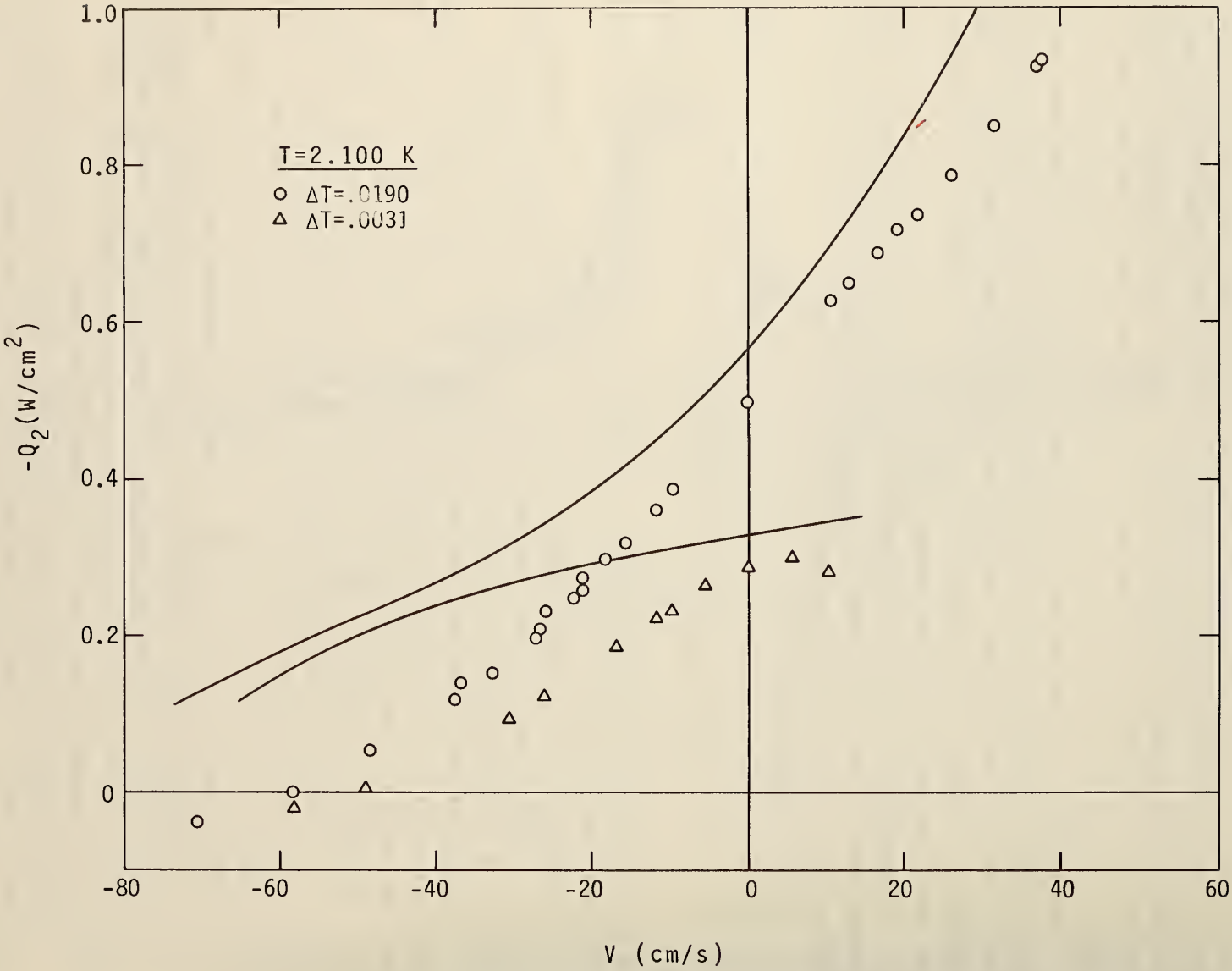

Figure 22. The useful heat current density vs the net fluid velocity at 2.100 K. The solid lines are the calculations that assume mutual friction is unaltered by the net fluid flow.

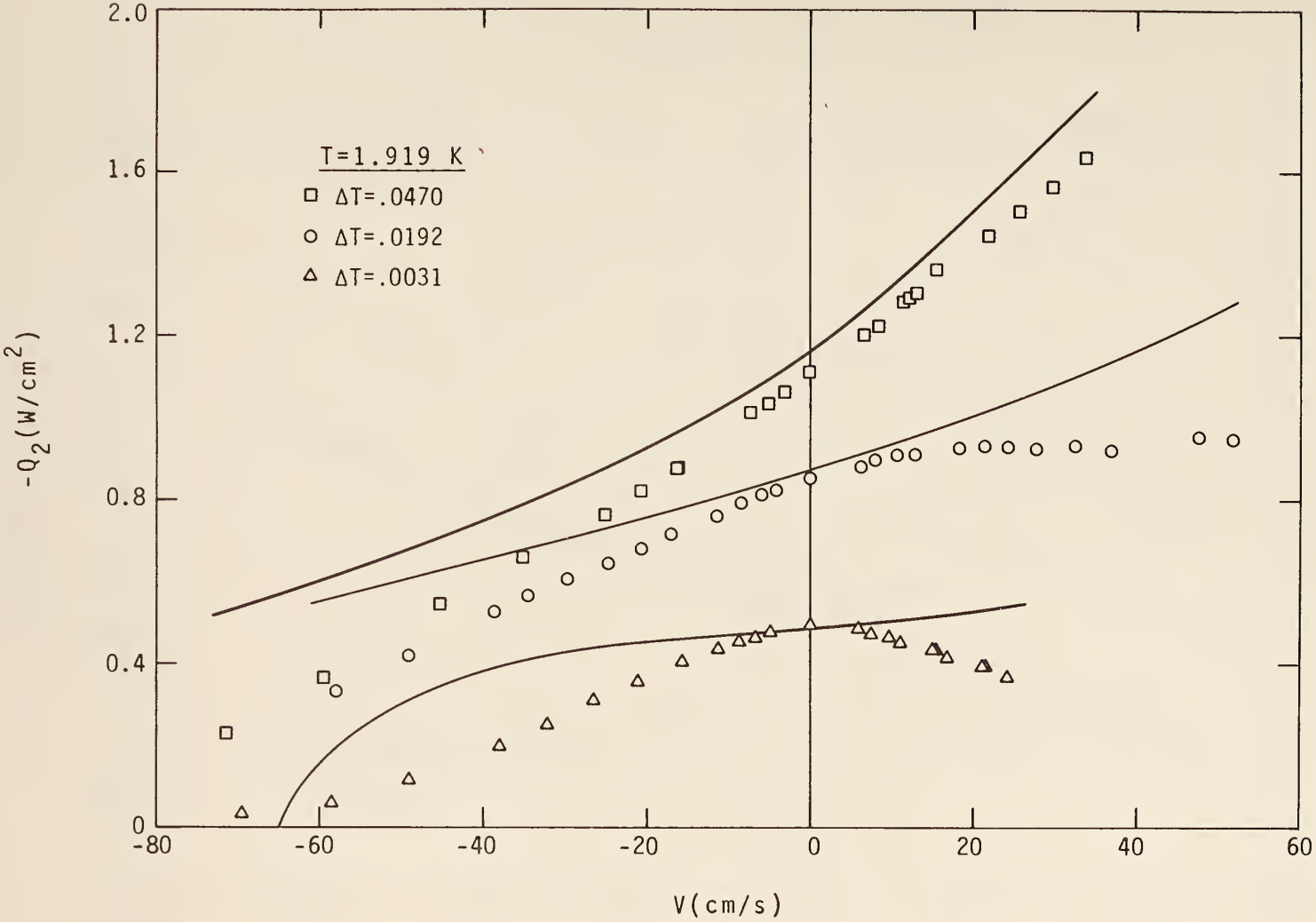

Figure 23. The useful heat current density vs the net fluid velocity at 1.919 K. The solid lines are the calculations that assume mutual friction is unaltered by the net fluid flow.

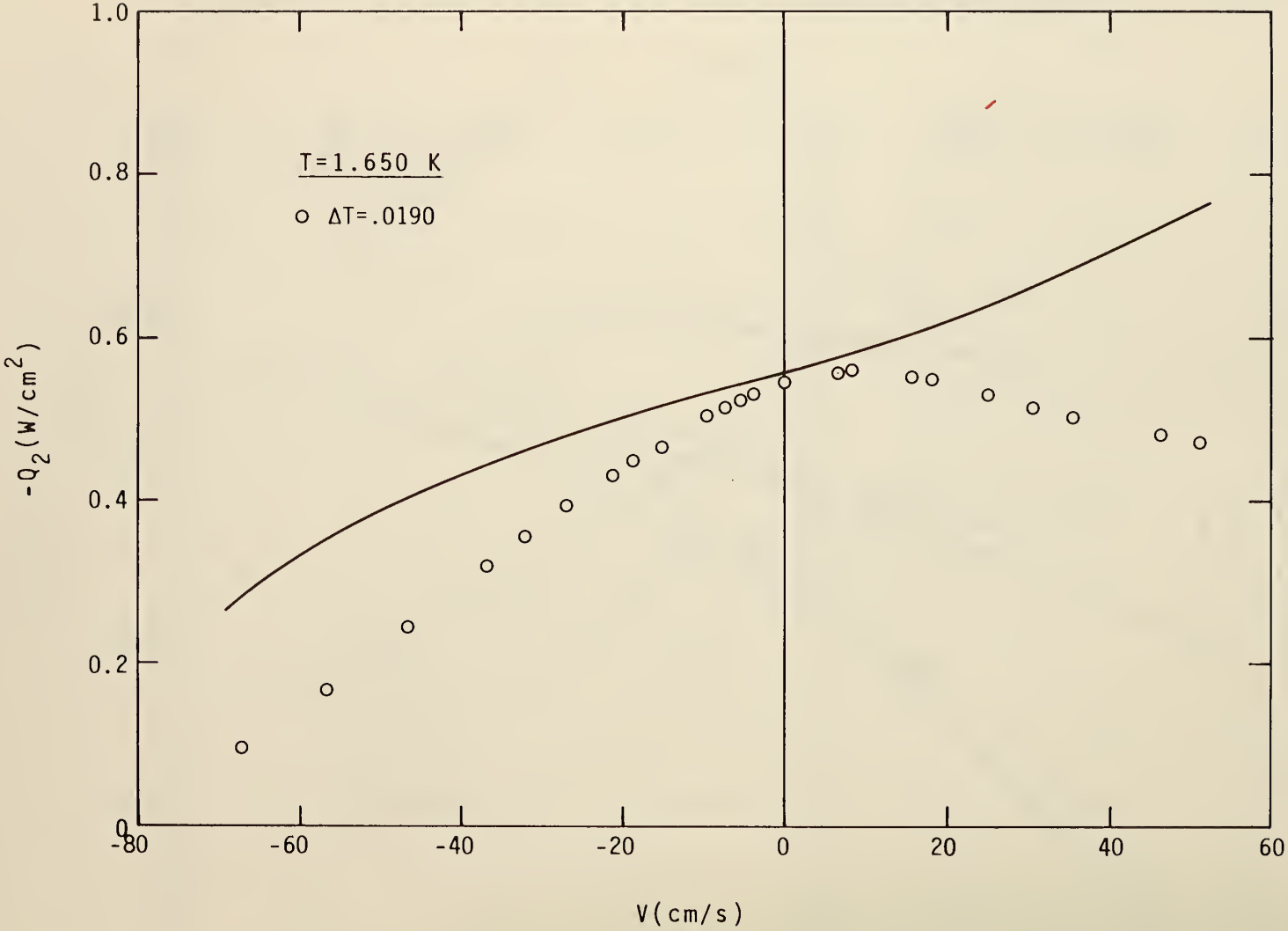

Figure 24. The useful heat current density vs the net fluid velocity at 1.650 K. The solid line is the calculation that assumes mutual friction is unaltered by the net fluid flow.

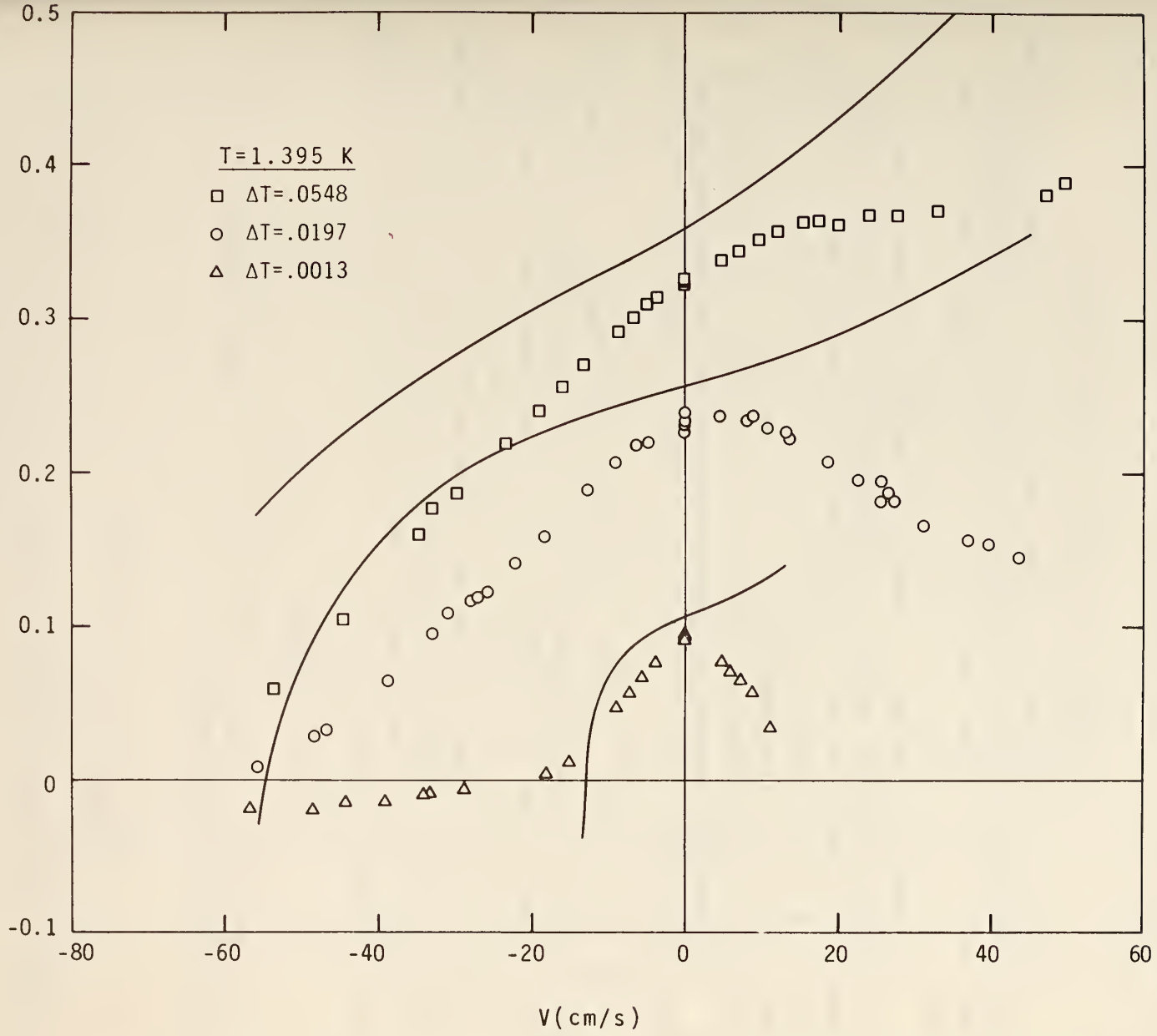

Figure 25. The useful heat current density vs the net fluid velocity at 1.395 K. The solid lines are the calculations that assume mutual friction is unaltered by the net fluid flow.

These results seem to be suggesting that we might retain Vinen's identification of the source of mutual friction with the presence of vorticity in the superfluid fraction, if we now suppose that the net fluid flow is capable of generating superfluid vorticity, in amounts over and above that generated by the mean counterflow of the two components.

5. ENHANCEMENT OF HEAT TRANSPORT BY FORCED CONVECTION

Without understanding quantitatively how mutual friction is increased by mass flow we can still draw some qualitative conclusions which indicate that in some circumstances at least, much more heat can be transported by forced convection than by "natural" convection.

Our reasoning is based again on investigating the limit as the heat current goes to zero everywhere except near the heater. The energy equation for He II also integrates immediately to give the now familiar result that the total heat absorbed by the fluid is equal to the enthalpy difference times the flow rate. For the incoming fluid ($V > 0$), we get $\dot{q}_2 = \rho V C_p \Delta T$; for the departing fluid ($V < 0$), we get $\dot{q}_2 = 0$. The positive velocity portion of the enthalpy-rise-heat-current is given on the graphs (Figs. 26-29) of $\dot{q}_2$ vs V. This value should, and does, act as a lower bound for the useful heat that can be rejected by the heat source. If the extra mutual friction caused by the mass flow has not "killed off" the heat current, then we can expect an extra contribution.

Now let us consider a comparison of "natural" to forced convection. Suppose we want to use the flow tube from these experiments to cool some localized heat source. First, let us estimate the best that we can do at 1.8 K with pure counterflow, with two tubes connected to the source, but no forcing of circulation around the loop. We suppose that we have a pressurized system so that we can increase the ΔT to 0.300 K. At best, the heat current per tube will increase as the cube root of T, and since $\dot{q}_2(T = 1.92, \Delta T = 0.047, V = 0) = -1.11\ W/cm^2$, the best we can do (ignoring the temperature dependence of the proportionality constant in equation (8)) is

$$(1.11) \times 2 \times \left(\frac{0.300}{0.047}\right)^{1/3} = 4.1\ W/cm^2$$

Second, how well can we do with forced convection? The enthalpy-difference-heat-current (the lower limit) for the same ΔT is

$$\rho V \int_{1.8}^{2.1} C_p\, dT = V \times (0.21\ J/cm^3)$$

If we have enough head (2.5 m) to force the flow at 200 cm/s, we get

$$42\ W/cm^2$$

which is 10 times larger. The pump work divided by the heat transported is

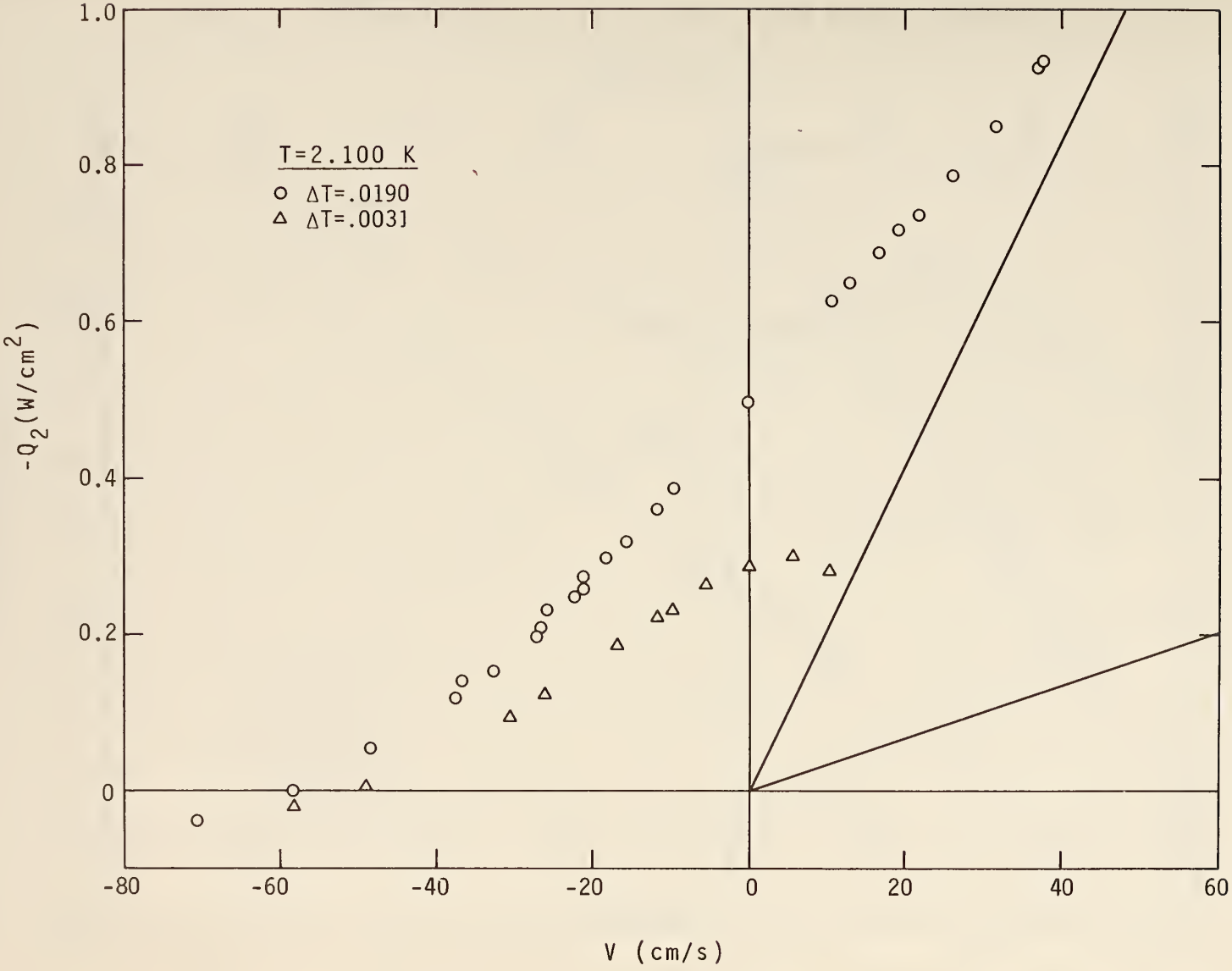

Figure 26. The data of Fig. 22. The lines are the enthalpy rise values for the different ΔT's.

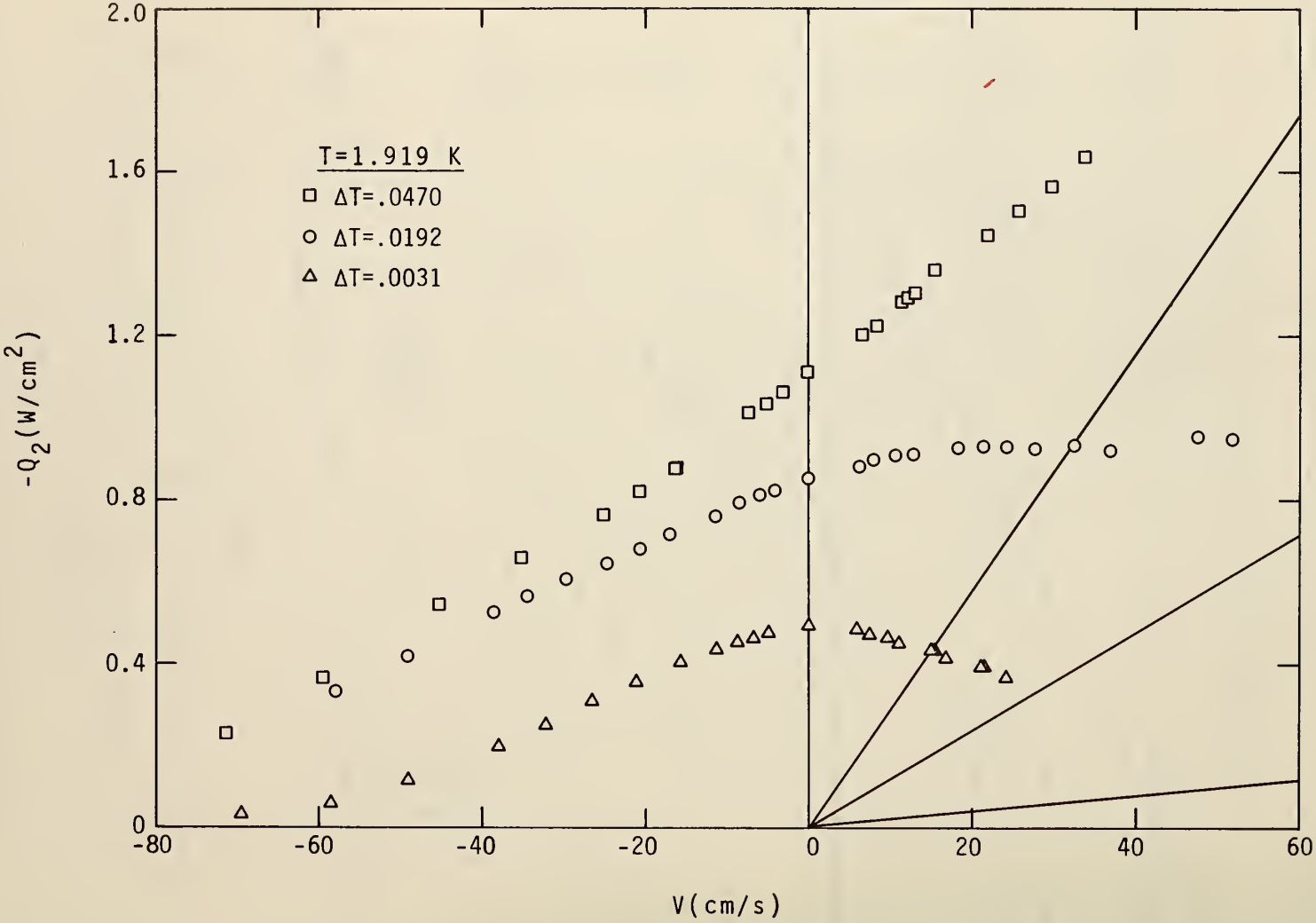

Figure 27. The data of Fig. 23. The lines are the enthalpy rise values for the different ΔT's.

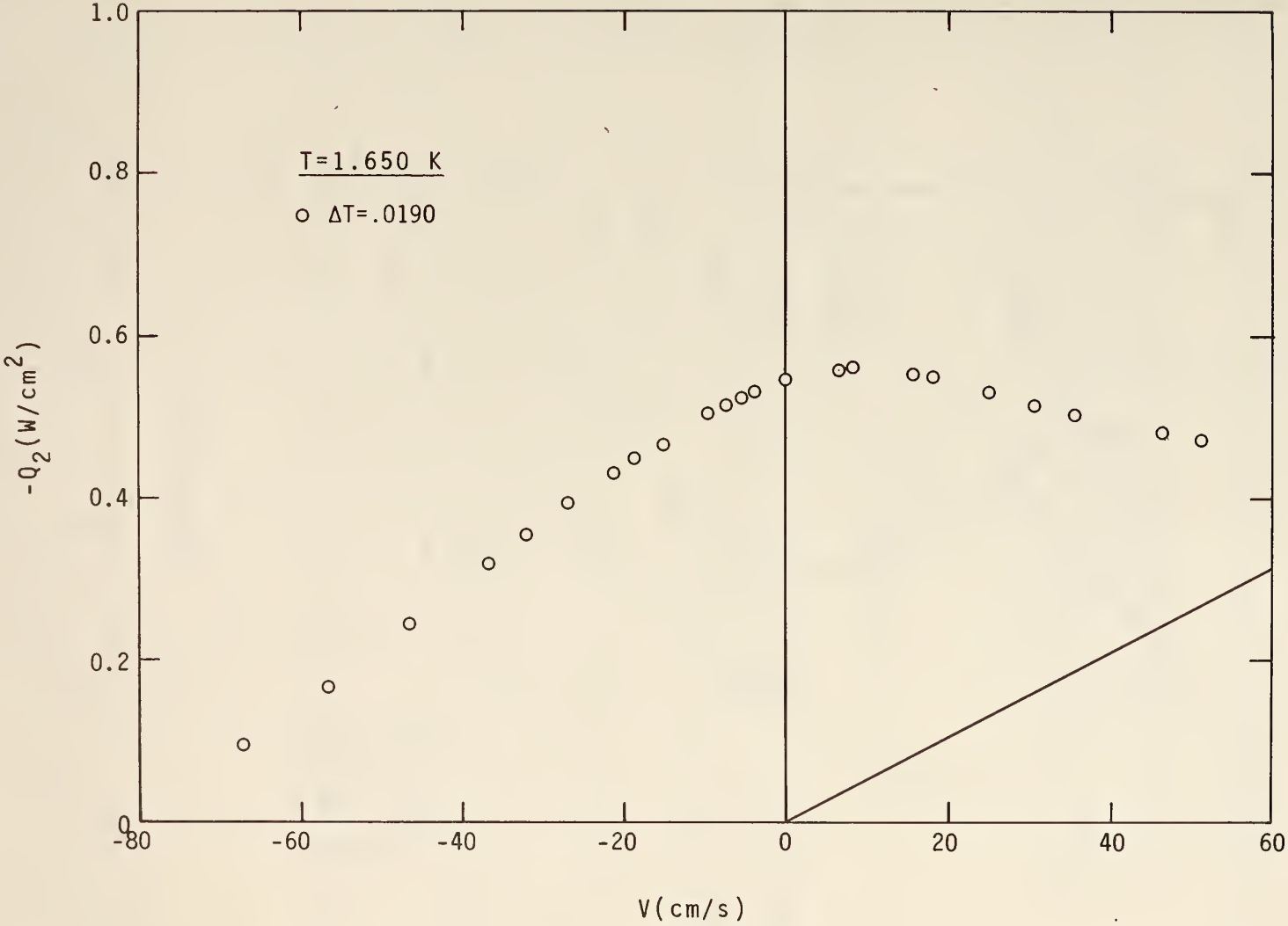

Figure 28. The data of Fig. 24. The lines are the enthalpy rise values for the different ΔT's.

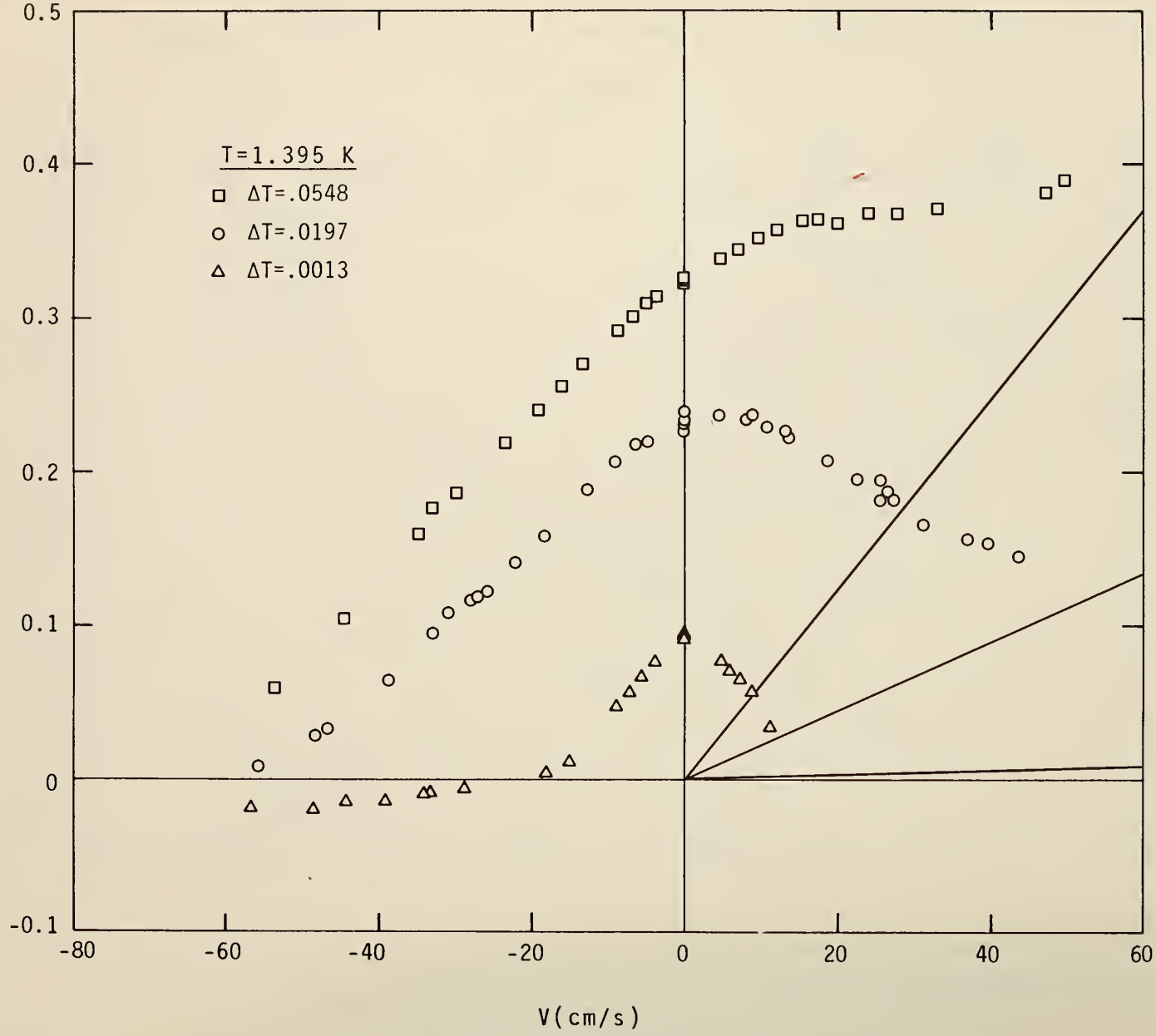

Figure 29. The data of Fig. 25. The lines are the enthalpy rise values for the different ΔT's.

$$\frac{\Delta P \cdot V}{\rho V \int C_p \, dT} \simeq \frac{3.6 \times 10^3 \text{ Pa}}{0.21 \text{ J/cm}^3} \simeq \frac{3.6 \times 10^3}{2.1 \times 10^5} \simeq 1.7\%$$

If 17% pumpwork were acceptable, then another factor of 3 increase in heat absorbed is possible.

While this example may not be typical of any prospective application, it does illustrate how in some situations forced cooling might be of interest.

These experimental results for $\dot{q}_2$ show the transition from this purely classical and predictable heat transport to the more or less predictable values for zero mass flow -- the pure counterflow regime.

6. CONCLUSIONS

This experimental study enables the following generalizations to be made regarding combined heat and mass flow in Helium II.

1. Velocity of flow is primarily a function of pressure gradient. Towards the higher velocities encountered in these experiments, the relationship between velocity and pressure gradient is independent of the temperature gradient and strongly resembles a classical fluid. At lower velocities a complex relationship exists between V, ΔT and ΔP, which needs further clarification.
2. At zero velocity, axial heat transport typical of the "mutual friction" regime is again confirmed. Either positive or negative velocities reduce this heat transport below what would be calculated from the Vinen theory, and, as the magnitude of the velocity increases, classical forced convection heat transport is approached. For strongly negative velocities there is some evidence that a reversal in the direction of the heat current takes place as predicted from the Vinen theory. More definitive experiments would be required to confirm this.
3. In practical situations, axial heat transport far in excess of the usual pure counterflow values may be achieved by imposing mass flow or forced convection with the usual classical pressure drop.

7. ACKNOWLEDGEMENTS

Vincent Arp played a vital role in initiating and encouraging this project, and in defining the problems which it addresses. Jim Siegwarth generously loaned experimental equipment and expertise. One of us (W.J.) would like to acknowledge support provided through the National Bureau of Standards Postdoctoral Research Associateship Program in association with the National Research Council.

8. REFERENCES

[1] G.v.d. Heijden, W.J.P. de Voogt, and H.C. Kramers, "Forces in the Flow of Liquid Helium II, I" Physica 59, 473 (1972).

[2] G.v.d. Heijden, A.G.M.v.d. Boog and H.C. Kramers, "Forces in the Flow of Liquid He II, III," Physica 77, 487 (1974)

[3] W. de Haas, A. Hartoog, H.v. Beelen, R. de Bruyn Ouboter and K.W. Taconis, "Dissipation in the Flow of He II," Physica 75, 311 (1974).

[4] W. de Haas and H. van Beelen, " A Synthesis of Flow Phenomena in He II," Physica 83B, 129-146 (1976).

[5] J. Wilks, The Properties of Liquid and Solid Helium, Oxford University Press (1967).

[6] W.E. Keller, Helium-3 and Helium-4, Plenum Press (1969).

[7] R.J. Donnelly, W.I. Glaberson and P.E. Parks, Experimental Superfluidity, University of Chicago (1967).

[8] S.J. Putterman, Superfluid Hydrodynamics, North-Holland (1974).

[9] W.F. Vinen, "Mutual Friction in a Heat Current in Liquid Helium II," I - Proc. Roy. Soc. A240, 114 (1957); II - Proc. Roy. Soc. A240, 128 (1957); III - Proc. Roy. Soc. A242, 493 (1957); IV - Proc. Roy. Soc. A243, 400 (1958).

[10] R.K. Childers and J.T. Tough, "Helium II Thermal Counterflow: Temperature -and Pressure - Difference Data and Analysis in Terms of the Vinen Theory," Physical Rev. B13, 1040 (1976).

[11] D.R. Ladner, R.K. Childers and J.T. Tough, "He II Thermal Counterflow at Large Heat Currents," Phys. Rev. B13, 2919 (1976).

[12] V. Arp, "Heat Transport Through Helium II," Cryogenics 10, 96 (1970).

[13] C. Linnet and T.H.K. Frederking, "Thermal Conditions at the Gorter-Mellink Counterflow Limit Between 0.01 and 3 Bar," J. Low Temp. Phys. 21, 447, (1975).

[14] G. Krafft, "Kuhlung Langer Rohrsysteme mit Superfluidem Helium," Kern Forschungszentrum Karlsruhe Report KFK1786, (1973).

[15] R.K. Childers and J.T. Tough, "Superheating in He II," Low Temp. Phys. LT13, 1, 359 (1972).

[16] R. Eaton III, W.D. Lee and F.J. Agee, "High-Heat Flux Regime of Superfluid Cooling in Vertical Channels," Phys. Rev. A5, 1342 (1972).

[17] L.D. Landau and E.M. Lifshitz, Fluid Mechanics, Pergamon Press (1959).

[18] R.B. Bird, W.E. Stewart and E.N. Lightfoot, Transport Phenomena, John Wiley (1960).

[19] S.R. de Groot, Thermodynamics of Irreversible Processes, North-Holland (1951).

[20] E.F. Hammel and W.E. Keller, "Dissipation and Critical Velocities in Superfluid Helium," International Conference of Low Temperature Physics - LT10, Moscow, Vol I, p. 30 (1967).

[21] P.H. Roberts and R.J. Donnelly, "Superfluid Mechanics," Ann. Rev. of Fluid Mech. 6, 179 (1974).

[22] R. Meservey, "Superfluid Flow in a Venturi Tube," Phys. of Fluids 8, 1209 (1965).

[23] P.M. McConnell, "Liquid Helium Pumps," (U.S.) National Bureau of Standards Internal Report NBSIR-73-316 (1973).

[24] F.G. Brickwedde, H.v. Dijk, M. Durieux, J.R. Clement and J.K. Logan, "The 1958 He^4 Scale of Temperatures," J. of Res. NBS 64A, 1 (1960).

[25] S.G. Sydoriak and R.H. Sherman, "The 1962 He^3 Scale of Temperatures I," J. of Res. 68A, 547 (1974).

[26] R.D. McCarty, "Thermophysical Properties of Helium-4 from 2 to 1500 K with Pressures to 1000 Atmospheres," (U.S.) National Bureau of Standards Tech. Note 631 (1972).

[27] H.J.M. Hanley and J. Ely, "The Viscosity and Thermal Conductivity Coefficients of Dilute Nitrogen and Oxygen," J. Phys. Chem. Ref. Data 2, 735 (1973).

[28] C.M. White, "Streamline Flow Through Curved Pipes," Proc. Roy. Soc. A123, 645 (1929).

[29] H. Ito, "Friction Factors for Turbulent Flow in Curved Pipes," Trans. ASME, J. of Basic. Eng., June 1959, p 123.

9. NOMENCLATURE

English

A	Gorter-Mellink constant
A_d, A_i, A_o	horizontal cross-sectional area
A_x	cross-sectional area of the flow tube
C_p	isobaric heat capacity per unit mass
C, C_v, C_1, C_2	capacitance
D	diameter of the flow tube
E	total energy of the helium
g	gravitational constant
h, h_1, h_2, h_{ent}	enthalpy per unit mass
j_u (j_e)	the energy (total energy) current density
ℓ	active capacitor length
L	flow tube length
L_o	length of quantized vortex line per unit volume
M (m, m')	the total (liquid, vapor) mass of helium within the inner vessel
P, P_1, P_2, P_{sv}	pressure
P_o, P_s	(for gas flow measurements) the ambient pressure, the partial pressure of water vapor
$\dot{Q}$	heat current or rate of heat addition
$\dot{q}$, $\dot{q}_1$, $\dot{q}_2$, $\dot{q}_{ent}$	heat current density
Re	Reynolds' number
s, s', s_1, s_2	entropy per unit mass
T, T_1, T_2, T_{ent}	temperature
U	total internal energy of the helium within the inner vessel
u, u', u_1, u_2, u_{ent}	internal energy density per unit mass
v, v'	volume per unit mass
v_n, v_s	normal and super component velocities (cross-sectional average)
V	net fluid velocity (cross-sectional average)
V_b, V_e, V_i, V_o	vertical velocities
x	axial coordinate
z_1, z_2, z_b, z_{ent}	altitudes

Greek

Δ	(indicates the difference of two values)
ε, ε'	dielectric constant
η, η_n	coefficient of viscosity
ρ, ρ_n, ρ_s	mass per unit volume
μ	Gibbs potential per unit mass (chemical potential)
ω	vorticity
Ω	volumetric flow rate

Subscripts

1 (2) or o (i)	for the outside helium bath (inner vessel)
e, (b, d)	for evaporation measurements (the vacuum can, the dewar)
ent	at the entrance of the flow tube to the inner vessel
SV, svp	along the liquid-vapor coexistence line
u (e)	associated with the internal (total) energy density

Superscripts

primed and unprimed quantities distinguish between the vapor and the liquid, respectively

APPENDIX 1

The following tables give the important results for almost every data point taken during the long run. Listed are the average and the difference of the temperatures of the inside and the outside helium vessels (TMEAN,DT), the altitude difference calculated from the preceeding two quantities (DP), the velocity of net fluid flow through the flow tube (V), and the nominal heat current density at the inside end of the flow tube (Q2).

The sign convention is determined by taking the positive direction to run from the outside toward the inside. Therefore positive temperature differences indicate that the inside was hotter than the outside; a positive pressure difference, that the inside end of the flow tube is at a higher pressure than the outside end. The negative values of Q2 indicate that heat is flowing towards the (cooler) outside, etc.

All temperatures are given in kelvins (measured on the T_{58} He^4 vapor pressure scale), the pressure difference is given in pascals (= 1 newton/meter^2 = 10 dyne/centimeter^2), the altitude difference in centimeters, and the velocities are given in centimeters/second. The reader should be alert to a practice that is commonly found in the He II literature and this paper, and that is the mixing of MKS and cgs units. Therefore, when various quantities are multiplied together, further multiplication by powers of ten may be necessary to maintain consistent units.

Each data point is identified by numbers found in the ninth column of the table; the month and day on which a data-taking session was started is indicated by the numbers under DATE , the sequence number for that data point is indicated under NN, and the mode number that indicates the location of the liquid interfaces is given under MO (see Table 1). The data points have been sorted: first by TMEAN, then by whether they are regular data points or equilibrium points (Q2 = 0) and finally by chronological order.

In columns 7 and 8 are given the results for the two auxiliary thermometers TIB and TOB. They were intended to measure the temperatures near, but not at, the inside and outside ends respectively. (See the text for an account of the relatively large uncertainties in this particular measurement). The temperature of the outside helium bath was subtracted from the indicated temperature at each location to give the listed values of DTIB and DTOB.

Several other quantities of possible interest can be calculated from the experimental results by using known values for some thermodynamic properties and some formulas from section 2 and 3. We have listed RDMU, the density times the difference in the chemical potential, which is given by $\Delta P - \rho \bar{s} \Delta T$. Also tabulated is Q1, ($Q1 \equiv \dot{q}_1$), the nominal heat flux density at the outside end of the flow tube, defined by $Q1 \equiv Q2 + (z_2 - z_1)\rho V$. Finally, we have tabulated the nominal values for the normal- and super-fluid velocities at the two ends from the formulas

$$VN1 = V + \frac{Q1}{\rho s_1 T_1} ,$$

$$VS1 = - \frac{\rho_n}{\rho_s} \frac{Q1}{s_1 T_1} , \text{ etc.}$$

The thermodynamic properties were taken from a power-law interpolation of tables A and E of Putterman [8].

Appendix 1. Experimental Data.

TMEAN (K)	DT (K)	DZ (CM)	DP (PA)	V (CM/S)	Q2 (W/CM2)	DTOB (K)	DTIB (K)	DATENNMO	RDMU (PA)	Q1 (W/CM2)	VN2 (CM/S)	VN1 (CM/S)	VS2 (CM/S)	VS1 (CM/S)
2.10035	.01913	-14.96	-.1	0.00	-.497	.00095	.01877	917 7 1	-3542.4	-.497	-1.24	-1.32	4.87	3.68
2.10034	.01911	-24.34	-134.3	37.55	-.933	-.00030	.01212	917 8 4	-3673.7	-.164	35.22	37.11	46.69	38.76
2.10032	.01897	-5.58	132.1	-37.81	-.118	.00402	.01731	917 9 3	-3380.3	-.896	-38.10	-40.18	-36.65	-31.16
2.10029	.01897	-14.85	-.3	0.00	-.498	.00036	.01704	91710 1	-3513.3	-.498	-1.24	-1.32	4.87	3.69
2.10038	.01867	16.30	441.5	-70.72	.038	.01053	.01952	91713 3	-3015.8	-1.417	-70.62	-74.47	-71.09	-60.19
2.10034	.01876	6.92	305.4	-58.47	-.001	.00804	.01877	91714 3	-3164.6	-1.201	-58.48	-61.66	-58.47	-49.56
2.10036	.01874	.67	218.9	-48.56	-.054	.00623	.01832	91715 3	-3250.7	-1.046	-48.70	-51.34	-48.03	-40.80
2.10027	.01893	-14.76	.4	0.00	-.499	.00076	.01795	91716 1	-3503.8	-.499	-1.24	-1.32	4.87	3.70
2.10052	.01912	-14.94	.2	0.00	-.494	.00151	.02021	920 3 1	-3542.5	-.494	-1.23	-1.31	4.86	3.66
2.10054	.01905	-21.61	-98.8	31.67	-.850	-.00040	.01262	920 4 4	-3629.2	-.202	29.55	31.13	40.03	33.17
2.10053	.01901	-8.08	87.2	-32.82	-.154	.00340	.01762	920 5 3	-3424.2	-.830	-33.21	-35.02	-31.31	-26.66
2.10056	.01903	-19.63	-67.8	26.15	-.789	-.00038	.01346	920 6 4	-3594.5	-.253	24.18	25.48	33.91	28.03
2.10061	.01903	-10.20	66.2	-27.20	-.199	.00306	.01885	920 7 3	-3480.0	-.762	-27.78	-29.30	-25.32	-21.63
2.10064	.01907	-16.66	-49.6	21.58	-.736	-.00010	.01472	920 8 4	-3579.9	-.293	19.75	20.81	28.84	23.75
2.10061	.01903	-10.23	66.2	-25.99	-.230	.00306	.01885	920 9 4	-3480.0	-.766	-26.57	-28.02	-23.73	-20.31
2.10061	.01903	-10.23	66.2	-26.93	-.208	.00306	.01885	92010 3	-3480.0	-.763	-27.45	-28.95	-24.89	-21.27
2.10065	.01899	-11.81	43.5	-21.24	-.272	.00221	.01825	92011 4	-3476.2	-.708	-21.91	-23.11	-18.56	-15.98
2.10065	.01899	-11.81	43.5	-22.21	-.248	.00221	.01825	92012 3	-3476.2	-.705	-22.83	-24.08	-19.77	-16.97
2.10065	.01899	-11.81	43.5	-21.36	-.259	.00221	.01825	92013 1	-3476.2	-.698	-22.01	-23.21	-18.81	-16.18
2.10072	.01906	-14.34	-.4	0.00	-.497	.00106	.01908	92014 1	-3534.1	-.497	-1.24	-1.31	4.91	3.69
2.10036	.01911	-14.69	.7	0.00	-.496	.00015	.01644	92110 1	-3538.4	-.496	-1.23	-1.31	4.86	3.67
2.10048	.01897	-16.45	-23.3	16.73	-.687	-.00028	.01470	92111 1	-3536.4	-.345	15.02	15.82	23.48	19.29
2.10048	.01897	-13.33	21.4	-15.58	-.319	.00084	.01686	92112 1	-3491.8	-.638	-16.38	-17.27	-12.45	-10.85
2.10045	.01897	-17.08	-32.2	19.27	-.717	-.00031	.01438	92113 1	-3545.6	-.323	17.48	18.41	26.30	21.66
2.10046	.01897	-12.76	30.4	-18.12	-.297	.00136	.01698	92114 1	-3483.0	-.668	-18.85	-19.89	-15.20	-13.16
2.10044	.01895	-14.85	-.7	0.00	-.496	.00004	.01629	92115 1	-3511.4	-.496	-1.24	-1.31	4.86	3.68
2.10044	.01895	-15.60	-14.1	12.93	-.649	-.00021	.01510	92116 1	-3524.8	-.384	11.32	11.91	19.29	15.78
2.10045	.01895	-13.93	12.7	-11.78	-.360	.00071	.01682	92117 1	-3497.8	-.601	-12.68	-13.37	-8.25	-7.32
2.10045	.01895	-15.55	-10.5	10.67	-.627	-.00023	.01527	92118 1	-3521.0	-.409	9.10	9.58	16.82	13.70
2.10045	.01890	-14.18	8.6	-9.46	-.388	.00052	.01674	92119 1	-3492.9	-.581	-10.42	-11.00	-5.65	-5.14
2.10045	.01890	-14.65	-1.1	0.00	-.497	.00001	.01624	92120 1	-3502.6	-.497	-1.24	-1.32	4.87	3.69
2.10037	.01913	-15.00	-.8	0.00	-.497	.00005	.01648	10 2 3 1	-3542.8	-.497	-1.24	-1.32	4.87	3.68
2.10039	.01906	-24.38	-135.6	37.32	-.926	-.00052	.01170	10 2 4 4	-3665.2	-.163	35.01	36.88	46.39	38.53
2.10036	.01893	-5.63	131.1	-36.99	-.140	.00394	.01714	10 2 5 3	-3374.8	-.901	-37.34	-39.38	-35.62	-30.31
2.10073	.00332	-2.60	.0	0.00	-.288	-.00036	.00224	10 210 1	-616.1	-.288	-.74	-.74	2.41	2.28
2.10069	.00336	-1.66	13.3	-11.68	-.222	-.00045	.00183	10 211 1	-609.0	-.265	-12.25	-12.37	-9.83	-9.59
2.10074	.00329	-3.29	-10.2	10.38	-.282	-.00047	.00182	10 212 1	-620.0	-.245	9.66	9.74	12.73	12.32
2.10068	.00334	-1.91	10.1	-9.95	-.232	-.00047	.00173	10 213 1	-609.9	-.268	-10.55	-10.65	-8.02	-7.83
2.10071	.00326	-2.56	-.1	0.00	-.289	-.00044	.00205	10 214 1	-604.5	-.289	-.74	-.75	2.41	2.29
2.10075	.00327	-2.87	-4.5	5.71	-.298	-.00054	.00172	10 215 1	-611.1	-.278	4.95	4.99	8.19	7.91
2.10074	.00324	-2.25	4.1	-5.59	-.265	-.00057	.00164	10 216 1	-596.8	-.284	-6.27	-6.32	-3.38	-3.34
2.10071	.00308	3.69	87.2	-30.69	-.094	-.00059	.00143	10 217 3	-484.0	-.199	-30.93	-31.21	-29.91	-29.12
2.10067	.00307	19.32	310.4	-58.45	.021	.00022	.00285	10 218 3	-258.5	-.191	-58.39	-58.94	-58.62	-56.93
2.10066	.00302	13.07	220.6	-49.12	-.005	-.00034	.00170	10 219 3	-339.4	-.176	-49.13	-49.57	-49.07	-47.72
2.10065	.00314	2.13	65.5	-26.16	-.124	-.00044	.00156	10 220 3	-515.8	-.215	-26.49	-26.73	-25.14	-24.48
2.10072	.00306	-2.43	-.4	0.00	-.286	-.00058	.00149	10 221 1	-568.4	-.286	-.73	-.74	2.38	2.27
2.10070	.00307	-.24	30.9	-17.15	-.184	-.00002	.00264	10 222 1	-537.4	-.242	-17.62	-17.77	-15.61	-15.24

Appendix 1 (continued). Experimental Data.

TMEAN (K)	DT (K)	DZ (CM)	DP (PA)	V (CM/S)	Q2 (W/CM2)	DTOB (K)	DTIB (K)	DATENNMO	ROMU (PA)	Q1 (W/CM2)	VN2 (CM/S)	VN1 (CM/S)	VS2 (CM/S)	VS1 (CM/S)
2.10983	-.00005	-.01	-.7	0.00	0.000	.00071	-.04057	917 1 1	8.6	0.000	0.00	0.00	0.00	0.00
2.10495	.00004	-.01	.2	0.00	0.000	.00067	.00255	917 2 1	-6.8	0.000	0.00	0.00	0.00	0.00
2.10035	.00002	-.00	.2	0.00	0.000	.00083	.00294	917 3 1	-3.8	0.000	0.00	0.00	0.00	0.00
2.09573	.00000	-.01	-.0	0.00	0.000	.00069	.00253	917 4 1	-.8	0.000	0.00	0.00	0.00	0.00
2.09074	.00005	-.01	.5	0.00	0.000	.00065	.00233	917 5 1	-9.3	0.000	0.00	0.00	0.00	0.00
2.09080	-.00004	-.03	-.7	0.00	0.000	.00026	.00123	917 6 1	5.6	0.000	0.00	0.00	0.00	0.00
2.09082	.00003	536.19	7663.2	0.00	0.000	.00011	.00066	91711 1	7657.8	0.000	0.00	0.00	0.00	0.00
2.09083	.00003	-.02	-.0	0.00	0.000	.00006	.00054	91712 1	-5.1	0.000	0.00	0.00	0.00	0.00
2.09087	-.00001	.01	-.0	0.00	0.000	.00024	.00129	91717 1	1.6	0.000	0.00	0.00	0.00	0.00
2.09071	.00006	-.00	.6	0.00	0.000	.00014	.00078	918 1 1	-9.8	0.000	0.00	0.00	0.00	0.00
2.09071	-.00001	-.03	-.1	0.00	0.000	-.00012	.00008	918 2 1	1.5	0.000	0.00	0.00	0.00	0.00
2.08994	.00002	.03	.6	0.00	0.000	.00122	.00426	920 1 1	-3.1	0.000	0.00	0.00	0.00	0.00
2.09098	.00001	.03	.6	0.00	0.000	.00096	.00339	920 2 1	-1.7	0.000	0.00	0.00	0.00	0.00
2.09113	.00003	.01	.9	0.00	0.000	.00025	.00126	92015 1	-4.1	0.000	0.00	0.00	0.00	0.00
2.10100	-.00001	536.19	7662.7	0.00	0.000	.00052	.00237	921 1 1	7665.1	0.000	0.00	0.00	0.00	0.00
2.10111	-.00004	-.01	-.6	0.00	0.000	-.00074	-.00158	921 2 1	6.9	0.000	0.00	0.00	0.00	0.00
2.11030	-.00001	-.01	-.3	0.00	0.000	-.00078	-.00156	921 3 1	2.0	0.000	0.00	0.00	0.00	0.00
2.10543	-.00001	-.01	-.3	0.00	0.000	-.00072	-.00156	921 4 1	1.4	0.000	0.00	0.00	0.00	0.00
2.10111	-.00001	-.01	-.3	0.00	0.000	-.00073	-.00158	921 5 1	1.1	0.000	0.00	0.00	0.00	0.00
2.09643	.00001	-.01	-.1	0.00	0.000	-.00072	-.00157	921 6 1	-1.8	0.000	0.00	0.00	0.00	0.00
2.09148	.00003	-.02	.0	0.00	0.000	-.00068	-.00151	921 7 1	-5.0	0.000	0.00	0.00	0.00	0.00
2.09124	.00000	-.01	-.1	0.00	0.000	-.00067	-.00153	921 8 1	-.6	0.000	0.00	0.00	0.00	0.00
2.09092	.00002	-.01	.1	0.00	0.000	-.00065	-.00151	921 9 1	-3.4	0.000	0.00	0.00	0.00	0.00
2.10033	-.00004	.01	-.4	0.00	0.000	-.00074	-.00159	10 2 1 1	7.5	0.000	0.00	0.00	0.00	0.00
2.09075	-.00003	.01	-.2	0.00	0.000	-.00073	-.00157	10 2 2 1	5.2	0.000	0.00	0.00	0.00	0.00
2.10167	-.00002	.01	-.1	0.00	0.000	-.00074	-.00155	10 2 6 1	2.9	0.000	0.00	0.00	0.00	0.00
2.09894	-.00001	.01	-.1	0.00	0.000	-.00075	-.00156	10 2 7 1	2.4	0.000	0.00	0.00	0.00	0.00
2.10246	-.00011	.03	-.9	0.00	0.000	-.00066	-.00129	10 2 8 1	20.2	0.000	0.00	0.00	0.00	0.00
2.09902	-.00005	.03	-.2	0.00	0.000	-.00052	-.00098	10 2 9 1	9.9	0.000	0.00	0.00	0.00	0.00
2.09913	-.00003	536.19	7662.5	0.00	0.000	.00000	.00050	10 223 1	7668.7	0.000	0.00	0.00	0.00	0.00
1.92368	.02883	-15.53	6.2	0.00	-.961	.00139	.02685	9 2 2 1	-3276.8	-.961	-4.18	-4.60	3.78	3.56
1.92415	.02898	-15.67	6.1	0.00	-.961	.00137	.02702	9 2 3 1	-3296.5	-.961	-4.18	-4.60	3.78	3.56
1.92413	.02901	-18.82	-38.2	24.78	-1.161	.00117	.02572	9 2 4 1	-3344.7	-.720	19.65	21.25	29.26	27.36
1.92407	.02867	-12.65	48.2	-24.19	-.709	.00257	.02728	9 2 5 1	-3218.9	-1.138	-27.28	-29.63	-21.40	-19.98
1.91935	.04728	-25.53	6.7	0.00	-1.108	.00231	.04438	910 1 1	-5309.7	-1.108	-4.75	-5.56	4.40	4.00
1.91942	.04721	-26.73	-11.6	15.28	-1.361	.00136	.04242	910 2 4	-5321.8	-.922	9.45	10.66	20.69	18.61
1.91941	.04719	-27.72	-25.1	21.94	-1.448	.00120	.04142	910 3 4	-5332.5	-.818	15.73	17.84	27.69	24.90
1.91941	.04711	-12.71	183.1	-45.23	-.545	.01011	.04565	910 4 4	-5110.4	-1.850	-47.57	-54.51	-43.07	-38.55
1.91948	.04716	-31.78	-83.7	33.87	-1.635	.00099	.03940	910 5 4	-5382.3	-.667	26.86	30.53	40.37	36.28
1.91944	.04709	-30.22	-61.5	29.74	-1.569	.00106	.04002	910 6 4	-5358.9	-.718	23.02	26.15	35.98	32.34
1.91953	.04706	-28.66	-39.4	25.65	-1.508	.00109	.04074	910 7 4	-5334.1	-.774	19.19	21.77	31.64	28.45
1.91952	.04702	-15.65	102.3	-35.21	-.660	.00767	.04550	910 8 4	-5187.5	-1.671	-38.03	-43.58	-32.59	-29.17
1.91969	.04684	-26.22	-.2	11.93	-1.299	.00136	.04264	910 9 2	-5278.6	-.959	6.36	7.13	17.09	15.40
1.91954	.04693	-25.37	6.8	0.00	-1.109	.00226	.04412	91010 1	-5279.0	-1.109	-4.75	-5.55	4.40	4.01
1.91946	.04698	-25.37	6.7	0.00	-1.108	.00226	.04410	911 1 2	-5277.4	-1.108	-4.75	-5.55	4.40	4.00
1.91943	.04687	-24.09	15.6	-7.13	-1.014	.00298	.04455	911 2 2	-5256.3	-1.217	-11.47	-13.22	-3.10	-2.73
1.91943	.04687	-24.09	15.6	-7.20	-1.013	.00298	.04455	911 3 1	-5256.3	-1.218	-11.54	-13.30	-3.18	-2.80
1.91943	.04686	-26.06	-4.1	11.07	-1.286	.00161	.04276	911 4 1	-5274.8	-.970	5.56	6.22	16.18	14.58
1.91943	.04686	-26.06	-4.1	10.99	-1.282	.00161	.04276	911 5 2	-5274.8	-.968	5.49	6.14	16.08	14.49

Appendix 1 (continued). Experimental Data.

TMEAN (K)	DT (K)	LZ (CM)	DP (PA)	V (CM/S)	Q2 (W/CM2)	DTOB (K)	DTIB (K)	DATENNMO	RDMU (PA)	Q1 (W/CM2)	VN2 (CM/S)	VN1 (CM/S)	VS2 (CM/S)	VS1 (CM/S)
1.91941	.04684	-25.23	6.7	0.00	-1.108	.00224	.04395	911 6 2	-5261.0	-1.108	-4.75	-5.55	4.40	4.00
1.91939	.04682	-24.98	11.0	-3.30	-1.063	.00259	.04421	911 7 2	-5255.0	-1.157	-7.86	-9.09	.93	.88
1.91941	.04679	-25.61	1.9	6.53	-1.205	.00175	.04324	911 8 2	-5260.6	-1.019	1.36	1.43	11.31	10.21
1.91939	.04674	-25.26	6.4	0.00	-1.108	.00221	.04385	911 9 2	-5250.5	-1.108	-4.75	-5.55	4.40	4.00
1.91934	.04664	6.00	451.1	-71.56	-.233	.01554	.04538	91110 3	-4793.3	-2.297	-72.56	-83.07	-70.64	-63.27
1.91933	.04658	-3.38	317.6	-59.76	-.368	.01280	.04522	91111 3	-4920.7	-2.080	-61.34	-70.18	-58.30	-52.24
1.91934	.04643	-25.10	0.2	0.00	-1.105	.00222	.04353	91112 2	-5215.2	-1.105	-4.74	-5.53	4.38	3.99
1.91925	.04631	-21.98	49.7	-25.09	-.763	.00543	.04463	91113 1	-5156.9	-1.472	-28.37	-32.46	-22.07	-19.78
1.91922	.04622	-24.97	6.3	0.00	-1.104	.00220	.04336	91114 2	-5189.5	-1.104	-4.74	-5.53	4.38	3.99
1.91922	.04623	-22.78	37.0	-20.77	-.824	.00463	.04447	91115 1	-5159.4	-1.409	-24.31	-27.83	-17.50	-15.68
1.91925	.04627	-25.91	-6.6	13.06	-1.309	.00149	.04199	91116 1	-5208.1	-.942	7.44	8.35	18.26	16.46
1.91925	.04627	-25.91	-6.6	13.00	-1.308	.00149	.04199	91117 2	-5208.1	-.942	7.38	8.29	18.19	16.41
1.91920	.04628	-23.40	29.3	-15.90	-.886	.00405	.04437	91118 2	-5172.6	-1.334	-19.70	-22.58	-12.39	-11.08
1.91920	.04624	-23.40	29.0	-16.21	-.881	.00405	.04437	91119 1	-5172.6	-1.338	-20.00	-22.91	-12.72	-11.38
1.91923	.04619	-24.94	6.5	0.00	-1.104	.00224	.04335	91120 1	-5185.6	-1.104	-4.74	-5.53	4.38	3.99
1.91925	.04620	-25.41	-.0	8.19	-1.227	.00168	.04253	91121 1	-5193.8	-.997	2.92	3.20	13.06	11.79
1.91922	.04618	-24.47	13.1	-5.28	-1.036	.00270	.04373	91122 1	-5177.6	-1.184	-9.73	-11.21	-1.18	-1.00
1.92388	.02866	-15.47	0.5	0.00	-.958	.00144	.02670	914 4 1	-3259.2	-.958	-4.17	-4.58	3.76	3.55
1.92389	.02857	-12.35	50.2	-25.05	-.703	.00263	.02718	914 5 1	-3203.3	-1.146	-29.12	-30.54	-22.29	-20.81
1.91942	.00315	-1.68	.8	0.00	-.496	.00023	.00273	928 9 1	-353.3	-.496	-2.29	-2.31	1.88	1.87
1.91942	.00315	-4.80	-43.8	20.99	-.395	.00014	.00247	92810 1	-397.8	-.356	19.17	19.34	22.49	22.33
1.91942	.00315	1.45	45.4	-21.22	-.364	.00022	.00248	92811 1	-308.7	-.406	-22.90	-23.11	-19.84	-19.69
1.91940	.00315	-4.80	-43.8	21.23	-.396	.00031	.00276	92812 1	-398.0	-.357	19.40	19.57	22.73	22.57
1.91940	.00315	1.45	45.4	-21.28	-.359	.00024	.00243	92813 1	-308.9	-.401	-22.93	-23.14	-19.92	-19.77
1.91936	.00317	-4.80	-43.8	21.35	-.395	.00030	.00263	92814 1	-399.6	-.354	19.53	19.70	22.84	22.68
1.91939	.00313	.51	31.8	-18.15	-.385	.00034	.00265	92815 1	-320.0	-.420	-19.92	-20.10	-16.69	-16.57
1.91939	.00313	-3.96	-36.6	17.86	-.416	.00041	.00310	92816 1	-382.3	-.383	15.94	16.08	19.44	19.30
1.91938	.00313	-.11	22.9	-15.73	-.405	.00038	.00276	92817 1	-329.0	-.435	-17.60	-17.76	-14.20	-14.10
1.91942	.00309	-3.24	-21.9	15.21	-.437	.00035	.00304	92818 1	-369.5	-.408	13.20	13.31	16.86	16.75
1.91937	.00314	-1.64	1.3	0.00	-.496	.00026	.00268	92819 1	-352.0	-.496	-2.29	-2.31	1.88	1.87
1.91935	.00312	-.70	14.5	-11.40	-.436	.00049	.00307	92820 1	-336.4	-.460	-13.42	-13.54	-9.74	-9.67
1.91939	.00307	-2.98	-12.7	11.05	-.453	.00036	.00310	92821 1	-357.9	-.433	8.96	9.03	12.76	12.68
1.91939	.00313	-.95	11.0	-8.90	-.457	.00030	.00267	92822 1	-340.8	-.474	-11.00	-11.10	-7.17	-7.11
1.91945	.00303	-2.33	-9.4	9.56	-.464	.00043	.00325	92823 1	-350.2	-.446	7.42	7.48	11.31	11.24
1.91937	.00311	-1.17	7.7	-6.78	-.406	.00034	.00282	92824 1	-341.7	-.479	-8.93	-9.01	-5.01	-4.98
1.91943	.00307	-2.11	-8.0	7.47	-.473	.00043	.00333	92825 1	-350.9	-.459	5.29	5.33	9.26	9.20
1.91940	.00313	-1.33	5.6	-5.09	-.474	.00040	.00303	92826 1	-346.0	-.484	-7.28	-7.34	-3.30	-3.27
1.91935	.00312	-1.95	-3.4	5.97	-.486	.00040	.00302	92827 1	-354.1	-.477	3.72	3.75	7.82	7.76
1.91936	.00313	-1.63	1.3	0.00	-.495	.00033	.00284	92828 1	-350.7	-.495	-2.28	-2.30	1.87	1.86
1.91946	.00322	-1.69	1.2	0.00	-.498	.00019	.00250	929 4 1	-361.6	-.498	-2.30	-2.32	1.89	1.88
1.91953	.00316	-5.75	-57.3	24.17	-.370	.00016	.00243	929 5 3	-412.9	-.325	22.46	22.65	25.57	25.39
1.91950	.00316	3.00	67.5	-26.82	-.308	.00019	.00242	929 6 3	-298.3	-.362	-28.24	-28.50	-25.65	-25.46
1.91947	.01928	-10.34	3.8	0.00	-.850	.00094	.01780	929 9 1	-2164.6	-.850	-3.82	-4.07	3.28	3.15
1.91947	.01931	-25.97	-218.8	93.26	-.956	.00059	.01664	92910 4	-2391.0	-.399	43.97	46.35	51.94	49.74
1.91950	.01924	5.23	226.3	-49.36	-.420	.00219	.01808	92911 3	-1938.2	-1.010	-51.26	-54.21	-47.76	-45.64
1.91953	.01923	-29.09	-264.0	81.84	-.944	.00055	.01641	92912 4	-2427.2	-.351	47.64	50.20	55.51	53.17
1.91951	.01925	-.96	137.3	-38.89	-.527	.00190	.01807	92913 3	-2028.6	-.988	-41.25	-43.61	-36.86	-35.22
1.91955	.01926	-19.72	-130.0	36.65	-.929	.00062	.01093	92914 4	-2297.2	-.504	32.49	34.24	40.23	38.52
1.91955	.01922	11.54	315.3	-58.13	-.333	.00247	.01807	92915 3	-1846.8	-1.031	-59.62	-63.05	-56.84	-54.30
1.91958	.01931	-10.35	3.9	0.00	-.852	.00096	.01782	92916 1	-2168.5	-.852	-3.82	-4.07	3.28	3.16
1.91966	.01929	-10.38	3.4	0.00	-.851	.00092	.01778	930 3 1	-2167.9	-.351	-3.82	-4.07	3.28	3.15

Appendix 1 (continued). Experimental Data.

TMEAN (K)	DT (K)	DZ (CM)	DP (PA)	V (CM/S)	Q2 (W/CM2)	DTOB (K)	DTIB (K)	DATENNMO	RDMU (PA)	Q1 (W/CM2)	VN2 (CM/S)	VN1 (CM/S)	VS2 (CM/S)	VS1 (CM/S)
1.91963	.01929	-17.25	-94.7	32.47	-.935	.00064	.01707	930 4 4	-2265.9	-.556	28.27	29.81	36.07	34.53
1.91962	.01925	-3.50	101.1	-34.51	-.564	.00176	.01803	930 5 3	-2065.0	-.972	-37.04	-39.16	-32.34	-30.91
1.91959	.01921	-15.07	-64.1	27.61	-.927	.00066	.01711	930 6 4	-2226.2	-.605	23.46	24.72	31.18	29.86
1.91961	.01919	-5.69	89.4	-29.27	-.612	.00159	.01795	930 7 3	-2090.1	-.956	-32.01	-33.84	-26.91	-25.72
1.91962	.01918	-13.80	-42.1	24.19	-.932	.00067	.01715	930 8 4	-2200.3	-.651	20.01	21.08	27.78	26.60
1.91958	.01918	-7.25	47.0	-24.89	-.648	.00152	.01794	930 9 3	-2111.1	-.940	-27.80	-29.39	-22.40	-21.41
1.91962	.01919	-10.31	3.5	0.00	-.851	.00092	.01768	93010 1	-2156.0	-.851	-3.82	-4.07	3.28	3.15
1.91945	.00318	-1.68	1.0	0.00	-.498	.00015	.00246	10 1 4 1	-356.7	-.498	-2.29	-2.32	1.89	1.87
1.91944	.00316	-3.24	-21.5	14.94	-.439	.00017	.00241	10 1 5 1	-376.7	-.410	12.92	13.03	16.61	16.49
1.91942	.00317	-.12	23.2	-16.24	-.405	.00019	.00243	10 1 6 1	-333.5	-.437	-18.10	-18.27	-14.70	-14.59
1.91960	.01927	-10.35	3.0	0.00	-.851	.00093	.01775	10 3 4 1	-2165.0	-.851	-3.82	-4.07	3.28	3.15
1.91962	.01925	-12.54	-27.3	21.14	-.933	.00067	.01733	10 3 5 1	-2193.8	-.686	16.95	17.86	24.73	23.68
1.91959	.01928	-8.26	34.9	-26.87	-.684	.00142	.01803	10 3 6 1	-2135.0	-.930	-23.94	-25.31	-18.23	-17.42
1.91965	.01929	-11.91	-18.5	18.27	-.930	.00078	.01745	10 3 7 1	-2189.7	-.715	14.11	14.86	21.85	20.92
1.91963	.01928	-8.79	26.3	-17.08	-.715	.00134	.01801	10 3 8 1	-2143.9	-.916	-20.29	-21.46	-14.33	-13.69
1.91965	.01927	-10.35	3.5	0.00	-.853	.00094	.01778	10 3 9 1	-2165.1	-.853	-3.82	-4.07	3.28	3.16
1.91971	.01930	-11.29	-9.6	12.77	-.916	.00076	.01757	10 310 1	-2182.2	-.766	8.66	9.11	16.30	15.60
1.91970	.01928	-9.42	17.1	-11.50	-.767	.00119	.01795	10 311 1	-2154.3	-.902	-14.93	-15.81	-8.54	-8.16
1.91974	.01923	-11.04	-6.6	10.41	-.912	.00073	.01756	10 312 1	-2171.5	-.790	6.32	6.64	13.93	13.34
1.91970	.01928	-9.67	13.4	-8.46	-.794	-.64072	.01792	10 313 1	-2156.6	-.894	-12.02	-12.73	-5.40	-5.14
1.91974	.01923	-10.83	-3.4	8.33	-.900	.00078	.01761	10 314 1	-2168.3	-.806	3.99	4.18	11.49	11.01
1.91973	.01928	-9.69	10.3	-6.34	-.816	.01805	.01789	10 315 1	-2159.8	-.887	-9.70	-10.28	-2.90	-2.76
1.91975	.01931	-10.37	3.7	0.00	-.853	.00097	.01781	10 316 1	-2170.3	-.853	-3.82	-4.07	3.29	3.16
1.91973	.01925	-10.08	-1.2	6.08	-.806	.00081	.01758	10 317 1	-2168.7	-.814	2.11	2.19	9.49	9.10
1.91976	.01931	-10.38	0.2	-4.30	-.828	.00104	.01788	10 318 1	-2165.8	-.879	-8.01	-8.49	-1.10	-1.04
1.91951	.00317	-1.69	.8	0.00	-.496	.00017	.00244	10 321 1	-356.3	-.496	-2.29	-2.31	1.88	1.87
1.91954	.00310	29.57	445.8	-69.64	-.031	.00026	.00243	10 322 3	96.9	-.194	-69.78	-70.54	-69.52	-68.91
1.91953	.00316	26.19	312.6	-58.56	-.059	.00026	.00244	10 323 3	-43.0	-.190	-58.83	-59.45	-58.34	-57.85
1.91955	.00316	13.94	223.5	-49.23	-.114	.00024	.00242	10 324 3	-131.9	-.219	-49.76	-50.26	-48.80	-48.41
1.91958	.00311	7.69	134.0	-38.01	-.201	.00016	.00237	10 325 3	-215.9	-.278	-38.94	-39.31	-37.25	-36.96
1.91959	.00314	5.19	98.6	-32.33	-.254	.00018	.00238	10 326 3	-255.1	-.319	-33.50	-33.81	-31.36	-31.13
1.91960	.00317	-1.68	.8	0.00	-.499	.00016	.00241	10 327 1	-355.4	-.499	-2.30	-2.32	1.89	1.88
1.90935	-.00003	.00	-.2	0.00	0.000	.00004	-.00052	9 2 1 1	3.1	0.000	0.00	0.00	0.00	0.00
1.90964	-.00001	.01	.1	0.00	0.000	.00005	-.00051	9 3 1 1	1.2	0.000	0.00	0.00	0.00	0.00
1.89614	.00003	.01	.3	0.00	0.000	.00008	-.00044	91123 1	-2.5	0.000	0.00	0.00	0.00	0.00
1.90503	.00003	-.00	.2	0.00	0.000	.00008	-.00050	91124 1	-2.6	0.000	0.00	0.00	0.00	0.00
1.91368	.00001	-.01	.0	0.00	0.000	.00004	-.00053	91125 1	-1.5	0.000	0.00	0.00	0.00	0.00
1.92229	.00002	-.01	.0	0.00	0.000	.00004	-.00058	91126 1	-2.0	0.000	0.00	0.00	0.00	0.00
1.93152	.00005	-.01	.2	0.00	0.000	.00002	-.00060	91127 1	-5.1	0.000	0.00	0.00	0.00	0.00
1.93971	.00002	-.01	-.1	0.00	0.000	-.00001	-.00066	91128 1	-1.9	0.000	0.00	0.00	0.00	0.00
1.94237	.00003	-.01	.1	0.00	0.000	-.00003	-.00068	91129 1	-3.5	0.000	0.00	0.00	0.00	0.00

Appendix 1 (continued). Experimental Data.

TMEAN (K)	DT (K)	DZ (CM)	DP (PA)	V (CM/S)	Q2 (W/CM2)	DTDB (K)	DTIB (K)	DATENNMO	RDMU (PA)	Q1 (W/CM2)	VN2 (CM/S)	VN1 (CM/S)	VS2 (CM/S)	VS1 (CM/S)
1.91272	.00002	-.01	.1	0.00	0.000	.00009	-.00046	914 1 1	-2.7	0.000	0.00	0.00	0.00	0.00
1.90418	.00001	-.01	.0	0.00	0.000	.00010	-.00044	914 2 1	-1.5	0.000	0.00	0.00	0.00	0.00
1.90949	.00003	-.01	.1	0.00	0.000	.00009	-.00046	914 3 1	-3.5	0.000	0.00	0.00	0.00	0.00
1.91367	-.00003	.02	.0	0.00	0.000	.00076	.00151	928 1 1	3.4	0.000	0.00	0.00	0.00	0.00
1.91506	-.00001	.02	.2	0.00	0.000	.00056	.00089	928 2 1	1.1	0.000	0.00	0.00	0.00	0.00
1.91640	.00001	.01	.2	0.00	0.000	.00041	.00040	928 3 1	-.7	0.000	0.00	0.00	0.00	0.00
1.91782	.00001	.01	.1	0.00	0.000	.00024	-.00002	928 4 1	-.6	0.000	0.00	0.00	0.00	0.00
1.91910	-.00001	.01	-.0	0.00	0.000	.00009	-.00041	928 5 1	1.7	0.000	0.00	0.00	0.00	0.00
1.92114	-.00002	.00	-.1	0.00	0.000	.00008	-.00042	928 6 1	2.5	0.000	0.00	0.00	0.00	0.00
1.92234	.00001	.00	.1	0.00	0.000	.00009	-.00041	928 7 1	-.8	0.000	0.00	0.00	0.00	0.00
1.91781	-.00000	.00	.0	0.00	0.000	.00011	-.00038	928 8 1	.3	0.000	0.00	0.00	0.00	0.00
1.91782	-.00003	.02	.1	0.00	0.000	.00016	-.00014	92829 1	3.3	0.000	0.00	0.00	0.00	0.00
1.91776	.00000	.00	.1	0.00	0.000	.00003	-.00056	929 1 1	-.0	0.000	0.00	0.00	0.00	0.00
1.91913	-.00001	.00	-.0	0.00	0.000	.00002	-.00057	929 2 1	.7	0.000	0.00	0.00	0.00	0.00
1.92119	-.00000	.00	.0	0.00	0.000	.00001	-.00058	929 3 1	.5	0.000	0.00	0.00	0.00	0.00
1.92902	-.00000	.00	.0	0.00	0.000	.00000	-.00062	929 7 1	.2	0.000	0.00	0.00	0.00	0.00
1.90981	-.00007	.01	-.3	0.00	0.000	-.00000	-.00055	929 8 1	7.2	0.000	0.00	0.00	0.00	0.00
1.92914	-.00004	-.02	-.0	0.00	0.000	-.00001	-.00064	930 1 1	3.8	0.000	0.00	0.00	0.00	0.00
1.90993	-.00003	-.01	-.1	0.00	0.000	.00005	-.00053	930 2 1	.2	0.000	0.00	0.00	0.00	0.00
1.91782	.00001	0.00	.1	0.00	0.000	-.00069	-.00057	10 1 3 1	-.7	0.000	0.00	0.00	0.00	0.00
1.89603	-.00001	536.12	7642.3	0.00	0.000	-.00010	-.00187	10 3 1 4	7643.8	0.000	0.00	0.00	0.00	0.00
1.92916	-.00004	-.02	-.5	0.00	0.000	-.00004	-.00070	10 3 2 1	4.1	0.000	0.00	0.00	0.00	0.00
1.90983	-.00002	-.01	-.3	0.00	0.000	.00005	-.00053	10 3 3 1	2.1	0.000	0.00	0.00	0.00	0.00
1.91788	-.00002	-.02	-.4	0.00	0.000	.00002	-.00060	10 319 1	2.2	0.000	0.00	0.00	0.00	0.00
1.92108	-.00002	-.02	-.4	0.00	0.000	-.00001	-.00062	10 320 1	1.6	0.000	0.00	0.00	0.00	0.00
1.66786	.02941	-8.25	2.4	0.00	-.660	.00161	.02840	9 2 7 1	-1526.5	-.660	-7.19	-8.07	1.98	1.96
1.66789	.02936	-5.13	[illegible]	-22.62	-.517	.00237	.02865	9 2 8 1	-1479.3	-.710	-28.25	-31.30	-21.07	-20.52
1.66791	.02940	-11.36	-42.1	21.65	-.708	.00123	.02782	9 2 9 1	-1570.4	-.525	13.93	15.23	23.77	23.20
1.64977	.01902	-4.92	3.2	0.00	-.544	.00096	.01837	925 6 1	-927.1	-.544	-6.49	-7.00	1.62	1.61
1.64976	.01897	-14.35	-135.4	35.78	-.501	.00076	.01785	925 7 4	-1058.1	-.320	29.80	31.66	37.27	36.72
1.64976	.01892	4.45	136.3	-36.76	-.319	.00151	.01838	925 8 3	-789.1	-.515	-40.57	-43.38	-35.81	-35.24
1.64978	.01891	-11.86	-35.0	30.64	-.514	.00076	.01786	925 9 4	-1019.8	-.357	24.51	26.04	32.16	31.69
1.64977	.01887	1.95	100.5	-32.12	-.354	.00140	.01833	92510 3	-822.5	-.524	-36.35	-38.86	-31.07	-30.58
1.64977	.01885	-4.38	3.2	0.00	-.546	.00094	.01819	92511 1	-918.9	-.546	-6.52	-7.02	1.62	1.61
1.64976	.01895	-4.91	3.1	0.00	-.545	.00094	.01830	92516 1	-923.7	-.545	-6.51	-7.02	1.62	1.61
1.64978	.01893	-7.10	-28.1	18.27	-.548	.00075	.01805	92517 1	-954.0	-.454	11.73	12.43	19.90	19.61
1.64975	.01894	-2.73	34.2	-18.70	-.448	.00122	.01839	92518 1	-892.0	-.546	-24.04	-25.72	-17.37	-17.08
1.64975	.01894	-7.10	-28.1	18.42	-.549	.00078	.01804	92519 1	-954.3	-.453	11.87	12.58	20.05	19.76
1.64973	.01888	-2.73	34.0	-18.58	-.449	.00120	.01835	92520 1	-889.3	-.546	-23.94	-25.60	-17.24	-16.96
1.64973	.01888	-7.10	-28.3	18.57	-.551	.00078	.01801	92521 1	-951.6	-.455	11.99	12.71	20.20	19.91
1.64974	.01887	-4.90	3.0	0.00	-.545	.00093	.01822	92522 1	-919.9	-.545	-6.51	-7.02	1.62	1.61
1.64975	.01886	-6.45	-19.2	15.82	-.554	.00086	.01805	92524 1	-941.9	-.473	9.21	9.74	17.47	17.22
1.64975	.01886	-3.34	25.2	-15.36	-.467	.00119	.01831	92525 1	-897.4	-.547	-20.94	-22.40	-13.97	-13.74
1.64977	.01881	-5.84	-10.6	12.51	-.558	.00085	.01805	92526 1	-930.6	-.494	5.85	6.16	14.17	13.97
1.64977	.01881	-3.95	16.1	-9.60	-.503	.00107	.01822	92527 1	-903.9	-.553	-15.61	-16.72	-8.11	-7.97
1.64979	.01876	-5.84	-10.7	12.54	-.559	.00079	.01799	92528 1	-928.4	-.494	5.88	6.19	14.20	14.00
1.64977	.01876	-4.21	12.4	-7.40	-.514	.00099	.01818	92529 1	-905.3	-.552	-13.54	-14.50	-5.87	-5.77
1.64979	.01874	-5.59	-7.3	10.64	-.562	.00080	.01800	92530 1	-923.7	-.507	3.93	4.11	12.31	12.14
1.64977	.01875	-4.87	3.0	0.00	-.545	.00091	.01816	92531 1	-914.1	-.545	-6.50	-7.01	1.62	1.61

Appendix 1 (continued). Experimental Data.

TMEAN (K)	DT (K)	DZ (CM)	DP (PA)	V (CM/S)	Q2 (W/CM2)	DTOB (K)	DTIB (K)	DATENNMO	RDMU (PA)	Q1 (W/CM2)	VN2 (CM/S)	VN1 (CM/S)	VS2 (CM/S)	VS1 (CM/S)
1.64976	.01874	-4.40	9.6	-5.53	-.524	.00100	.01818	92532 1	-906.9	-.552	-11.78	-12.63	-3.98	-3.90
1.64976	.01874	-5.34	-3.7	8.24	-.560	.00086	.01802	92533 1	-920.2	-.518	1.55	1.58	9.90	9.77
1.64977	.01872	-4.55	7.4	-3.88	-.532	.00095	.01814	92534 1	-908.5	-.552	-10.23	-10.98	-2.30	-2.25
1.64977	.01870	-5.18	-1.6	6.48	-.556	.00083	.01798	92535 1	-916.3	-.523	-.16	-.25	8.13	8.03
1.64977	.01869	-4.85	3.0	0.00	-.544	.00092	.01805	92536 1	-911.4	-.544	-6.50	-7.00	1.62	1.61
1.64983	.01909	-4.95	3.1	0.00	-.546	.00114	.01892	927 4 1	-931.1	-.546	-6.51	-7.02	1.62	1.61
1.64983	.01911	-23.71	-203.7	51.55	-.471	.00075	.01800	927 5 4	-1198.4	-.214	45.93	48.80	52.95	52.19
1.64983	.01911	16.93	314.5	-56.61	-.166	.00219	.01920	927 6 3	-620.3	-.481	-58.59	-62.80	-56.12	-55.19
1.64983	.01911	10.65	225.5	-46.55	-.244	.00196	.01903	927 7 3	-709.2	-.499	-49.46	-52.97	-45.83	-45.08
1.64991	.01908	-20.58	-219.3	46.49	-.479	.00079	.01805	927 8 4	-1152.9	-.246	40.78	43.33	47.91	47.22
1.64991	.01909	-.27	89.8	-26.99	-.394	.00139	.01863	927 9 3	-864.1	-.537	-31.69	-33.91	-25.82	-25.40
1.64993	.01910	-9.64	-63.6	25.74	-.531	.00080	.01820	92710 3	-998.3	-.398	19.40	20.62	27.32	26.92
1.64993	.01910	-9.64	-62.6	25.18	-.529	.00080	.01820	92711 4	-998.3	-.398	18.87	20.05	26.75	26.35
1.64997	.01906	20.31	447.7	-67.54	-.095	.00272	.01993	92712 3	-435.2	-.479	-68.67	-73.70	-67.26	-66.13
1.65001	.01913	-8.63	-41.2	21.66	-.547	.00110	.01894	92713 1	-977.7	-.433	15.34	16.28	23.49	23.14
1.65001	.01913	-.34	2.9	0.00	-.547	.00104	.01870	92714 1	-933.5	-.547	-6.53	-7.04	1.63	1.62
1.65001	.01913	-1.33	+7.6	-21.90	-.430	-.37111	-.37111	92715 1	-888.7	-.546	-27.03	-28.92	-20.62	-20.29
1.65296	.00000	.02	.2	0.00	0.000	.00001	.00014	9 2 6 1	.1	0.000	0.00	0.00	0.00	0.00
1.68352	.00003	.01	.2	0.00	0.000	.00007	-.41417	9 210 1	-1.3	0.000	0.00	0.00	0.00	0.00
1.65923	-.00000	.00	.3	0.00	0.000	-.00001	.00017	925 1 1	.2	0.000	0.00	0.00	0.00	0.00
1.65463	.00004	.00	.2	0.00	0.000	-.00000	.00016	925 2 1	-1.6	0.000	0.00	0.00	0.00	0.00
1.64993	.00001	.01	.1	0.00	0.000	-.00004	.00015	925 3 1	-.3	0.000	0.00	0.00	0.00	0.00
1.64524	.00001	.01	.1	0.00	0.000	-.00003	.00016	925 4 1	-.4	0.000	0.00	0.00	0.00	0.00
1.64026	.00001	.01	.1	0.00	0.000	-.00005	.00016	925 5 1	-.2	0.000	0.00	0.00	0.00	0.00
1.64024	.00001	0.00	.0	0.00	0.000	-.00002	.00023	92512 1	-.4	0.000	0.00	0.00	0.00	0.00
1.64990	-.00001	-.00	-.1	0.00	0.000	-.00002	.00020	92513 1	.2	0.000	0.00	0.00	0.00	0.00
1.65941	.00004	-.01	.1	0.00	0.000	.00004	.00021	92514 1	-1.8	0.000	0.00	0.00	0.00	0.00
1.64020	.00002	-.00	.0	0.00	0.000	-.00004	.00018	92515 1	-.9	0.000	0.00	0.00	0.00	0.00
1.65921	-.00001	.00	-.0	0.00	0.000	.00061	.00170	927 1 1	.7	0.000	0.00	0.00	0.00	0.00
1.64971	-.00002	.00	-.0	0.00	0.000	.00020	.00069	927 2 1	1.0	0.000	0.00	0.00	0.00	0.00
1.64024	-.00003	.01	-.0	0.00	0.000	.00009	.00050	927 3 1	1.2	0.000	0.00	0.00	0.00	0.00
1.63985	-.00002	-.01	-.2	0.00	0.000	-.00009	.00012	10 1 1 1	.7	0.000	0.00	0.00	0.00	0.00
1.63997	-.00001	-.01	-.2	0.00	0.000	-.00011	.00009	10 1 2 1	.4	0.000	0.00	0.00	0.00	0.00
1.39517	.01926	-1.80	3.9	0.00	-.231	.00102	.01785	9 3 8 1	-357.6	-.231	-8.42	-9.25	.69	.69
1.39520	.01926	-4.93	-40.5	18.71	-.208	.00101	.01768	9 3 9 1	-402.0	-.169	11.12	11.93	19.33	19.22
1.39519	.01925	1.33	48.3	-18.25	-.158	.00130	.01786	9 310 1	-312.9	-.198	-24.02	-26.19	-17.78	-17.66
1.39534	.01940	-1.82	3.9	0.00	-.231	.00102	.01804	9 4 2 1	-360.5	-.231	-8.41	-9.25	.69	.69
1.39539	.01949	-8.07	-84.9	26.24	-.182	.00102	.01776	9 4 3 1	-451.1	-.127	19.62	21.14	26.78	26.62
1.39539	.01949	-8.07	-84.3	26.70	-.186	.00102	.01776	9 4 4 3	-451.1	-.130	19.95	21.49	27.25	27.09
1.39539	.01949	-8.07	-84.9	25.97	-.181	.00102	.01776	9 4 5 3	-451.1	-.127	19.37	20.87	26.51	26.35
1.39538	.01954	4.43	92.9	-30.87	-.108	.00144	.01818	9 4 6 3	-274.0	-.178	-34.81	-38.01	-30.55	-30.34
1.39538	.01954	4.43	92.9	-27.20	-.118	.00144	.01818	9 4 7 3	-274.0	-.180	-31.50	-34.40	-26.85	-26.66
1.39538	.01954	4.43	92.9	-25.57	-.122	.00144	.01818	9 4 8 1	-274.0	-.180	-30.01	-32.78	-25.21	-25.03
1.39561	.01983	-14.35	-173.7	37.15	-.154	.00091	.01794	9 4 9 4	-546.4	-.078	31.56	34.01	37.60	37.38
1.39557	.01963	10.65	161.9	-38.86	-.064	.00167	.01858	9 410 3	-190.9	-.157	-41.18	-45.14	-38.67	-38.39
1.39567	.02003	23.16	359.9	-55.62	-.008	.00242	.01936	9 411 3	-16.7	-.152	-55.89	-61.69	-55.60	-55.16

Appendix 1 (continued). Experimental Data.

TMEAN (K)	DT (K)	DZ (CM)	DP (PA)	V (CM/S)	Q2 (W/CM2)	DTOB (K)	DTIB (K)	DATENNMO	RDMU (PA)	Q1 (W/CM2)	VN2 (CM/S)	VN1 (CM/S)	VS2 (CM/S)	VS1 (CM/S)
1.39572	.02007	-18.73	-235.5	43.71	-.144	.00076	.01806	9 412 4	-613.0	-.057	38.48	41.43	44.14	43.88
1.39569	.02001	16.91	271.0	-48.18	-.029	.00199	.01886	9 413 3	-105.4	-.150	-49.25	-54.18	-48.10	-47.74
1.39551	.01957	-11.18	-129.0	31.76	-.164	.00096	.01782	9 415 4	-496.7	-.099	25.79	27.78	32.25	32.06
1.39553	.01964	16.95	271.1	-46.67	-.031	.00197	.01852	9 416 3	-98.0	-.145	-47.78	-52.48	-46.58	-46.23
1.39555	.01969	-15.87	-195.4	39.56	-.152	.00086	.01782	9 417 4	-565.6	-.073	34.03	36.63	40.02	39.78
1.39546	.01961	7.57	137.7	-32.97	-.091	.00156	.01828	9 418 3	-230.8	-.167	-36.28	-39.67	-32.70	-32.47
1.39538	.01945	-1.61	4.0	0.00	-.233	.00102	.01804	9 419 1	-361.4	-.233	-8.47	-9.32	.69	.70
1.39551	.01959	-6.50	-82.4	22.73	-.194	.00112	.01791	9 420 1	-430.5	-.146	15.69	16.90	23.30	23.16
1.39553	.01972	-.25	26.7	-12.84	-.188	.00122	.01835	9 421 1	-344.0	-.217	-19.68	-21.52	-12.28	-12.19
1.39557	.01977	-3.38	-17.7	13.28	-.226	.00104	.01824	9 422 1	-389.4	-.197	5.08	5.40	13.95	13.87
1.39559	.01980	2.88	71.2	-22.41	-.140	.00141	.01842	9 423 1	-301.0	-.191	-27.50	-30.07	-21.99	-21.83
1.39563	.01984	-2.44	-4.2	8.63	-.236	.00115	.01835	9 424 1	-377.3	-.217	.06	-.06	9.33	9.28
1.39565	.01992	-1.19	13.7	-6.55	-.216	.00115	.01856	9 425 1	-360.9	-.231	-14.39	-15.79	-5.90	-5.85
1.39569	.02001	-2.13	.5	4.57	-.236	.00108	.01856	9 426 1	-376.0	-.226	-3.98	-4.46	5.27	5.25
1.39574	.02004	-1.50	9.4	-4.13	-.223	.00111	.01868	9 427 1	-367.6	-.233	-12.24	-13.45	-3.47	-3.43
1.39580	.02007	-1.90	3.8	0.00	-.235	.00106	.01864	9 428 1	-373.8	-.235	-8.51	-9.39	.70	.70
1.39620	.02115	-2.04	3.6	0.00	-.238	.00115	.01971	9 8 5 1	-395.0	-.238	-8.60	-9.55	.71	.71
1.39517	.01902	-1.80	3.6	0.00	-.229	.00098	.01764	9 8 6 1	-353.4	-.229	-8.35	-9.18	.68	.69
1.39528	.01915	-8.06	-85.2	27.08	-.181	.00090	.01742	9 8 7 3	-444.8	-.126	20.48	22.04	27.62	27.46
1.39538	.01930	4.45	92.8	-27.72	-.117	.00138	.01791	9 8 8 3	-269.7	-.179	-31.98	-34.89	-27.37	-27.18
1.39574	.05517	-5.61	5.1	0.00	-.326	.00385	.05295	9 8 9 1	-1032.9	-.326	-10.86	-14.24	.96	.99
1.39577	.05523	-24.35	-201.5	47.46	-.381	.00158	.04926	9 810 4	-1300.6	-.102	34.74	43.00	48.59	47.77
1.39580	.05523	10.02	227.4	-44.54	-.104	.00963	.05371	9 811 3	-811.8	-.388	-48.00	-61.50	-44.23	-43.37
1.39580	.05523	-27.49	-305.9	49.92	-.387	.00154	.04890	9 812 4	-1345.1	-.096	36.99	45.72	51.06	50.21
1.39583	.05528	16.27	316.3	-53.55	-.059	.01128	.05397	9 813 3	-724.0	-.406	-55.53	-71.30	-53.37	-52.32
1.39593	.05533	3.77	138.7	-34.66	-.159	.00804	.05368	9 814 3	-903.0	-.377	-39.96	-51.16	-34.19	-33.52
1.39580	.05516	-5.61	5.0	0.00	-.326	.00386	.05288	9 816 1	-1032.8	-.326	-10.89	-14.27	.96	.99
1.39585	.05515	-14.99	-128.3	33.45	-.371	.00212	.05063	9 817 4	-1166.2	-.170	21.08	26.02	34.55	33.97
1.39585	.05521	1.27	102.9	-29.88	-.186	.00726	.05349	9 818 3	-936.2	-.373	-36.08	-46.17	-29.33	-28.75
1.39589	.05525	-12.49	-92.5	28.30	-.368	.00224	.05109	9 819 4	-1132.5	-.196	16.04	19.72	29.38	28.89
1.39580	.05525	17.11	324.1	0.00	-.327	.00385	.05298	9 9 1 1	-711.6	-.327	-10.91	-14.32	.97	.99
1.39578	.05513	-5.59	5.2	0.00	-.327	.00383	.05286	9 9 2 1	-1032.0	-.327	-10.92	-14.31	.97	.99
1.39577	.05511	-5.59	5.3	0.00	-.327	.00377	.05284	9 9 3 1	-1031.7	-.327	-10.92	-14.31	.97	.99
1.39574	.05497	-10.28	-61.6	24.32	-.367	.00253	.05122	9 9 4 1	-1095.8	-.220	12.05	14.69	25.40	24.98
1.39573	.05493	-.90	71.7	-23.44	-.218	.00654	.05318	9 9 5 1	-961.7	-.363	-30.71	-39.29	-22.80	-22.34
1.39496	.05422	-5.46	5.4	0.00	-.323	.00374	.05198	9 911 1	-1011.3	-.323	-10.84	-14.15	.95	.98
1.39494	.05424	-8.59	-39.0	20.32	-.362	.00253	.05080	9 912 1	-1055.9	-.240	8.19	9.80	21.39	21.05
1.39495	.05431	-2.34	50.0	-19.08	-.239	.00593	.05253	9 913 1	-968.3	-.355	-27.09	-34.62	-18.38	-18.01
1.39499	.05431	-5.46	5.6	0.00	-.324	.00379	.05207	9 914 1	-1012.8	-.324	-10.88	-14.21	.96	.98
1.39499	.05432	-7.65	-25.5	17.64	-.363	.00250	.05102	9 915 1	-1044.2	-.257	5.47	6.38	18.72	18.42
1.39499	.05434	-3.27	36.7	-15.98	-.255	.00557	.05251	9 916 1	-982.2	-.352	-24.54	-31.41	-15.23	-14.92
1.39501	.05435	-7.02	-16.6	15.59	-.362	.00260	.05118	9 917 1	-1035.9	-.268	3.45	3.84	16.66	16.40
1.39504	.05435	-3.90	27.8	-12.91	-.270	.00517	.05251	9 918 1	-991.5	-.348	-21.96	-28.16	-12.11	-11.86
1.39505	.05437	-5.46	5.6	0.00	-.325	.00379	.05211	9 919 1	-1014.3	-.325	-10.90	-14.24	.96	.98
1.39504	.05433	-6.40	-7.8	12.07	-.357	.00271	.05141	9 920 1	-1026.9	-.284	.10	-.37	13.12	12.93
1.39507	.05437	-4.53	19.0	-8.56	-.290	.00471	.05245	9 921 1	-1000.9	-.342	-18.30	-23.56	-7.70	-7.53
1.39505	.05437	-6.15	-4.2	9.92	-.351	.00298	.05159	9 922 1	-1024.0	-.292	-1.87	-2.86	10.96	10.80
1.39508	.05439	-4.78	15.4	-6.65	-.300	.00445	.05241	9 923 1	-1004.8	-.340	-16.71	-21.55	-5.77	-5.62
1.39506	.05439	-5.48	5.5	0.00	-.325	.00378	.05213	9 924 1	-1014.7	-.325	-10.89	-14.22	.96	.98
1.39509	.05440	-5.95	-1.2	7.21	-.343	.00309	.05176	9 925 1	-1021.7	-.300	-4.29	-5.91	8.23	8.12
1.39513	.05439	-5.01	12.2	-4.86	-.308	.00426	.05237	9 926 1	-1008.4	-.337	-15.17	-19.62	-3.95	-3.84
1.39511	.05441	-5.73	1.1	4.98	-.337	.00323	.05188	9 927 1	-1019.8	-.307	-6.32	-8.46	5.97	5.90
1.39513	.05441	-5.16	10.0	-3.61	-.314	.00415	.05232	9 928 1	-1010.9	-.336	-14.13	-18.30	-2.68	-2.59

TMEAN (K)	DT (K)	DZ (CM)	DP (PA)	V (CM/S)	Q2 (W/CM2)	DTOB (K)	DTIB (K)	DATENNMO	ROMU (PA)	Q1 (W/CM2)	VN2 (CM/S)	VN1 (CM/S)	VS2 (CM/S)	VS1 (CM/S)
1.39512	.05443	-5.49	5.3	0.00	-.325	.00378	.05217	9 929 1	-1015.8	-.325	-10.88	-14.22	.96	.98
1.39531	.01924	-1.79	4.0	0.00	-.231	.00154	.01903	915 8 1	-357.2	-.231	-8.41	-9.25	.69	.69
1.39530	.01917	-4.91	-6.5	18.95	-.206	.00128	.01841	915 9 1	-400.4	-.167	11.43	12.26	19.56	19.45
1.39529	.01918	1.34	46.4	-18.46	-.158	.00199	.01954	91510 1	-311.8	-.198	-24.22	-26.41	-17.99	-17.87
1.39344	.00128	-.04	1.3	0.00	-.093	.00048	.00214	91512 1	-22.5	-.093	-3.58	-3.61	.28	.28
1.39343	.00125	3.08	45.7	-18.09	-.003	.00050	.00215	91513 1	22.4	-.006	-18.21	-18.34	-18.08	-18.07
1.39346	.00128	-.05	1.1	0.00	-.093	.00005	.00105	91516 1	-22.7	-.093	-3.57	-3.60	.28	.28
1.39347	.00128	18.70	267.7	-48.88	.019	.00014	.00102	91517 3	244.0	-.001	-48.17	-48.93	-48.94	-48.88
1.39349	.00130	12.44	178.9	-39.35	.014	.00003	.00091	91518 3	154.7	.001	-38.83	-39.31	-39.39	-39.36
1.39349	.00127	-.05	1.2	0.00	-.095	-.00003	.00088	91519 1	-22.4	-.095	-3.65	-3.67	.28	.28
1.39349	.00123	-.05	1.1	0.00	-.093	.00034	.00181	916 5 1	-21.8	-.093	-3.58	-3.61	.28	.28
1.39350	.00124	-1.62	-21.1	12.10	-.333	.00031	.00166	916 6 1	-44.9	-.032	10.83	10.88	12.20	12.19
1.39352	.00124	1.51	23.3	-12.52	-.017	.00045	.00203	916 7 1	.2	-.019	-13.19	-13.27	-12.47	-12.47
1.39351	.00123	-.05	1.1	0.00	-.093	.00034	.00178	916 8 1	-21.8	-.093	-3.58	-3.61	.28	.28
1.39347	.00123	-.99	-12.2	8.79	-.057	.00037	.00167	916 9 1	-35.1	-.056	6.59	6.62	8.96	8.96
1.39351	.00123	.88	14.4	-9.01	-.047	.00037	.00175	91610 1	-8.4	-.048	-10.80	-10.87	-8.87	-8.86
1.39348	.00118	-.74	-8.7	7.24	-.065	.00036	.00170	91611 1	-30.8	-.064	4.76	4.77	7.43	7.43
1.39345	.00115	.63	10.8	-7.34	-.054	.00041	.00177	91612 1	-10.6	-.055	-9.43	-9.48	-7.18	-7.17
1.39345	.00109	-.04	1.0	0.00	-.090	.00033	.00163	91613 1	-19.3	-.090	-3.44	-3.46	.27	.27
1.39349	.00125	-.05	1.1	0.00	-.093	.00034	.00175	91616 1	-22.2	-.093	-3.57	-3.59	.28	.28
1.39349	.00121	-.74	-8.7	7.46	-.065	.00038	.00171	91617 1	-31.3	-.064	4.98	5.00	7.65	7.65
1.39348	.00120	.63	10.8	-7.26	-.057	.00035	.00171	91618 1	-11.5	-.058	-9.44	-9.49	-7.10	-7.09
1.39350	.00118	-.37	-3.4	4.84	-.077	.00039	.00172	91619 1	-25.4	-.076	1.90	1.91	5.07	5.07
1.39349	.00118	.25	5.5	-3.96	-.076	.00034	.00171	91620 1	-16.6	-.077	-6.89	-6.92	-3.73	-3.73
1.39351	.00114	-.04	1.1	0.00	-.091	.00032	.00168	91621 1	-20.1	-.091	-3.49	-3.51	.27	.27
1.39352	.00119	-.36	-3.3	4.84	-.076	.00038	.00167	91622 1	-25.5	-.076	1.91	1.92	5.06	5.06
1.39348	.00114	.27	5.6	-4.05	-.075	.00033	.00165	91623 1	-15.7	-.075	-6.92	-6.96	-3.82	-3.82
1.39353	.00115	-.51	-5.5	5.88	-.071	.00036	.00166	91624 1	-27.0	-.071	3.14	3.15	6.09	6.09
1.39356	.00119	.43	7.9	-5.54	-.067	.00037	.00171	91625 1	-14.4	-.068	-8.13	-8.17	-5.34	-5.33
1.39355	.00116	-.04	1.1	0.00	-.092	.00030	.00166	91626 1	-20.5	-.092	-3.54	-3.56	.28	.28
1.39347	.00117	-.05	1.0	0.00	-.092	-.00010	.00072	10 330 1	-20.9	-.092	-3.53	-3.55	.27	.27
1.39375	.00141	24.95	396.9	-56.61	.019	.00016	.00107	10 331 3	330.6	-.010	-55.89	-57.00	-56.67	-56.58
1.39382	.00141	6.82	99.1	-28.92	.006	-.00008	.00094	10 332 3	72.7	-.001	-28.69	-28.97	-28.93	-28.91
1.39387	.00149	9.32	134.8	-34.16	.010	-.00005	.00103	10 333 3	107.0	-.000	-33.79	-34.18	-34.19	-34.16
1.39384	.00146	-.05	1.4	0.00	-.099	-.00010	.00098	10 334 3	-25.9	-.099	-3.81	-3.84	.30	.30
1.39349	.00134	-.04	1.5	0.00	-.096	-.00009	.00087	10 5 3 1	-23.5	-.096	-3.67	-3.70	.29	.29
1.39357	.00127	-.04	1.4	0.00	-.094	-.00010	.00079	10 5 4 1	-22.3	-.094	-3.61	-3.63	.28	.28
1.39360	.00125	24.97	396.9	-56.67	.019	.00013	.00089	10 5 5 3	333.7	-.009	-55.92	-57.00	-56.73	-56.64
1.39357	.00121	15.59	223.5	-44.13	.015	-.00003	.00079	10 5 6 3	200.9	-.001	-43.57	-44.17	-44.18	-44.13
1.39357	.00124	9.34	134.7	-33.06	.009	-.00006	.00079	10 5 7 3	111.5	-.000	-32.72	-33.06	-33.08	-33.06
1.39362	.00126	9.34	134.7	-33.93	.010	-.00008	.00077	10 5 8 3	110.9	.001	-33.54	-33.90	-33.96	-33.93
1.39360	.00128	6.84	99.2	-28.83	.007	-.00010	.00079	10 5 9 3	75.3	.000	-28.55	-28.81	-28.85	-28.83
1.39361	.00125	2.15	32.5	-15.04	-.011	-.00009	.00077	10 510 1	9.1	-.013	-15.45	-15.55	-15.00	-15.00
1.39364	.00126	-.04	1.3	0.00	-.094	-.00009	.00077	10 511 1	-22.2	-.094	-3.61	-3.63	.28	.28
1.39515	.01910	-1.78	3.9	0.00	-.231	.00095	.01771	10 514 1	-354.5	-.231	-8.42	-9.25	.69	.69
1.39519	.01924	-3.35	-18.1	13.80	-.222	.00083	.01765	10 515 1	-379.3	-.193	5.70	6.06	14.46	14.38
1.39515	.01925	-.22	26.3	-12.88	-.188	.00118	.01786	10 516 1	-334.9	-.216	-19.75	-21.55	-12.32	-12.24
1.39522	.01920	-2.72	-9.3	10.99	-.229	.00088	.01765	10 517 1	-369.7	-.206	2.65	2.76	11.67	11.61
1.39519	.01923	-.85	17.4	-8.80	-.207	.00112	.01783	10 518 1	-343.6	-.226	-16.35	-17.86	-8.18	-8.12
1.39518	.01917	-1.80	3.8	0.00	-.232	.00098	.01776	10 519 1	-356.0	-.232	-8.44	-9.28	.69	.69
1.39518	.01920	-2.27	-2.8	8.12	-.234	.00092	.01770	10 520 1	-353.2	-.217	-.40	-.56	8.82	8.77

Appendix 1 (continued). Experimental Data.

TMEAN (K)	DT (K)	DZ (CM)	DP (PA)	V (CM/S)	Q2 (W/CM2)	DTOB (K)	DTIB (K)	DATENNMO	RDMU (PA)	Q1 (W/CM2)	VN2 (CM/S)	VN1 (CM/S)	VS2 (CM/S)	VS1 (CM/S)
1.39514	.01920	-1.33	10.5	-4.87	-.219	.00104	.01783	10 521 1	-349.9	-.230	-12.87	-14.08	-4.22	-4.18
1.39517	.01918	-3.35	-18.4	13.88	-.222	-.11624	.01755	10 522 1	-378.3	-.192	5.79	6.16	14.54	14.45
1.39516	.01909	-1.79	3.8	0.00	-.231	.00095	.01766	10 523 1	-354.6	-.231	-8.42	-9.25	.69	.69
1.40459	-.00002	-.01	-.1	0.00	0.000	-.00051	-.00067	9 3 2 1	.3	0.000	0.00	0.00	0.00	0.00
1.39974	.00010	-.01	.1	0.00	0.000	-.00031	-.00049	9 3 3 1	-1.9	0.000	0.00	0.00	0.00	0.00
1.39487	-.00000	-.01	-.1	0.00	0.000	-.00012	-.00041	9 3 4 1	-.1	0.000	0.00	0.00	0.00	0.00
1.39015	.00001	-.00	-.0	0.00	0.000	-.00003	-.00033	9 3 5 1	-.2	0.000	0.00	0.00	0.00	0.00
1.38551	-.00003	-.00	-.1	0.00	0.000	-.00007	-.00044	9 3 6 1	.5	0.000	0.00	0.00	0.00	0.00
1.40481	-.00003	-.00	-.1	0.00	0.000	-.00051	-.00064	9 3 7 1	.5	0.000	0.00	0.00	0.00	0.00
1.38561	.00001	.01	.1	0.00	0.000	-.00004	-.00040	9 4 1 1	-.1	0.000	0.00	0.00	0.00	0.00
1.40497	-.00004	.03	.3	0.00	0.000	-.00053	-.00070	9 414 1	1.1	0.000	0.00	0.00	0.00	0.00
1.38561	.00000	-.01	-.1	0.00	0.000	-.00003	-.00040	9 429 1	-.2	0.000	0.00	0.00	0.00	0.00
1.40484	.00004	-.02	-.3	0.00	0.000	-.00054	-.00070	9 8 1 1	-1.0	0.000	0.00	0.00	0.00	0.00
1.38556	.00004	-.02	-.2	0.00	0.000	-.00003	-.00045	9 8 2 1	-.9	0.000	0.00	0.00	0.00	0.00
1.36775	.00006	-.02	-.1	0.00	0.000	.00003	-.00065	9 8 3 1	-1.1	0.000	0.00	0.00	0.00	0.00
1.42185	-.00000	-.02	-.3	0.00	0.000	-.00054	-.00045	9 8 4 1	-.3	0.000	0.00	0.00	0.00	0.00
1.38681	-.00002	.00	.0	0.00	0.000	.00001	-.00062	9 9 6 1	.3	0.000	0.00	0.00	0.00	0.00
1.42190	.00001	-.00	-.0	0.00	0.000	-.00053	-.00050	9 9 7 1	-.1	0.000	0.00	0.00	0.00	0.00
1.40485	.00001	0.00	.0	0.00	0.000	-.00051	-.00065	9 9 8 1	-.2	0.000	0.00	0.00	0.00	0.00
1.38561	.00005	.00	.1	0.00	0.000	-.00003	-.00040	9 9 9 1	-.8	0.000	0.00	0.00	0.00	0.00
1.38785	.00002	.00	.1	0.00	0.000	.00004	-.00061	9 910 1	-.2	0.000	0.00	0.00	0.00	0.00
1.40487	-.00001	.00	.0	0.00	0.000	-.00032	-.00021	915 1 1	.3	0.000	0.00	0.00	0.00	0.00
1.40009	.00013	.00	.3	0.00	0.000	-.00002	.00018	915 2 1	-2.3	0.000	0.00	0.00	0.00	0.00
1.39519	.00000	.01	.1	0.00	0.000	.00027	.00062	915 3 1	.0	0.000	0.00	0.00	0.00	0.00
1.39528	-.00002	.01	.1	0.00	0.000	.00047	.00120	915 4 1	.4	0.000	0.00	0.00	0.00	0.00
1.39057	.00001	.01	.1	0.00	0.000	.00062	.00130	915 5 1	-.0	0.000	0.00	0.00	0.00	0.00
1.38588	.00005	.01	.2	0.00	0.000	.00058	.00112	915 6 1	-.7	0.000	0.00	0.00	0.00	0.00
1.38564	-.00000	.01	.1	0.00	0.000	.00049	.00093	915 7 1	.2	0.000	0.00	0.00	0.00	0.00
1.39276	.00003	.01	.2	0.00	0.000	.00047	.00093	91511 1	-.4	0.000	0.00	0.00	0.00	0.00
1.39282	.00006	536.02	7620.2	0.00	0.000	.00008	.00016	91514 1	7619.0	0.000	0.00	0.00	0.00	0.00
1.39282	-.00000	-.00	-.0	0.00	0.000	.00003	-.00009	91515 1	.0	0.000	0.00	0.00	0.00	0.00
1.39286	-.00002	-.01	-.1	0.00	0.000	.00034	.00071	916 1 1	.3	0.000	0.00	0.00	0.00	0.00
1.39374	-.00001	-.01	-.1	0.00	0.000	.00031	.00072	916 2 1	.0	0.000	0.00	0.00	0.00	0.00
1.39467	.00001	-.01	-.1	0.00	0.000	.00030	.00071	916 3 1	-.2	0.000	0.00	0.00	0.00	0.00
1.39293	.00000	-.00	-.0	0.00	0.000	.00028	.00065	916 4 1	-.1	0.000	0.00	0.00	0.00	0.00
1.39293	.00001	-.00	-.0	0.00	0.000	.00027	.00057	91614 1	-.3	0.000	0.00	0.00	0.00	0.00
1.39289	-.00001	-.00	-.1	0.00	0.000	.00029	.00059	91615 1	.1	0.000	0.00	0.00	0.00	0.00
1.39291	-.00001	0.00	-.0	0.00	0.000	.00029	.00057	91627 1	.1	0.000	0.00	0.00	0.00	0.00
1.39412	-.00000	0.00	-.0	0.00	0.000	.00025	.00057	91628 1	.0	0.000	0.00	0.00	0.00	0.00
1.39278	-.00002	.00	.0	0.00	0.000	-.00011	-.00042	10 328 1	.3	0.000	0.00	0.00	0.00	0.00

Appendix 1 (continued). Experimental Data.

TMEAN (K)	DT (K)	DZ (CM)	DF (PA)	V (CM/S)	Q2 (W/CM2)	DTOB (K)	DTIB (K)	DATENNMO	ROMU (PA)	Q1 (W/CM2)	VN2 (CM/S)	VN1 (CM/S)	VS2 (CM/S)	VS1 (CM/S)
1.39424	-.00003	.03	-.0	0.00	0.000	-.00014	-.00043	10 329 1	.6	0.000	0.00	0.00	0.00	0.00
1.39413	-.00002	.02	.2	0.00	0.000	-.00016	-.00042	10 5 1 1	.6	0.000	0.00	0.00	0.00	0.00
1.39286	-.00005	.02	.2	0.00	0.000	-.00019	-.00046	10 5 2 1	1.1	0.000	0.00	0.00	0.00	0.00
1.40463	-.00004	0.00	-.1	0.00	0.000	-.00057	-.00073	10 512 1	.7	0.000	0.00	0.00	0.00	0.00
1.38552	-.00002	.00	.0	0.00	0.000	-.00012	-.00049	10 513 1	.4	0.000	0.00	0.00	0.00	0.00

APPENDIX 2

The purpose of this appendix is to prove the assertion that the formulas already given for the overall energy balance and energy flux -- in particular eq (36) -- are still correct when the gravitational and work terms are taken into account. Our procedure is as before, i.e., equating the change in energy calculated by two different methods.

In the first method, we calculate the change in the total energy E of the helium contained within the control volume (the inside vessel), due to the increment in its mass, when the temperature is held constant. It is

$$dE = dU + dE_{grav} \tag{A2.1}$$

where dE_{grav} is the change in the gravitational potential energy, and dU is again the change in internal energy of the helium.

We can prove that the variation of u within the liquid is negligible, by considering its variation with depth,

$$\frac{du}{dz} = \left(\frac{\partial u}{\partial T}\right)_P \frac{dT}{dz} + \left(\frac{\partial u}{\partial P}\right)_T \frac{dP}{dz} \tag{A2.2}$$

For equilibrium within the control volume, with a gravitational field present, we still have $dT = 0$, but now $dP/dz = -\rho g$, i.e., the pressure varies with depth within the liquid. However, using the measured values of expansivity and compressibility for the liquid to evaluate the size of the pressure derivative, we find that

$$\frac{du}{dz} = -\rho\left(\frac{\partial u}{\partial P}\right)_T g$$

is much smaller (< 1%) than the corresponding variation of the gravitational potential energy density with depth (= d(gz)/dz = g), so that it can be safely neglected.

Since u everywhere within the liquid has nearly the same value that it has at the surface, we can repeat the entire argument used to eliminate from dU any explicit dependence on the vapor; we obtain the same equations [eqs (31) - (35)], as long as we realize that the pressure in eq (33) is the pressure of the vapor. Therefore, eq (35) is still valid if we evaluate the enthalpy of the liquid at the pressure of the surface, which we designate as P'_2.

We may evaluate the change in the gravitational potential, without loss of generality, by assuming the inside space to have a constant horizontal cross-section A_i, and by evaluating the gain or loss of liquid at the surface (altitude z_2) and at the bottom of the inside space (altitude z_b). It is

$$dE_{grav} = g(z_2 \rho A_i dz_2 - z_b \rho A_i dz_b) \tag{A2.3}$$

We can express this differently by using eq (28) and the identities $dz_2/dt = V_i$ and $dz_b/dt = V_b$, and then combine it with the result for dU, to obtain

$$dE = \left(\rho u_2 + P'_2 - T_2\left(\frac{\partial P}{\partial T}\right)_{svp,T_2}\right) VA_x dt$$

$$+ \rho g(z_2 - z_b)\, V_b A_i dt + \rho g z_2 V A_x dt \qquad \text{(A2.4)}$$

where, as before, T_2 is the inside temperature, and u_2 is the liquid energy density at this temperature.

The second method is to calculate the energy that passes through the boundary of the control volume. It is the sum of the electrical heat, the work done on the fluid by the walls of its container, and the energy that enters through the flow tube.

$$dE = dQ - dW + j_e A_x dt \qquad \text{(A2.5)}$$

The work term is evaluated simply by the pressure-volume work done on the fluid by the top and bottom of the inside space, taking into account the hydrostatic pressure difference.

$$-dW = -P'_2 V_b A_i dt + \left(P'_2 + g(z_2 - z_b)\right) V_b A_i dt$$

$$= g(z_2 - z_b)\, V_b A_i dt \qquad \text{(A2.6)}$$

The total energy current j_e contains, as before, the enthalpy current and the heat current, but we must also add a gravitational potential energy current, $gz_{ent}\rho V$, where z_{ent} is the altitude at which the fluid enters the inside space. The enthalpy is to be evaluated at the pressure at which the liquid enters, which is, by continuity in the pressure, the local fluid pressure at the altitude of entry, $P'_2 + \rho g(z_2 - z_{ent})$. Collecting terms, we find that the z_{ent} terms cancel to give

$$j_e = \left(\rho u_{ent} + P'_2 + \dot{q}_{ent} + \rho g z_2\right) V \quad . \qquad \text{(A2.7)}$$

Then substituting into eq (A2.5), and equating it to eq (A2.4), we find that all the remaining terms containing g cancel, and we recover eq (36).

NBS-114A (REV. 7-73)

U.S. DEPT. OF COMM. BIBLIOGRAPHIC DATA SHEET	1. PUBLICATION OR REPORT NO. NBS TN-1002	2. Gov't Accession No.	3. Recipient's Accession No.

4. TITLE AND SUBTITLE

MEASUREMENTS OF COMBINED AXIAL MASS AND HEAT TRANSPORT IN He II

5. Publication Date: February 1978

6. Performing Organization Code: 275.05

7. AUTHOR(S): WARREN W. JOHNSON AND MICHAEL C. JONES

8. Performing Organ. Report No.

9. PERFORMING ORGANIZATION NAME AND ADDRESS

NATIONAL BUREAU OF STANDARDS
DEPARTMENT OF COMMERCE
WASHINGTON, D.C. 20234

10. Project/Task/Work Unit No.: 2750551

11. Contract/Grant No.

12. Sponsoring Organization Name and Complete Address *(Street, City, State, ZIP)*

13. Type of Report & Period Covered

14. Sponsoring Agency Code

15. SUPPLEMENTARY NOTES

16. ABSTRACT *(A 200-word or less factual summary of most significant information. If document includes a significant bibliography or literature survey, mention it here.)*

An experiment was performed that allowed measurements of both axial mass and heat transport of He-II in a long tube. The apparatus allowed the pressure difference and the temperature difference across the flow tube to each be independently adjusted, and the resulting steady-state values of net fluid velocity and axial heat transport to be measured. For the larger Reynolds numbers, it was found that the relation between pressure difference and net fluid velocity was nearly indistinguishable from that of an ordinary fluid in turbulent flow. The axial heat transported was found to be suppressed from the values that were calculated by assuming that "mutual friction" was unchanged by the net fluid flow, but it was always found to be larger than the "enthalpy rise" value. Taking this second value as a lower limit, it is shown that a mild extrapolation of these results suggests that (in appropriate circumstances) forced convection would allow much greater heat to be transported in long cooling channels than could be transported by "natural" convection alone.

17. KEY WORDS *(six to twelve entries; alphabetical order; capitalize only the first letter of the first key word unless a proper name; separated by semicolons)*

Axial heat transport; forced convection; helium II; measurements; 1.4 - 2.1 K; pressure drop.

18. AVAILABILITY

[X] Unlimited

[ ] For Official Distribution. Do Not Release to NTIS

[XX] Order From Sup. of Doc., U.S. Government Printing Office Washington, D.C. 20402, SD Cat. No. C13.46:1002

[ ] Order From National Technical Information Service (NTIS) Springfield, Virginia 22151

19. SECURITY CLASS (THIS REPORT): UNCLASSIFIED

21. NO. OF PAGES: 84

20. SECURITY CLASS (THIS PAGE): UNCLASSIFIED

22. Price: $2.40

USCOMM-DC 29042-P74

☆U.S. Government Printing Office: 1978-777-067/1230 Region 8

NBS TECHNICAL PUBLICATIONS

PERIODICALS

JOURNAL OF RESEARCH—The Journal of Research of the National Bureau of Standards reports NBS research and development in those disciplines of the physical and engineering sciences in which the Bureau is active. These include physics, chemistry, engineering, mathematics, and computer sciences. Papers cover a broad range of subjects, with major emphasis on measurement methodology, and the basic technology underlying standardization. Also included from time to time are survey articles on topics closely related to the Bureau's technical and scientific programs. As a special service to subscribers each issue contains complete citations to all recent NBS publications in NBS and non-NBS media. Issued six times a year. Annual subscription: domestic $17.00; foreign $21.25. Single copy, $3.00 domestic; $3.75 foreign.

Note: The Journal was formerly published in two sections: Section A "Physics and Chemistry" and Section B "Mathematical Sciences."

DIMENSIONS/NBS

This monthly magazine is published to inform scientists, engineers, businessmen, industry, teachers, students, and consumers of the latest advances in science and technology, with primary emphasis on the work at NBS. The magazine highlights and reviews such issues as energy research, fire protection, building technology, metric conversion, pollution abatement, health and safety, and consumer product performance. In addition, it reports the results of Bureau programs in measurement standards and techniques, properties of matter and materials, engineering standards and services, instrumentation, and automatic data processing.

Annual subscription: Domestic, $12.50; Foreign $15.65.

NONPERIODICALS

Monographs—Major contributions to the technical literature on various subjects related to the Bureau's scientific and technical activities.

Handbooks—Recommended codes of engineering and industrial practice (including safety codes) developed in cooperation with interested industries, professional organizations, and regulatory bodies.

Special Publications—Include proceedings of conferences sponsored by NBS, NBS annual reports, and other special publications appropriate to this grouping such as wall charts, pocket cards, and bibliographies.

Applied Mathematics Series—Mathematical tables, manuals, and studies of special interest to physicists, engineers, chemists, biologists, mathematicians, computer programmers, and others engaged in scientific and technical work.

National Standard Reference Data Series—Provides quantitative data on the physical and chemical properties of materials, compiled from the world's literature and critically evaluated. Developed under a world-wide program coordinated by NBS. Program under authority of National Standard Data Act (Public Law 90-396).

NOTE: At present the principal publication outlet for these data is the Journal of Physical and Chemical Reference Data (JPCRD) published quarterly for NBS by the American Chemical Society (ACS) and the American Institute of Physics (AIP). Subscriptions, reprints, and supplements available from ACS, 1155 Sixteenth St. N.W., Wash., D.C. 20056.

Building Science Series—Disseminates technical information developed at the Bureau on building materials, components, systems, and whole structures. The series presents research results, test methods, and performance criteria related to the structural and environmental functions and the durability and safety characteristics of building elements and systems.

Technical Notes—Studies or reports which are complete in themselves but restrictive in their treatment of a subject. Analogous to monographs but not so comprehensive in scope or definitive in treatment of the subject area. Often serve as a vehicle for final reports of work performed at NBS under the sponsorship of other government agencies.

Voluntary Product Standards—Developed under procedures published by the Department of Commerce in Part 10, Title 15, of the Code of Federal Regulations. The purpose of the standards is to establish nationally recognized requirements for products, and to provide all concerned interests with a basis for common understanding of the characteristics of the products. NBS administers this program as a supplement to the activities of the private sector standardizing organizations.

Consumer Information Series—Practical information, based on NBS research and experience, covering areas of interest to the consumer. Easily understandable language and illustrations provide useful background knowledge for shopping in today's technological marketplace.

Order **above** *NBS publications from: Superintendent of Documents, Government Printing Office, Washington, D.C. 20402.*

Order **following** *NBS publications—NBSIR's and FIPS from the National Technical Information Services, Springfield, Va. 22161.*

Federal Information Processing Standards Publications (FIPS PUB)—Publications in this series collectively constitute the Federal Information Processing Standards Register. Register serves as the official source of information in the Federal Government regarding standards issued by NBS pursuant to the Federal Property and Administrative Services Act of 1949 as amended, Public Law 89-306 (79 Stat. 1127), and as implemented by Executive Order 11717 (38 FR 12315, dated May 11, 1973) and Part 6 of Title 15 CFR (Code of Federal Regulations).

NBS Interagency Reports (NBSIR)—A special series of interim or final reports on work performed by NBS for outside sponsors (both government and non-government). In general, initial distribution is handled by the sponsor; public distribution is by the National Technical Information Services (Springfield, Va. 22161) in paper copy or microfiche form.

BIBLIOGRAPHIC SUBSCRIPTION SERVICES

The following current-awareness and literature-survey bibliographies are issued periodically by the Bureau:

Cryogenic Data Center Current Awareness Service. A literature survey issued biweekly. Annual subscription: Domestic, $25.00; Foreign, $30.00.

Liquified Natural Gas. A literature survey issued quarterly. Annual subscription: $20.00.

Superconducting Devices and Materials. A literature survey issued quarterly. Annual subscription: $30.00. Send subscription orders and remittances for the preceding bibliographic services to National Bureau of Standards, Cryogenic Data Center (275.02) Boulder, Colorado 80302.

U.S. DEPARTMENT OF COMMERCE
National Bureau of Standards
Washington, D.C. 20234

OFFICIAL BUSINESS

Penalty for Private Use, $300

POSTAGE AND FEES PAID
U.S. DEPARTMENT OF COMMERCE
COM-215

SPECIAL FOURTH-CLASS RATE
BOOK